Development of a Modelling Approach for High-Density Controlled Agriculture Environment Spaces for Energy and Yield Analysis

by

Marie-Hélène TALBOT

MANUSCRIPT-BASED THESIS PRESENTED TO ÉCOLE DE TECHNOLOGIE SUPÉRIEURE IN PARTIAL FULFILLEMENT OF THE REQUIREMENTS FOR THE DEGREE OF DOCTOR OF PHILOSOPHY
Ph.D.

MONTREAL, JANUARY 11, 2026

ÉCOLE DE TECHNOLOGIE SUPÉRIEURE
UNIVERSITÉ DU QUÉBEC

BOARD OF EXAMINERS

THIS THESIS HAS BEEN EVALUATED

BY THE FOLLOWING BOARD OF EXAMINERS

Mrs. Danielle Monfet, Thesis Supervisor
Department of Construction Engineering at École de technologie supérieure

Mrs.Tasseda Boukherroub, President of the Board of Examiners
Department of Systems Engineering at École de technologie supérieure

Mrs. Katherine Davignon, Member of the jury
Department of Construction Engineering at École de technologie supérieure

Mr. Didier Haillot, Member of the jury
Department of Mechanical Engineering at École de technologie supérieure

Mrs. Liping Wang, External Evaluator
Department of Civil and Architectural Engineering and Construction Management at University of Wyoming

THIS THESIS WAS PRENSENTED AND DEFENDED

IN THE PRESENCE OF A BOARD OF EXAMINERS AND PUBLIC

NOVEMBER 14, 2025

AT ÉCOLE DE TECHNOLOGIE SUPÉRIEURE

ACKNOWLEDGMENTS

I am deeply grateful to my supervisor, Prof. Danielle Monfet, whose support, patience, enthusiasm, and rigour have inspired me to grow as a researcher. Your mentorship, guidance on the project, and encouragement to pursue professional opportunities greatly shaped my PhD. I am also thankful for the expertise you shared in energy modelling, which was invaluable to my work.

I would like to sincerely thank the members of my thesis jury, Prof. Boukherroub, Prof. Davignon, Prof. Haillot, and Prof. Wang, for their time, valuable feedback, and insightful suggestions.

I extend my heartfelt thanks to my friends, my colleagues at the Laboratory of Thermal and Building Science and the Hydro-Québec Research Center, and my family, whose support and encouragement sustained me throughout this journey.

I am profoundly grateful to Tristan, my life partner, for standing by me through the most challenging moments. Your positivity, patience, encouragement, and love made all the difference.

This PhD journey was not without challenges and moments of doubt, but it helped me develop resilience and perspective, profoundly shaping the researcher I am today. I am grateful to continue growing professionally in a field I truly enjoy and am passionate about.

DÉVELOPPEMENT D'UNE APPROCHE DE MODÉLISATION DES ESPACES D'AGRICULTURE EN ENVIRONNEMENT CONTRÔLÉ À HAUTE DENSITÉ POUR L'ANALYSE ÉNERGÉTIQUE ET LE RENDEMENT

Marie-Hélène TALBOT

RÉSUMÉ

L'agriculture en environnement contrôlé à haute densité (AEC-HD), ou « vertical farming », consiste à cultiver verticalement des plantes dans un environnement contrôlé, assurant une production continue dans tous les climats et en zones urbaines. Bien que très productifs par unité de plancher, ces espaces sont énergivores en raison du contrôle précis de la température, de l'humidité, du dioxyde de carbone et de l'éclairage. Si l'optimisation des conditions intérieures pour améliorer la production a été largement étudiée, l'impact sur la consommation d'énergie reste souvent négligé, en raison de la complexité des interactions entre les plantes et leur environnement. Par exemple, la demande énergétique varie quotidiennement entre la photopériode et l'obscurité, et évolue avec la croissance. Cela requiert des systèmes de refroidissement et de déshumidification robustes pour maintenir des conditions d'air stables, ce qui constitue un défi important. La modélisation énergétique constitue un outil pertinent pour aborder ces enjeux. Cette thèse vise à développer une approche de modélisation énergétique permettant l'analyse conjointe de l'énergie et du rendement des espaces AEC-HD. La méthodologie repose sur la modélisation de la zone thermique, du système d'éclairage et des plantes dans un outil de simulation des performances du bâtiment. La laitue, culture dominante dans ces espaces, a été retenue comme cas d'étude. Pour atteindre l'objectif, trois étapes ont été réalisées : (1) l'examen des divergences de modélisation énergétique; (2) le développement et l'étalonnage expérimental d'un modèle dynamique de plantes intégrant un bilan énergétique et un modèle de croissance; et (3) l'application à une étude de cas afin d'analyser l'influence de la température, du déficit de pression de vapeur, de la densité de flux de photons photosynthétiques et de la photopériode. Les résultats ont mis en évidence l'importance de prendre en compte l'interception de la lumière et la croissance des plantes dans la modélisation énergétique. Le modèle dynamique de plantes développé a atteint une précision satisfaisante, avec des erreurs relatives maximales de 3,5 % et 4,1 % pour la charge énergétique spécifique et la durée de culture, respectivement. L'approche permet de simuler une large gamme de conditions intérieures et de scénarios opérationnels dans un outil de simulation des performances du bâtiment, soutenant l'analyse de 180 scénarios et fournissant des informations précieuses sur l'influence des conditions intérieures sur la charge énergétique et le rendement. Cette thèse par articles a conduit à la publication de quatre articles évalués par les pairs et à la diffusion de trois modèles de plantes accessibles à la communauté scientifique. L'approche proposée constitue une contribution significative pour améliorer la conception et l'exploitation des espaces AEC-HD en conciliant consommation énergétique et rendement, facilitant ainsi les analyses énergétiques, financières et environnementales

Mots-clés: agriculture en environnement contrôlé (AEC), *vertical farming*, modèle de plantes, modélisation énergétique, charge énergétique, modèle de croissance

DEVELOPMENT OF A MODELLING APPROACH FOR HIGH-DENSITY CONTROLLED AGRICULTURE ENVIRONMENT SPACES FOR ENERGY AND YIELD ANALYSIS

Marie-Hélène TALBOT

ABSTRACT

High-density controlled environment agriculture (CEA-HD), such as vertical farming, involves stacking crops in controlled indoor environments, enabling year-round food production across all climates and urban areas. Although CEA-HD spaces offer high productivity per unit of footprint, they are also energy-intensive due to precise regulation of temperature, humidity, carbon dioxide, and lighting. Many studies focus on optimizing growing conditions to improve yield, but the associated impact on energy consumption is often overlooked. One reason is the highly complex interplay between crops and their environment. For instance, energy demand varies daily between photoperiod and dark period and shifts throughout crop development. This necessitates robust cooling and dehumidification systems to maintain stable indoor air conditions, which is an ongoing challenge. Energy modelling is a valuable tool to address these types of issues. This thesis aims to develop an energy modelling approach to enable energy and yield analysis of CEA-HD spaces. The methodology involves modelling the thermal space, lighting system, and crops in a building performance simulation (BPS) tool. Given its dominance in CEA-HD spaces, lettuce was selected as the case crop. To achieve the objective, the following steps were undertaken: (1) the impact of discrepancies in energy modelling was examined; (2) a dynamic crop model, including an energy balance and growth model, was developed and calibrated with experimental data; and (3) the approach was applied to a case study analyzing the influence of temperature, vapour pressure deficit, photosynthetic photon flux density, and photoperiod. The results demonstrated the importance of accounting for light interception and crop growth in energy modelling. The developed model achieved a satisfactory level of accuracy, with maximum relative errors of 3.5% and 4.1% for the specific energy load and cultivation duration, respectively. The modelling approach enables simulations across a wide range of growing conditions and operational scenarios within a BPS tool, supporting the analysis of 180 scenarios and offering valuable insights into the influence of growing conditions on energy load and yield. This article-based thesis resulted in four peer-reviewed publications and the development of three crop models made available to the research community. The proposed modelling approach provides valuable support for enhancing CEA-HD design and operations by balancing energy consumption and crop yield. Overall, the work contributes a novel methodology to model CEA-HD spaces, facilitating energy, financial, and environmental assessments.

Keywords: controlled environment agriculture (CEA); vertical farming; crop model; energy modelling; energy load; growth model

TABLE OF CONTENTS

Page

LIST OF TABLES

LIST OF FIGURES

LIST OF ABREVIATIONS

ASHRAE	American Society of Heating, Refrigerating and Air-Conditioning Engineers
BELO	Building-integrated with electric lighting only
BIA	Building-integrated agriculture
BNEL	Building-integrated agriculture space with natural and electric lighting
BPS	Building performance simulation
CAC	Cultivation cover area
CEA	Controlled Agriculture Environment
CEA-HD	High-Density Controlled Agriculture Environment
CF	Container farm
CO_2	Carbon dioxide
COP	Coefficient of performance
CVRMSE	Coefficient of Variation of the Root Mean Square Error
DAT	Days after transplant
DWC	Deep-water culture
FAO	Food and Agriculture Organization
GH	Greenhouse
HPS	High-pressure sodium
HVAC	Heating, ventilation and air conditioning
HVAC&D	Heating, ventilation, air conditioning and dehumidification
MAD	Maximum Absolute Difference
NFT	Nutrient film technique

LED	Light-emitting diode
LA	Leaf area
LAI	Leaf area index
PAR	Photosynthetically active radiation
PCD	Planting crop density
PPE	Photosynthetic photon efficacy
PPF	Photosynthetic photon flux
PPFD	Photosynthetic photon flux density
RMSE	Root mean square error
RTGH	Rooftop greenhouse
SEC	Specific energy consumption
SHR	Sensible heat ratio
SLA	Specific leaf area
VF	Vertical farm
VPD	Vapour pressure deficit

LIST OF SYMBOLS

$[CO_2]$	air CO_2 concentration	[ppm]
A_v	total leaf area in the space	[m^2]
c	speed of light	[$m \cdot s^{-1}$]
c_ε	light use efficiency at very high CO_2 concentration	[$g \cdot J^{-1}$]
c_β	yield factor	[-]
$c_{gr,max}$	saturation growth rate	[s^{-1}]
c_τ	ratio of the root dry weight to the total dry weight	[-]
$c_{p_{a,i}}$	specific heat of the indoor air	[$J \cdot (kg \cdot °C)^{-1}$]
$c_{sol_{to}PAR}$	fraction of the total solar spectrum that is PAR	[-]
$c_{PPFD_{to}PAR}$	conversion factor from PPFD to the equivalent solar PAR	[$W \cdot m^{-2}_{cultivated} \cdot (\mu mol \cdot m^{-2} \cdot s^{-1})^{-1}$]
$DW_{content}$	dry weight content	[%]
DW_{leaf}	leaf dry weight	[$g \cdot m^{-2}_{cultivated}$]
DW_{sht}	shoot dry weight	[$g \cdot m^{-2}_{cultivated}$]
DW_{tot}	total dry weight	[$g \cdot m^{-2}_{cultivated}$]
f_{conv}	convective heat fraction	[-]
f_{LW}	long-wave radiation heat fraction	[-]
f_{SW}	short-wave radiation heat fraction	[-]
G	conductive flux between crops and soil	[$W \cdot m^{-2}_{cultivated}$]
h	Planck's constant	[J·s]
H	convective heat flux	[$W \cdot m^{-2}_{cultivated}$]
FW	fresh weight	[$g \cdot m^{-2}_{cultivated}$]

FW_{sht}	shoot fresh weight	[$g \cdot m^{-2}_{cultivated}$]
k_s	extinction coefficient	[-]
$k_{s,el}$	extinction coefficients associated with PAR from electric lighting	[-]
$k_{s,sol}$	extinction coefficients associated with PAR from sunlight	[-]
$\dot{m}_{CO2}$	CO_2 assimilation rate	[$kg \cdot hr^{-1}$]
M_{CO2}	CO_2 molar mass	[$kg \cdot \mu mol^{-1}$]
P_{cell}	cell net photosynthetic rate	[$\mu mol \cdot s^{-1}$]
P_{canopy}	canopy net photosynthetic rate	[$\mu mol \cdot m^{-2} \cdot s^{-1}$]
PPE_{max}	theoretical photosynthetic photon efficacy	[$\mu mol \cdot J^{-1}$]
$PPFD$	photosynthetic photon flux density	[$\mu mol \cdot m^{-2} \cdot s^{-1}$]
N_A	Avogadro's number	[μmol^{-1}]
q_{CE}	convective part of internal loads	[W]
q_{conv}	heat transfer from surfaces	[W]
$q_{IV,sens}$	sensible load caused by infiltration and ventilation	[W]
$q_{IV,lat}$	latent load caused by infiltration and ventilation	[W]
q_{LE}	latent part of internal loads	[W]
$q_{sys,sens}$	sensible heat transfer to/from HVAC&D systems	[W]
$q_{sys,lat}$	latent heat transfer to/from HVAC&D systems	[W]
q''_{el}	electric lighting power input	[$W \cdot m^{-2}_{cultivated}$]
$q''_{el,conv}$	convective heat flux from electric lighting	[$W \cdot m^{-2}_{cultivated}$]
$q''_{el,LW}$	net long-wave radiation flux from electric lighting	[$W \cdot m^{-2}_{cultivated}$]
$q''_{el,SW}$	short-wave radiation flux from electric lighting	[$W \cdot m^{-2}_{cultivated}$]

q''_{LWX}	net long-wave radiation flux exchange between surfaces	[$W \cdot m^{-2}_{cultivated}$]
q''_{LWS}	long-wave radiation from equipment in the zone	[$W \cdot m^{-2}_{cultivated}$]
q''_{morph}	flux used for photosynthesis	[$W \cdot m^{-2}_{cultivated}$]
$q''_{plt,conv}$	convective heat flux (gain or loss) from crops	[$W \cdot m^{-2}_{cultivated}$]
$q''_{plt,latent}$	latent heat flux from crops	[$W \cdot m^{-2}_{cultivated}$]
$q''_{plt,sol}$	net radiation flux absorbed by the crops from the sun	[$W \cdot m^{-2}_{cultivated}$]
$q''_{plt,SW}$	short-wave radiation flux absorbed by the crops from electric lighting	[$W \cdot m^{-2}_{cultivated}$]
$q''_{zone,SW}$	short-wave radiation flux converting into lighting heat	[$W \cdot m^{-2}_{cultivated}$]
q''_{sol}	transmitted solar radiation flux	[$W \cdot m^{-2}_{cultivated}$]
q''_{st}	flux stored within the leaves, stems and fruits	[$W \cdot m^{-2}_{cultivated}$]
PPE_{max}	theoretical photosynthetic photon efficacy	[$\mu mol \cdot J^{-1}$]
r_a	aerodynamic resistance	[$s \cdot m^{-1}$]
r_s	stomatal resistance	[$s \cdot m^{-1}$]
R_n	Net radiation heat flux absorbed by crops	[$W \cdot m^{-2}_{cultivated}$]
s	airflow speed	[$m \cdot s^{-1}$]
$T_{a,i}$	indoor air temperature	[°C]
T_{plt}	leaves temperature	[°C]
x_i	share of component *i* in the spectrum	[-]

Greek letters

α_{pl}	leaf absorption coefficient of PAR	[-]
χ_a	air vapour concentration	[$g \cdot m^{-3}$]
χ_s	vapour concentration at the canopy level	[$g \cdot m^{-3}$]

λ	heat of vaporisation of water	[kJ·kg^{-1}]
λE	evapotranspiration heat flux	[W·m$^{-2}_{cultivated}$]
λ_i	wavelength of the component *i*	nm
$\varphi_{a,i}$	air relative humidity	[%]
$\rho_{a,i}$	indoor air density	[kg·m^{-3}]
ρ_r	leaf reflection coefficient	[-]

INTRODUCTION

Controlled environment agriculture (CEA) takes various forms, such as standalone facilities like greenhouses, plant factories, vertical farms, and container farms, as well as building-integrated agriculture (BIA) facilities, such as rooftop greenhouses or indoor spaces that combine electric and natural lighting. When crops are grown in vertically stacked layers, these facilities are referred to as high-density controlled environment agriculture (CEA-HD) or vertical farms. These innovative spaces are well-suited for localized food production in cold climates and urban areas. CEA-HD are designed to maximize crop growth by regulating the indoor environment, such as temperature, humidity, carbon dioxide (CO_2) levels, light intensity, spectrum, and duration. These conditions are maintained using automated systems, including heating, ventilation, air conditioning, and dehumidification (HVAC&D) systems. By protecting crops from external conditions and ensuring precise control over their environment, CEA-HD achieve significantly higher yields and productivity compared to traditional outdoor farming (Kozai et al., 2015). These systems support various cultivation techniques (hydroponics, aeroponics, and soil-based methods) and irrigation systems (e.g., drip irrigation, nutrient film technique (NFT), and deep-water culture (DWC)). Despite their apparent advantages, CEA-HD spaces are recognized for their high energy requirements. The energy consumption is primarily driven by electric lighting, cooling, and dehumidification and, according to the 2021 Global CEA Census Report (Horomia & Gordon-Smith, 2021), the weighted average distribution in existing facilities worldwide is as follows: 55% for lighting, 35% for cooling and dehumidification and 10% for miscellaneous categories (heating, ventilation, automation, etc.).

Extensive research has focused on developing innovative cultivation methods and examining the influence of indoor environmental factors on crop yield, aiming to boost production without decreasing nutritional quality. For each crop, and even among different cultivars, different combinations of growing conditions can enhance both the quantity and quality of the yield. For example, Carotti et al. (2021) explored how varying the photosynthetic photon flux densities (PPFD), indoor air conditions, and root temperature affect lettuce growth. Similarly, extensive studies have been conducted on the effects of CO_2 enrichment on productivity (Kozai

et al., 2015). While optimizing growing conditions enhances productivity, it also directly influences the energy consumption of lighting and HVAC&D systems. However, the impact of these conditions on energy consumption is often overlooked, as most research prioritizes productivity and crop quality (Engler & Krarti, 2021). HVAC&D systems performance is also affected by the variation in sensible and latent cooling loads occurring in the space on a daily and growth cycle basis. This is due to variations in sensible and latent heat gains/losses between the photoperiod and the dark period, but is further influenced by leaf expansion as crops mature throughout a growth cycle. These variations require robust cooling and dehumidification systems to maintain a stable indoor air temperature and relative humidity. Beyond these thermal effects, crops also alter the air's gas composition, absorbing CO_2 and releasing oxygen during photosynthesis, while this process is reversed during respiration.

Since the relationship between growing conditions and the energy dynamics of CEA-HD spaces is highly complex, it presents significant challenges in designing and operating CEA spaces. Achieving a balance between yield and energy highlights the importance of a more integrated approach for energy design and management in controlled environments. To address these challenges, energy modelling is a valuable tool for analyzing the intricate heat exchanges involved in CEA operations. It facilitates the evaluation of energy-efficient strategies (Iddio et al., 2020) by estimating both energy consumption and crop yield. Effective energy modelling of CEA spaces often relies on the use of building performance simulation (BPS) tools, which must account for the heat exchanges between crops and their environment that vary as they grow (El Ghoumari et al., 2005). However, studies that have used energy modelling to estimate both energy consumption and fresh yield have reported significant discrepancies in their findings (Stanghellini & Katzin, 2023; Weidner et al., 2021). These differences stem from a variety of factors, including variations in growing conditions, the design of lighting and HVAC&D systems, and the proposed modelling approach. This variability highlights the lack of consensus within this emerging field on the approach to model CEA-HD spaces effectively for energy and yield analysis.

The main objective of this thesis is to develop a modelling approach adapted to CEA-HD spaces for energy and yield analysis. The developed approach includes a thermal space and crop model to support energy analysis for a wide range of growing conditions for lettuce. The first step involves exploring the impact of some of the discrepancies observed regarding crop modelling. Building on the findings from the first step, a crop model designed explicitly for vertical farm applications is developed and fully integrated into a BPS tool as a component for CEA-HD spaces analysis. The approach is then applied to a case study to gain valuable insights into the influence of growing conditions on energy load and yield. Overall, this research contributes to the body of knowledge by proposing a novel approach to model CEA-HD spaces, enabling the estimation of both energy and yield to support energy, financial and environmental analyses.

The thesis is composed of the following sections. Chapter 1 presents a foundational literature review and outlines the problem statement. Chapter 2 details the methodology followed to address the problem statement, including the structure of this article-based thesis. Chapters 3 to 6 consist of four published articles that represent the outcomes of this thesis. Chapter 7 is dedicated to an overall discussion of the research methods and findings, followed by the conclusion.

CHAPTER 1

LITERATURE REVIEW

This section provides a complementary literature review to that presented in the four articles of this thesis. Section 1.1 outlines the foundational literature and discrepancies regarding the energy consumption of CEA-HD spaces collected from existing facilities and estimated using models. To better understand the differences amongst the data generated with models, the modelling approaches are reviewed in sections 1.2 and 1.3. The approaches are presented for each component: the thermal space (section 1.2.1), the lighting system (section 1.2.2), the hydroponic solution (section 1.2.3) and the crops (section 1.3). Crop modelling is further divided into three parts: heat exchanges (section 1.3.1), growth (section 1.3.2) and CO_2 exchanges (section 1.3.3) modelling. Finally, section 1.4 provides a summary of identified literature gaps.

For this thesis, a total of 25 publications were selected to provide the state of the art in this literature review and the articles of the thesis regarding CEA-HD energy consumption and CEA modelling. They are grouped into two categories, A and B, as illustrated in Figure 1.1.

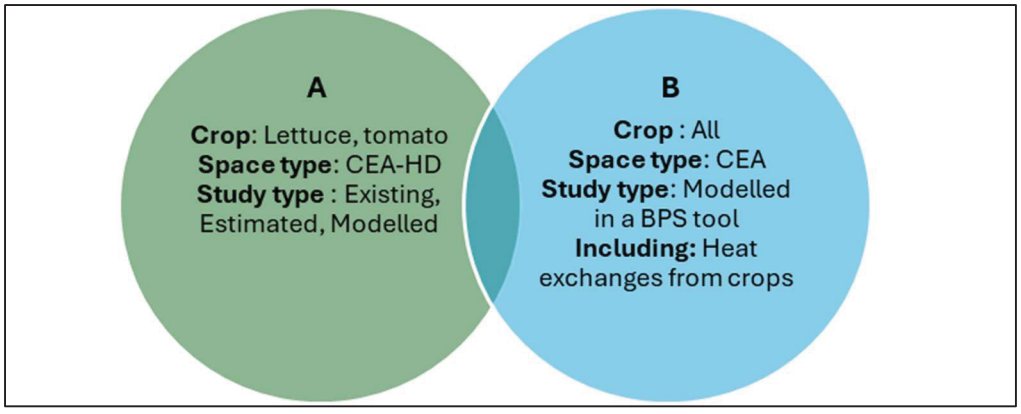

Figure 1.1 Categories and criteria used to classify the reviewed publications

Category A focuses specifically on studies related to cultivation in CEA-HD spaces, directly aligning with the focus of this thesis in terms of both space and crop type. In contrast, category B encompasses a broader scope of CEA space types, aiming to provide contextual insight into how crops are integrated into models when using BPS tools. These include different types of CEA space as proposed by Léveillé-Guillemette (2019) and illustrated in Figure 1.2: typical greenhouse built on ground (GH); rooftop greenhouse (RTGH); building-integrated agriculture space with natural and electric lighting (BNEL); building-integrated with electric lighting only (BELO). When integrated into a building, a CEA-HD space could also be referred to as a BELO. When CEA-HD is the unique usage in a building or a retrofitted shipping container, it can also be referred to as a vertical farm (VF) or a container farm (CF), respectively.

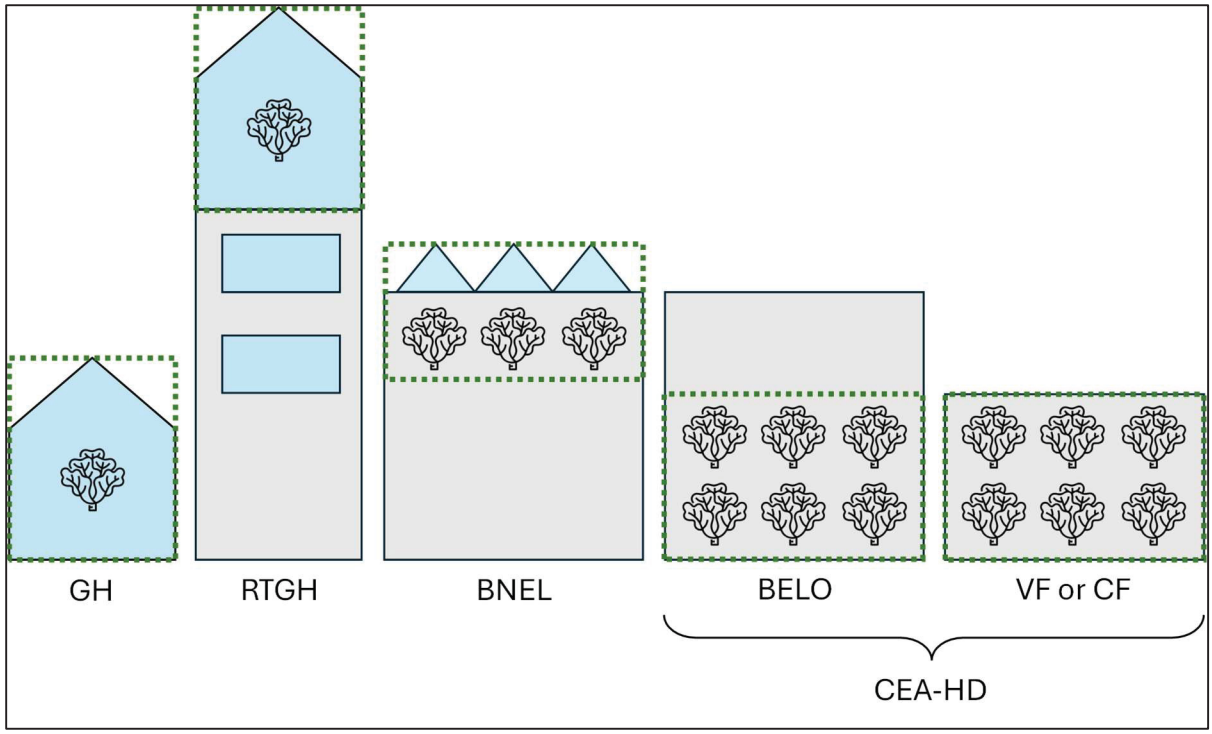

Figure 1.2 Illustration of different types of CEA spaces
Adapted from Léveillé-Guillemette (2019, p.42)

While publications in category A are mainly discussed in this literature review, publications in category B were mostly reviewed in the articles of the thesis, as there were few papers specifically addressing CEA-HD spaces at the time this research was conducted. The main

characteristics of the 25 publications are summarized in Table 1.1, by first specifying the space type, crop type, and type of data published. For energy consumption, two indicators are reported: (1) the specific energy consumption (SEC), which is the energy consumption per fresh yield produced, and (2) production intensity, which is the fresh yield produced per square meter, as reported in the publications. For studies that used a model, the modelling tool is specified, as well as an overview of the approach used to estimate the heat exchanges between crops and their environment, the purpose of the growth model and whether a CO_2 model is included. Publications shaded in light grey in Table 1.1 are selected to provide an overview of the state of the art on energy consumption in section 1.1. In contrast, the publications in the hatched box are used to provide an overview of the state of the art on modelling in sections 1.2 and 1.3. By compiling the characteristics of these publications in Table 1.1, some general observations can be made. Regarding energy consumption, 56% of the studies reported both indicators, the SEC and the production intensity. The use of these indicators has increased in recent years, as only 27% of the studies published before 2021 reported them. For CEA modelling, EnergyPlus is the most common BPS tool. For crop modelling, various approaches were used to estimate latent and convective heat exchanges, which are discussed in more detail in section 1.3.1. Convective heat exchanges were estimated more frequently, while radiative heat exchanges were largely overlooked. When included, growth modelling was often solely used to estimate yield, and only rarely to estimate yield and crop heat exchanges, which intensify as crops mature. Finally, CO_2 modelling is seldom included in crop modelling, with only five studies integrating it into their models.

Table 1.1 Main characteristics of the reviewed studies

Category	Space	Crop	Type of data	Energy consumption		CEA modelling	Crop modelling					Reference[1]
				Specific energy consumption, kWh·kg^{-1}	Production intensity, kg·m^{-2}		Heat exchanges			Growth	CO_2	
							Latent	Convective	Radiative			
A	CEA-HD	Lettuce	Ext	✓	-	-	-	-	-	-	-	Ohyama et al. (2020)
A					✗	-	-	-	-	-	-	Kozai (2019)
A					✓	-	-	-	-	-	-	Li et al. (2021)
A					✓	-	-	-	-	-	-	Blom et al. (2022)
A					✓	-	-	-	-	-	-	Casey et al. (2022)
A			Est	(✓)[2]	✓	-	-	-	-	-	-	Blom et al. (2023)
A				✓	✓	-	-	-	-	-	-	Stanghellini and Katzin (2023)
A, B			Mod	✓	✓	BPS (E+)	EB	EB	✗	✓ (Y)	✓	Graamans et al. (2018)
A, B					✓	BPS (E+)	FTR	EB	✗	✓ (Y)	✗	Zhang and Kacira (2020a), Zhang and Kacira (2020b)
A, B					✓	BPS (E+)	EB	EB	✗	✓ (Y)	✗	Eaton et al. (2023)
A					✓	HSim	EB	EB	✗	✓ (Y)	✗	Arcasi et al. (2024)
A, B					✗	BPS (E+)	EB	EB	✗	✓ (Y)	✗	Bu et al. (2024)
A					✓	HSim	EB	EB	✗	✓ (Y)	✓	Keyvan and Roshandel (2024)
A, B				✗	✗	BPS (E+)	FTR	✗	✗	✗	✗	Harbick and Albright (2016)
A, B					✗	BPS (TR)	EB	EB	✗	✗	✗	Lalonde et al. (2019)
A, B					✗	BPS (E+)	P-M	EB	✗	✗	✗	Liebman-Pelaez et al. (2021)
A, B					✗	BPS(E+)	EB	EB	✗	✓ (EB)	✗	Song et al. (2023)
A, B		Tomato	Mod	✓	✓	BPS (E+)	ST	✗	✗	✓ (Y)	✗	Benis et al. (2017b)
B	BNEL	Lettuce	Mod	✓	✓	BPS (E+)	EB	EB	EB	✓ (EB & Y)	✓	Jans-Singh et al. (2021)
B		Other	Mod	✗	✗	BPS (ESP)	P-M	EB	✗	✗	✗	Kokogiannakis and Cooper (2015)
B	RTGH, GH	Lettuce	Mod	✗	✗	BPS (E+)	ST	EB	✗	✓ (EB)	✓	Ledesma et al. (2022)
B		Tomato	Mod	✗	✗	BPS (TR)	EB	EB	EB	✓ (EB)	✓	Ward et al. (2015)
B			Mod	✗	✗	BPS (TR)	EMP	EB	✗	✓ (EB)	✗	Yeo et al. (2022)
B		Other	Mod	✗	✗	BPS (E+)	EMP	✗	✗	✗	✗	Nadal et al. (2017)
B			Mod	✗	✗	BPS (TR)	FAO	✗	✗	✗	✗	Baglivo et al. (2020)

Space *BNEL*: Building-integrated agriculture with natural and/or electric lighting, *CEA-HD*: High-density controlled environment agriculture, *GH*: Greenhouse, *RTGH*: Rooftop integrated greenhouse; **Data** *Est*: Estimated without modelling, *Ext*: From existing facilities, *Mod*: Estimated with modelling; **CEA modelling** *BPS*: Building performance simulation tool; *E+*: EnergyPlus, *HSim*: Hourly energy balance simulation, *TR*: TRNSYS; **Heat exchanges** *EB*: Heat exchanges are estimated with the energy balance approach, *EMP*: Latent heat flux is estimated with an empirical model, *FTR*: Latent heat flux is set to a fixed transpiration rate, *FAO*: Latent heat flux is estimated with FAO 56 Penman-Monteith model, *P-M*: Latent heat flux is estimated with Penman-Monteith model, *ST*: Latent heat flux is estimated with Stanghellini's model or a model derived from it; **Growth** *(EB)*: Growth is modelled to estimate dynamic crop heat exchanges, *(Y)*: Growth is modeled to estimate yield.

[1]Publications shaded in light grey and in the hatched box are respectively reviewed in sections 1.1 and 1.2 & 1.3.

[2]Incomplete, only the photoperiod was considered.

1.1 Energy consumption in CEA-HD

Energy consumption of well-insulated CEA-HD spaces is primarily driven by electric lighting, cooling, and dehumidification. It remains relatively unaffected by outdoor climatic conditions, highlighting the dominance of internal loads such as lighting and crop activity (Eaton et al., 2023; Graamans et al., 2018). The energy consumption of the electric lighting, cooling and dehumidification systems depends on various factors. Lighting and cooling energy consumption are influenced by the duration of the photoperiod, the light intensity and the photosynthetic photon efficacy (PPE) of the lights, which measures the photosynthetic photon flux emitted relative to the electrical power input. The PPE varies based on light efficiency and spectrum. In parallel, as crops grow, they generate heat and mass, and as crop foliage expands, more Photosynthetically Active Radiation (PAR) is intercepted, leading to increased transpiration rates. It results in additional dehumidification to maintain the humidity at the desired level (EPRI, 2018; Holden et al., 2021). Additionally, due to transpiration, crop leaves often exhibit lower temperatures than the surrounding air (Davis & Hirmer, 2015); thus, crops can cool their environment by radiative and convective heat transfer, which can be referred to as sensible heat loss. This evaporative cooling process also occurs during dark periods but differs in magnitude.

Energy consumption in CEA-HD facilities has been widely studied, revealing significant disparities in reported values. Most studies have used the SEC, the energy consumed per kilogram of fresh yield, as the key metric. These studies show significant variation in the reported SEC values, ranging from 15 to 26 $kWh \cdot kg^{-1}$ (Weidner et al., 2021), 6.2 to 23.0 $kWh \cdot kg^{-1}$ (Ahamed et al., 2023), and 4.4 to 38.5 $kWh \cdot kg^{-1}$ (Miserocchi & Franco, 2025). To better understand the factors contributing to this variation, 13 studies identified in light grey in Table 1.1 that reported a SEC value for lettuce cultivation were used for comparison. Five of those studies reported SEC values from existing facilities (Blom et al., 2022; Casey et al., 2022; Kozai, 2019; Li et al., 2021; Ohyama et al., 2018), seven studies from modelled facilities (Arcasi et al., 2024; Bu et al., 2024; Eaton et al., 2023; Graamans et al., 2018; Keyvan & Roshandel, 2024; Zhang & Kacira, 2020a, 2020b) while Stanghellini and Katzin (2023)

estimated the SEC based on a general rule of thumb. They proposed estimating lighting energy consumption based on the PPE of the lights, and assumed that HVAC systems contribute an additional 25% to the energy use to calculate the total energy consumption. Figure 1.3 compares the SEC values reported from existing facilities, modelled CEA-HD spaces, and estimated without using modelling. The latter are derived from the estimation method suggested by Stanghellini and Katzin (2023) for a photon production efficiency (PPE) of 1.8 µmol·J^{-1} and 2.6 µmol·J^{-1} for lighting intensities of 200, 400 and 750 µmol·m^{-2}·s^{-1} for a total of six estimated values.

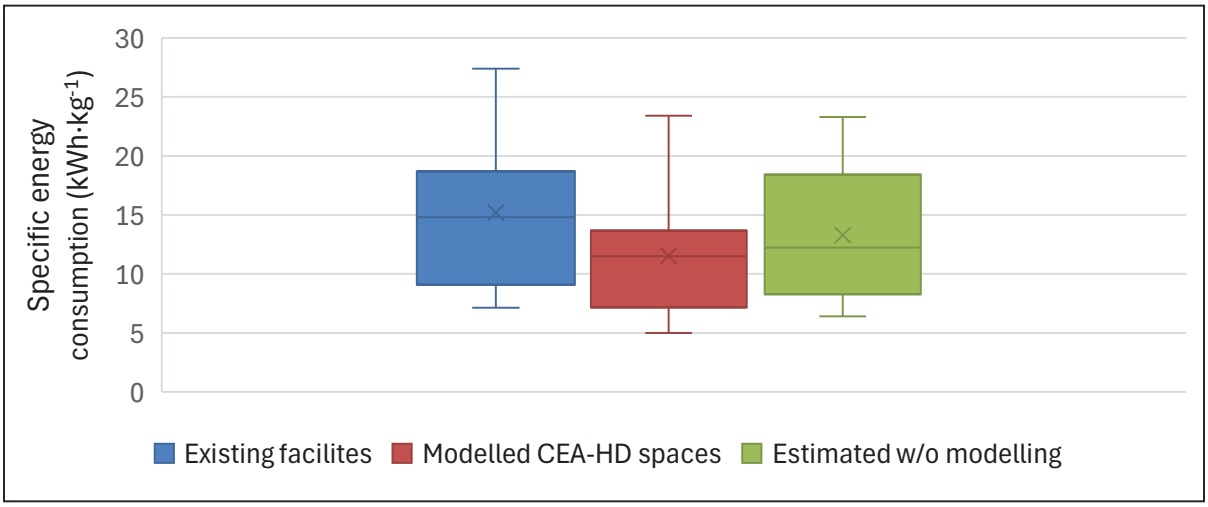

Figure 1.3 Specific energy consumption reported values from existing facilities, modelled facilities and estimated without modelling

1.1.1 Existing facilities

For the existing facilities, SEC varies between 7.1 and 27.4 kWh·kg^{-1}. However, it was recently suggested by Bu et al. (2024) that SEC of 6.3 to 9 kWh·kg^{-1} could be achieved with current installed lights, which have a PPE ranging from 1.8 µmol·J^{-1} (Bu et al., 2024) to 2.6 µmol·J^{-1} (Song et al., 2023). This gap suggests that current design and operation are suboptimal, with HVAC&D systems consuming more energy than necessary. However, when assessing the energy performance, SEC values alone do not fully reflect the performance of the installation: the production intensity must also be considered. As an example, Figure 1.4 reports the SEC

and production intensity for existing facilities that provided both information with a blue cross. These values are compared to those estimated using the method proposed by Stanghellini and Katzin (2023), forming a potential target range.

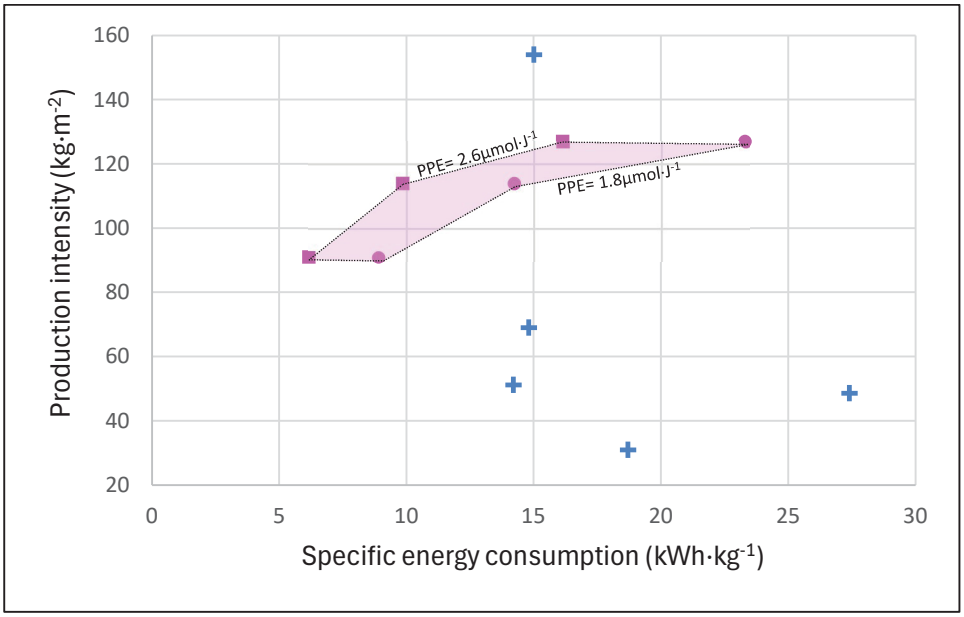

Figure 1.4 Production intensity plotted against specific energy consumption for existing facilities (blue crosses) compared with the estimations for PPE of 1.8 µmol·J^{-1} (pink circles) and 2.6 µmol·J^{-1} (pink squares), under three lighting intensities

The analysis of the energy consumption data (SEC and production intensity) reveals that most of the existing facilities are underproductive compared to the target area in pink, as derived from the approach proposed by Stanghellini and Katzin (2023). An exception, the facility reported by Casey et al. (2022), showed a high productivity of 154 kg·m^{-2} compared to other facilities with a similar SEC of around 15 kWh·kg^{-1}, exceeding the performance target range.

1.1.2 Modelled CEA-HD spaces

For the modelled CEA-HD spaces, some studies reported multiple SEC values, exploring various alternatives such as changes in location, overall heat transfer coefficient of the envelope, PPE, daily light integral, ventilation rate, CO_2 concentration, and more. As

illustrated in Figure 1.3, the SEC values vary between 5 and 23 $kWh \cdot kg^{-1}$, reflecting significant disparities across the results. Differences in growing conditions can explain the variation in SEC. For example, 56% of the SEC values reported in Figure 1.3 were for modelled spaces with CO_2 enrichment, 44% with indoor air temperature maintained within a narrow range, and 78% with controlled humidity, with only 43% of these spaces having a tight control over humidity. The modelling approaches can also explain the variation in SEC used: 71% of the studies modelled the crop energy balance to estimate both the latent and convective heat exchanges based on the PAR absorbed by crops, and 43% also integrated a mechanistic model for crop growth to estimate yield. However, none of the studies used the outputs from the growth model to dynamically assess heat exchanges from crops as they grow. Instead, the growth stage was set to a fixed value, meaning crop heat exchanges with their environment were considered constant at each simulation timestep.

1.2 Controlled agriculture environment modelling

To provide a comprehensive overview of the current state of CEA-HD space modelling, this section and the next draw on the 12 studies highlighted in the hatched box in Table 1.1, all of which modelled CEA-HD spaces for various crops. This section focuses on modelling approaches related to each component of a CEA model, as illustrated in Figure 1.5: the thermal space (1.2.1), lighting system (1.2.2) and hydroponic solution (1.2.3), while crop modelling is addressed in a dedicated section (1.3).

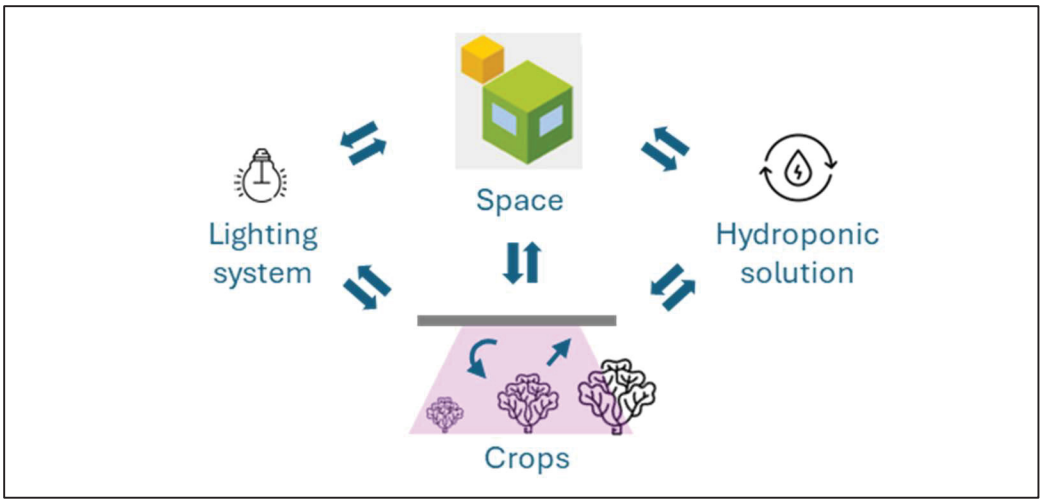

Figure 1.5 Simplified overview of a CEA-HD model

1.2.1 Thermal space

To model CEA-HD spaces, it is required to model them as a simplified energy representation, also referred to as a thermal space. The thermal space model typically includes at least one thermal zone and can be developed using a 3D representation that accounts for different parameters such as geometry, orientation, localization, envelope properties, surface convection coefficients, and infiltration rate. A weather file, corresponding to typical, actual or predictive weather, can also be linked to account for local climatic conditions. Thermal space modelling can either be programmed manually or with BPS tools, which are software specifically developed to perform building energy analysis based on a simplified energy model of multi-zone buildings. Figure 1.6 illustrates a typical flow chart for building energy modelling with BPS tools (ASHRAE, 2013a).

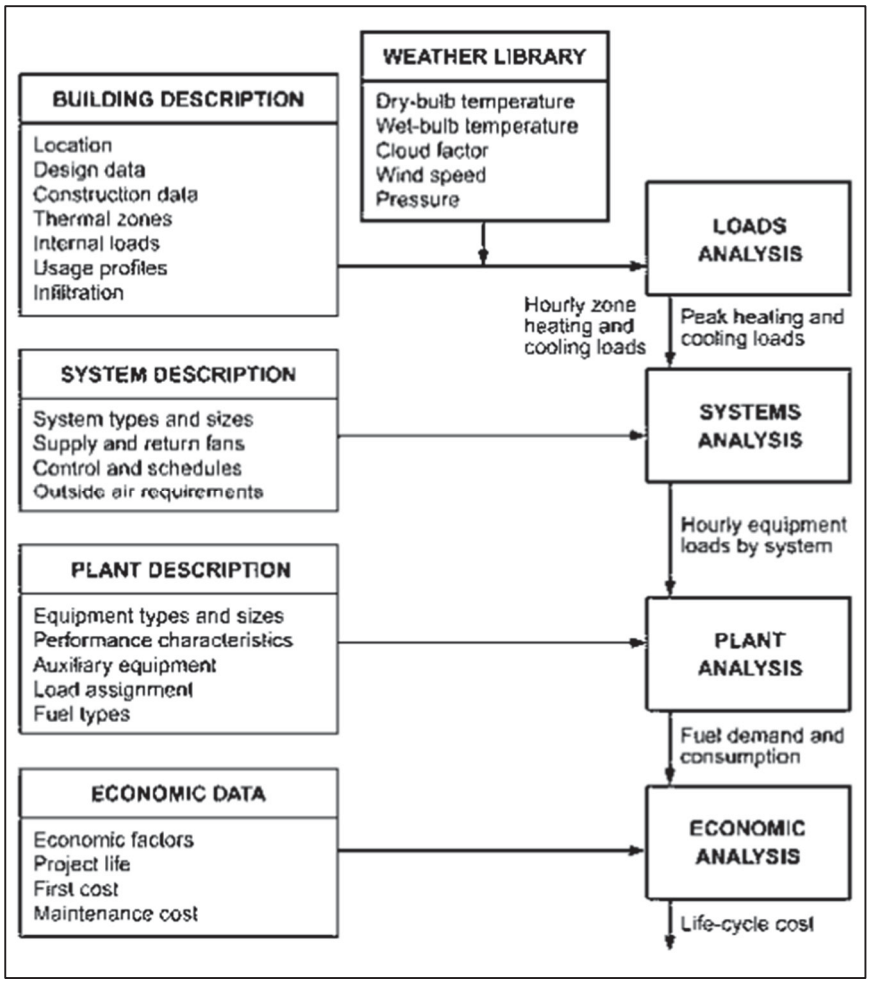

Figure 1.6 Flow chart for building energy modelling
Taken from ASHRAE (2013a, p.19.1)

The main advantage of BPS tools lies in their foundation on well-established mathematical models that are widely validated and accepted within the scientific community. These tools have gained broad adoption in both academic and professional settings for modelling multi-zone buildings, with applications ranging from research and design to performance assessment, optimization, and regulatory compliance. Several BPS tools are commonly used, each with its own strengths and limitations. For example, three widely used tools are summarized below:

- EnergyPlus (Crawley et al., 2000) is a widely adopted BPS engine that can be used directly or through interfaces such as OpenStudio and DesignBuilder. It incorporates validated mathematical models, is open-source and offers a good speed of execution.
- TRaNsient SYstem Simulation, or more commonly referred to as TRNSYS (Klein & al., 2017), is recognized for its modular structure and flexibility, particularly in modelling complex or custom energy systems.
- IDA Indoor Climate and Energy (IDA ICE) offers a balance between flexibility and ease of use, with a moderate learning curve.

Most BPS tools are based on the heat balance method (ASHRAE, 2021), which is schematically illustrated in Figure 1.7. The tools are built on mathematical models to estimate heat exchanges, conductive, convective, and radiative. Based on these exchanges, as well as temperature and humidity (if applicable) setpoints, BPS tools can estimate heating and cooling loads and/or the energy consumption of the HVAC systems, if modelled. A fundamental assumption of this method is that the indoor air is well-mixed. For CEA-HD spaces, the air heat balance and the moisture air heat balance can be expressed according to equations (1.1) and (1.2) for quasi-steady conditions (ASHRAE, 2021).

$$q_{conv} + q_{CE} + q_{IV,sens} + q_{sys,sens} = 0 \tag{1.1}$$

$$q_{LE} + q_{IV,lat} + q_{sys,lat} = 0 \tag{1.2}$$

where :

q_{conv} is the heat transfer from surfaces, W.

q_{CE} is the convective part of internal loads, W.

$q_{IV,sens}$ is the sensible load caused by infiltration and ventilation, W.

$q_{sys,sens}$ is the sensible heat transfer to/from HVAC&D systems, W.

q_{LE} is the latent part of internal loads, W.

$q_{IV,lat}$ is the latent load caused by infiltration and ventilation, W.

$q_{sys,lat}$ is the latent heat transfer to/from HVAC&D systems, W.

The crop heat exchanges and the convective heat gain for lights can be computed in the q_{CE} and q_{LE} terms. The coupling is explicitly described in section 1.3.1.

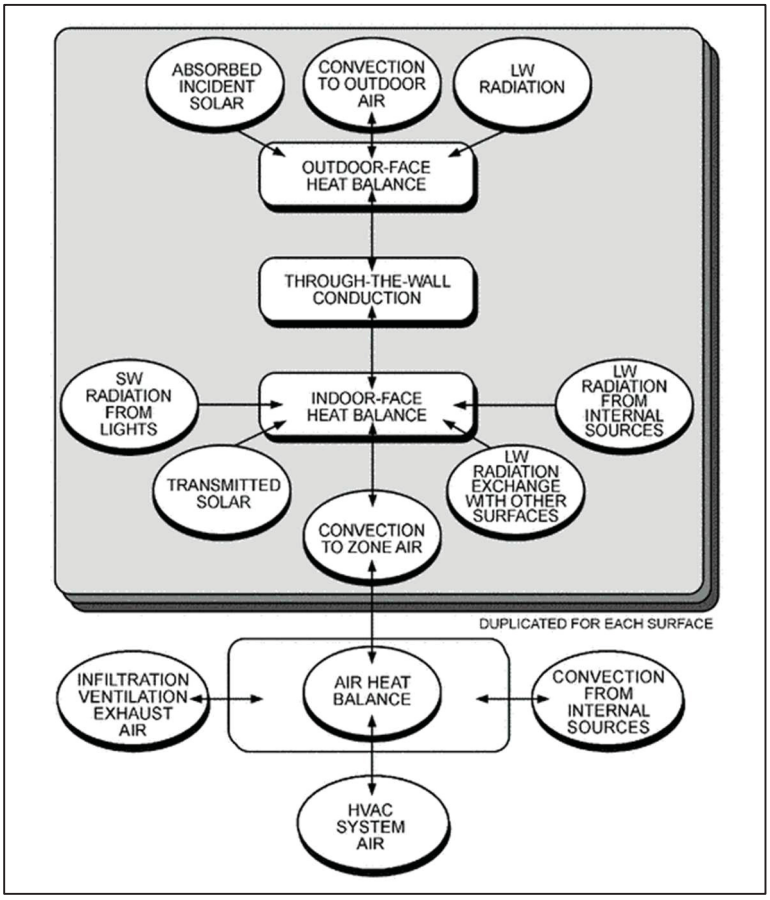

Figure 1.7 Schematic overview of the heat balance method
Taken from ASHRAE (2021, p.18.21)

Regarding CEA-HD space, out of the 12 studies reviewed, ten employed a BPS tool to simulate the thermal space. They all used EnergyPlus, except for Lalonde et al. (2019), who opted for TRNSYS. In contrast, two studies developed custom programs in software such as MATLAB to model hourly heat exchanges, requiring extensive programming that could have been streamlined by using a BPS tool. While integrating crops as internal heat sources in BPS tools presents some challenges, these tools offer significant advantages, such as faster model development, improved execution efficiency, and improved model quality.

While all reviewed studies accounted for crops and lighting as internal heat sources, modelling approaches varied based on the characteristics of the CEA-HD space or its climate control strategy. For instance, retrofitted containers were typically assumed not to be fully airtight, and infiltration was explicitly included (Bu et al., 2024; Keyvan & Roshandel, 2024; Liebman-Pelaez et al., 2021; Song et al., 2023). Some models also simulated outdoor air ventilation to manage cooling loads (Keyvan & Roshandel, 2024; Lalonde et al., 2019; Liebman-Pelaez et al., 2021).

In addition, several studies included internal heat sources from:

- Standalone dehumidification systems located within the thermal space (Eaton et al., 2023; Liebman-Pelaez et al., 2021);
- Pumps and fans (Song et al., 2023); and
- Occupants (Benis et al., 2017b).

1.2.2 Lighting

Lighting in CEA can be achieved using various technologies, including high-pressure sodium (HPS), fluorescent lights, and light-emitting diodes (LEDs). LEDs have become the preferred choice for CEA-HD spaces due to their low surface temperature, high PPE, and decreasing cost. The low surface temperature of LEDs is particularly important, as it allows crops to be placed much closer to the light source without the risk of leaf burn, enabling higher planting densities and improved space utilization. Furthermore, the modularity of LEDs, allowing fine-tuned control over both light intensity and spectral composition, has opened up new opportunities for optimizing light energy use, defined as the energy consumed per kilogram of crops produced (Kozai et al., 2015). However, LED lights, like HPS or fluorescent lights, are not 100% efficient, meaning that a portion of the electrical power input is directly converted into heat. The efficiency of LED, often referred to as the photosynthetically active radiation (PAR) fraction or short-wave heat fraction, ranges from 31% to 63% in the studies identified in the hatched box in Table 1.1. The efficiency depends on the PPE and light spectrum. It can

be estimated using data often provided by manufacturers. It is calculated as the ratio of the actual PPE to the theoretical maximum PPE (PPE_{max}) for a given spectral composition. The PPE_{max} is based on the energy content of photons, which can be determined with Planck's equation, and can be estimated with the proposed generalized formula in Equation (1.3).

$$PPE_{max} = \left\{ h \cdot c \cdot N_A \sum_i x_i \frac{1}{\lambda_i} \right\}^{-1} \quad (1.3)$$

where:

PPE_{max} is the theoretical photosynthetic photon efficacy, μmol·J^{-1};

h is Planck's constant, 6.626× 10^{-34} J·s;

c is the speed of light, 3.0× 10^{8} m·s^{-1};

N_A is the Avogadro's number, 6.022 × 10^{17} μmol^{-1}

λ_i is the wavelength of the component i, m; and

x_i is the share of component i in the spectrum.

The remaining energy is generally considered as heat gain, except for Arcasi et al. (2024), who assumed that all the electrical power input is converted into heat. For example, Zhang and Kacira (2020a), Zhang and Kacira (2020b), and Song et al. (2023) distributed the lighting heat gains between convective and radiative heat, whereas others did not clearly state how the heat gains were broken down. LED manufacturers rarely provide detailed information on the breakdown between long-wave radiative and convective heat fractions, and these values may vary significantly between models, as has been observed in building applications (Liu et al., 2017).

Furthermore, some of the PAR is intercepted and absorbed by crops, while the remaining can be accounted for as heat gains. Although all the studies included a portion of the PAR into the crop energy balance, only four, Lalonde et al. (2019), Liebman-Pelaez et al. (2021), Song et al. (2023), Keyvan and Roshandel (2024), explicitly accounted for the effect of light interception on lighting heat gains using a fixed light interception factor. However, it remains

unclear if it was considered in the other studies, but omitting to account for the effect of light interception can lead to an overestimation of lighting heat gains. To ensure energy conservation, this effect should be considered, even though the magnitude of the resulting error has yet to be quantified. Finally, only Song et al. (2023) dynamically modelled the effect of light interception on lighting heat gains, meaning the light interception factor increased as the crop leaves expanded.

1.2.3 Hydroponic solution

In CEA-HD spaces, operations alternate between two modes: the photoperiod, when the lights are on, and the dark period, when the lights are off. When switching between these modes, setpoints often change, contributing to the disruption of the thermal balance. Thermal storage occurring in CEA-HD spaces, such as in the surfaces (walls, ceiling, floor), crops, equipment, growing structures, and hydroponic solution, can potentially smooth the transition between operation modes and could even lower peak loads. However, aside from surfaces, whose properties are directly input into BPS tools, other thermal masses are often neglected. It would be valuable to investigate the impact of thermal storage in hydroponic solution on the load profile and determine whether it can be neglected in energy and yield analysis. From a thermal perspective, the hydroponic solution is essentially a mass of water with a heat capacity of 4.184 J kg^{-1} $°C^{-1}$. Like any thermal mass, it can store heat and release it later with a time delay. This behaviour is similar to hydroaccumulation reservoirs, which are used in greenhouses in cold climates as thermal storage to reduce heating equipment capacities (Hydro-Québec, 2025).

1.3 Crop modelling

This section presents the fundamentals and approaches for three facets of crop modelling that have been or can be integrated into energy and yield analysis: (1) crop heat exchanges (1.3.1), (2) yield and growth rate (1.3.2), and (3) CO_2 assimilation rate (1.3.3). This section reviews the approaches used in the same 12 studies of section 1.2, which were identified in a hatched box in Table 1.1.

1.3.1 Heat exchanges

Crops interact with their environment, and this interaction can be represented as an energy balance that includes energy inputs and outputs, as well as the energy stored and effectively used for photosynthesis. In CEA-HD spaces, where the photosynthetic active radiation from electric lighting is the primary energy input, the energy balance for the control volume, i.e., the canopy (Stanghellini, 1987), can be expressed as Equation (1.4) (adapted to CEA-HD from Talbot and Monfet (2020)), based on the heat balance method formulation (ASHRAE, 2021).

$$q"_{plt,SW} + q"_{plt,LWX} - q"_{st} - q"_{morph} - q"_{plt,conv} - q"_{plt,latent} = 0 \quad (1.4)$$

where:

$q"_{plt,SW}$ is the short-wave radiation flux absorbed by the crops from lights, $W \cdot m^{-2}_{cultivated}$;

$q"_{plt,LWX}$ is the net long-wave radiation flux exchange between surfaces, $W \cdot m^{-2}_{cultivated}$;

$q"_{st}$ and $q"_{morph}$ are the fluxes stored within the leaves, stems and fruits or used for the photosynthesis, respectively, $W \cdot m^{-2}_{cultivated}$;

$q"_{plt,conv}$ is the convective exchange flux between the leaves' surface with ambient air, which is typically a negative value in CEA-HD spaces, causing a cooling effect, $W \cdot m^{-2}_{cultivated}$; and

$q"_{plt,latent}$ is the latent exchange flux with ambient air, mostly by transpiration from the leaves, $W \cdot m^{-2}_{cultivated}$.

For CEA-HD applications, the energy balance is generally simplified by neglecting the net long-wave radiation heat flux ($q"_{plt,LWX}$), heat storage in crops ($q"_{st}$), and the energy used for photosynthesis ($q"_{morph}$). As a result, the formulation commonly adopted is given by Equation (1.5). It is worth noting that while long-wave radiation heat flux is often overlooked in CEA-HD spaces due to the relatively small temperature differences between surfaces, lighting, and crops, its actual impact has not yet been quantified.

$$q"_{plt,SW} - q"_{plt,conv} - q"_{plt,latent} = 0 \quad (1.5)$$

The crop heat exchanges, $q"_{plt,conv}$ and $q"_{plt,latent}$, can be found by solving this simplified energy balance. The crop and air heat balance equations, as defined by equations (1.1), (1.2) (detailed in section 1.1.2), and (1.5), are then coupled as illustrated in Figure 1.8.

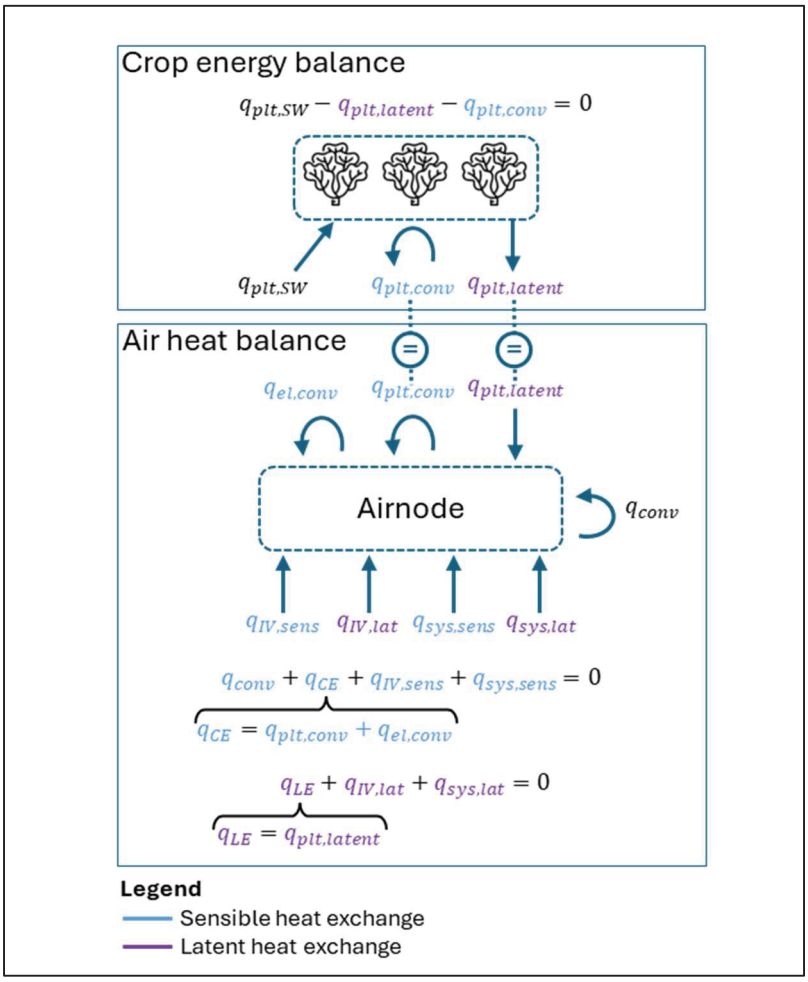

Figure 1.8 Coupling between the crop energy balance and the air heat balance

Furthermore, two studies, Harbick and Albright (2016) and Benis et al. (2017b), have also neglected the convective heat exchange from crops, which typically cool the surrounding air in CEA-HD spaces. They only included crop transpiration using either an average transpiration rate for lettuce grown in greenhouses of 100 ml $plant^{-1} \cdot day^{-1}$ (Harbick & Albright, 2016) or a crop transpiration model (Benis et al., 2017b). The crop transpiration model selected by Benis et al.(2017b) is derived from Stanghellini's crop transpiration model (Stanghellini, 1987),

which remains one of the models providing good performance for greenhouse application (Katsoulas & Stanghellini, 2019; Villarreal-Guerrero et al., 2012). Stanghellini's crop transpiration model is an adaptation of the foundational Penman-Monteith model (Monteith, 1965) for greenhouse applications. The main equation, variables, and parameters that compose the Penman-Monteith model are illustrated in Figure 1.9.

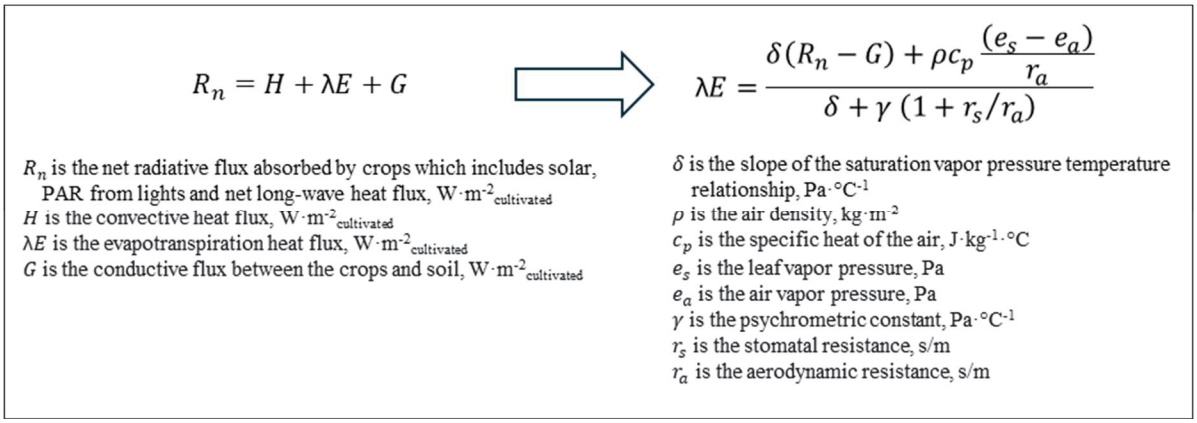

Figure 1.9 Penman-Monteith equation to estimate evapotranspiration
Adapted from Monteith (1965)

Since 2017, both latent and sensible heat exchanges from crops have been systematically included in CEA-HD spaces modelling. This shift appears to have been strongly influenced by Graamans et al. (2017), who introduced a validated model for estimating $q"_{plt,SW}$, $q"_{plt,conv}$, and $q"_{plt,latent}$ in CEA-HD spaces. Their model, referred to as the 'big leaf' model, is also an adaptation of the Penman-Monteith model. The procedure involves iteratively solving the energy balance, composed of three equations for $q"_{plt,SW}$, $q"_{plt,conv}$ and $q"_{plt,latent}$, as detailed in Figure 1.10, until the leaves' temperature converge to a solution. Consistent with the Penman-Monteith formulation, the leaf vapour pressure term is not evaluated psychometrically at leaf temperature but is approximated by a first-order linearization around the indoor air temperature. This approach accelerates convergence but partially decouples the leaf vapour pressure from the resolved leaf temperature. Moreover, although the water vapour transpired from the leaf surface is not necessarily at the air temperature, the procedure proposed by

Graamans et al. (2017) does not explicitly account for the potential sensible heat exchange associated with the newly added vapour in the air heat balance.

Graamans et al. (2017) term	Associated equation	Variables and parameters definition
Net radiation (R_{net}) Sensible heat exchange (H) Latent heat exchange (λE)	$R_{net} = q"_{plt,SW} = (1-\rho_r)\cdot CAC \cdot I_{electric}$ $H = q"_{plt,conv} = LAI \cdot \rho c_p \frac{T_{plt}-T_{air}}{r_a}$ $\lambda E = q"_{plt,latent} = LAI \cdot \lambda \frac{e_s - e_a}{r_s + r_a}$ $r_s = 60 \cdot \frac{1500+PPFD}{200+PPFD}$	ρ_r is the leaf reflection coefficient, % CAC is the cultivation cover area, % $I_{electric}$ is the PAR emitted by the electric horticultural lighting, $W \cdot m^{-2}_{cultivated}$ LAI is the leaf area index, $m^{-2}_{leaves} \cdot m^{-2}_{cultivated}$ ρ is the air density, $kg \cdot m^{-2}$ c_p is the specific heat of the air, $J \cdot kg^{-1} \cdot °C$ T_{plt} is the leaves temperature, °C T_a is the air temperature, °C e_s is the leaves vapor pressure, Pa e_a is the air vapor pressure, Pa r_s is the stomatal resistance, s/m r_a is the aerodynamic resistance, s/m $PPFD$ is the photosynthetic photon flux density, $\mu mol \cdot s^{-1} \cdot m^{-2}$

Figure 1.10 Details of the fluxes formulated in Graamans et al. (2017) lettuce model Adapted from Talbot and Monfet (2020, p.1453)

One of the key parameters in the model is the leaf area index (LAI), which influences each term, even the net radiation term, since the cultivation cover area (CAC) is a function of the LAI, as described by Tei et al. (1996). The LAI is a dimensionless variable defined as the total one-sided area of photosynthetic tissue per unit of ground surface area (Watson, 1947) and is one of the most influential variables affecting the gains or losses induced by crops (Prenger et al., 2002). It corresponds to the product of the leaf area per plant and the crop planting density. Therefore, the LAI reflects not only the growth stage (i.e., the size of the leaves) but also the plant spacing management method.

Out of the 10 studies published after 2017, 70% adopted the procedure outlined by Graamans et al. (2017). Among the few exceptions, Zhang and Kacira (2020a), Zhang and Kacira (2020b), and Song et al. (2023) applied the simplified energy balance from Equation (1.5) but did not use the procedure summarized in Figure 1.10. Zhang and Kacira (2020a) and Zhang and Kacira (2020b) adopted a fixed transpiration rate of 43 $ml \cdot plant^{-1} \cdot day^{-1}$, based on measured daily water consumption, while Song et al. (2023) used an adaptation of the Penman-Monteith model from Schymanski and Or (2017). This adaptation offers corrections of the Penman-Monteith model to account for the exchange of sensible heat from both sides of leaves

and accurately models crops with hypostomatous leaves (i.e., stomata on the underside of leaves). All seven studies that adopted the Graamans et al. (2017) model used their proposed formulation to estimate the short-wave radiative heat flux absorbed by crops. This formulation is based on the CAC as defined by Tei et al. (1996) and the leaf reflection coefficient. However, the CAC is estimated using an empirical correlation that is a function of the LAI, which is restricted to a specific planting density of 17.6 plants·m^{-2}.

Except for Song et al. (2023), the approaches selected to model the crop energy balance share a significant limitation: they assume constant latent and sensible heat exchanges from crops, using a fixed LAI value. Bu et al. (2024) identified this as one of the main limitations of their approach, noting the need to "improve the model's dynamics". Assuming a fixed LAI value can be reasonable depending on the growth management method. Growers can adopt two strategies: all crops may be grown at a single stage of development, or simultaneously at different stages. In the latter case, as the number of overlapping growth stages increases, variations in the overall canopy leaf area over time tend to decrease, making the use of a fixed average LAI value justifiable. Thus, by adopting a fixed LAI value, most studies implicitly or explicitly assumed a diversified stage growth management method, meaning their models may not be suitable for CEA-HD spaces managed under a single stage approach (Talbot & Monfet, 2020). Moreover, the fixed LAI value commonly used for lettuce of 2.1, according to Graamans et al. (2018), may not reflect actual conditions. The actual average LAI depends on several factors, including crop planting density, transplant and harvest size – all of which also influence yield. As such, using a fixed LAI can lead to inconsistencies if energy balance and growth models are not properly aligned.

1.3.2 Growth

The primary purpose of integrating a growth model into an energy model is to support yield estimation, expressed in kilograms of fresh or dry weight per year or per production cycle, which depends on various factors. The rate of photosynthesis, the main driver of biomass accumulation, is mainly influenced by temperature, light intensity, and indoor CO_2

concentration. The response of the rate of photosynthesis to these factors can be illustrated as shown in Figure 1.11. Each plant species has an optimal temperature and saturation points regarding light intensity and CO_2 concentration. While photosynthetic efficiency is highest at the optimal temperature, it cannot be further increased once light intensity or CO_2 concentration reaches its saturation point. As a result, the actual rate of photosynthesis corresponds to the minimum limiting rate among the three. For example, suppose a space is maintained at a CO_2 concentration below the saturation point. In that case, temperature does not need to be at its optimum and light intensity can remain below the saturation point without impacting the rate of photosynthesis. Other environmental factors, such as humidity, air speed, and irrigation, must also be maintained within acceptable ranges to avoid limiting crop growth.

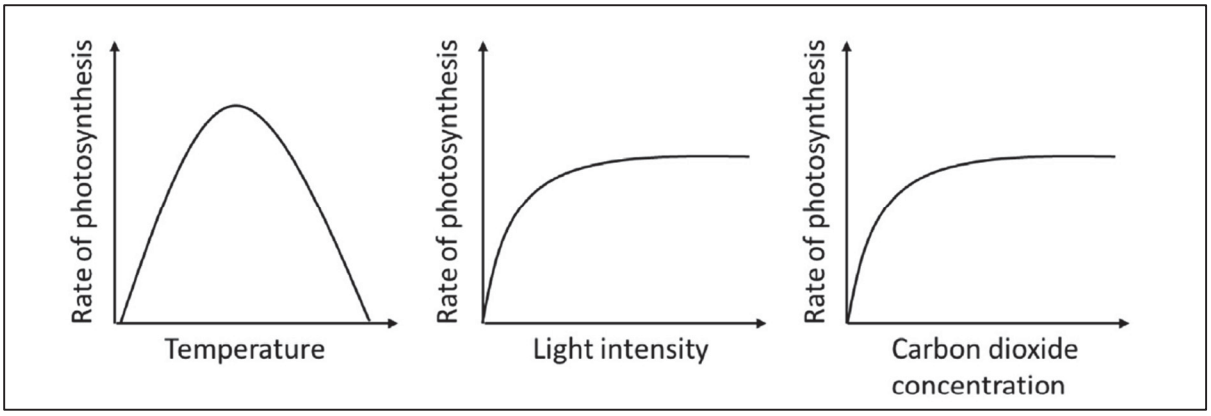

Figure 1.11 Illustration of the response of the rate of photosynthesis to temperature, light intensity, and CO_2 concentration
Taken from Li et al. (2020, p.4)

Growth models can also serve to estimate crop heat exchanges dynamically, but they require some manipulations. Models often estimate crop biomass accumulation throughout a growth cycle. Then, the leaf area (LA) can be estimated from crop biomass using a key parameter, the Specific Leaf Area (SLA), as expressed in Equation (1.6). From the LA, the LAI can then be calculated considering the crop planting density. Assuming a constant crop planting density throughout a growth cycle, LAI is lowest at the beginning of the cycle and reaches its peak at harvest.

$$LA(t) = SLA \cdot DW_{tot}(t) \quad (1.6)$$

where:

LA is the leaf area per plant, $m^2 \cdot plant^{-1}$;

SLA is the Specific Leaf Area, $m^{-2} \cdot kg$; and

DW_{tot} is the total (structural and non-structural) accumulated dry weight, $kg \cdot plant^{-1}$

SLA is not only species-specific but also varies significantly between cultivars (Kim & van Iersel, 2022). It is a growth parameter that represents the ratio of leaf area to leaf dry weight, often measured and reported in studies within the fields of plant physiology and crop science. SLA has been shown to be strongly influenced by environmental conditions, including light intensity, air and root temperatures, light spectrum, and CO_2 concentration. Certain conditions increase SLA, which may reflect larger and/or thinner leaves, while others reduce SLA, leading to smaller and/or thicker leaves. However, these changes in area and thickness do not always occur simultaneously. Specifically for cultivation in CEA spaces, Carotti et al. (2021) showed that SLA is particularly sensitive to PPFD, with air and root temperatures having a noticeable but lesser effect. Light spectrum also plays a role; for example, an increased proportion of far-red wavelengths has been shown to raise SLA (Carotti et al., 2024). For low-tech greenhouse applications, Sun et al. (2025) concluded that SLA was strongly correlated with both light intensity and relative humidity. However, it remains unclear whether relative humidity is an influential factor in CEA spaces, where humidity is typically well-controlled.

Growth modelling can follow different approaches and may incorporate one or several influential factors. Nine studies integrated a growth model, with eight applying it solely for yield estimation, without accounting for dynamic crop heat exchanges. Only the study by Song et al. (2023) used a growth model to estimate these heat exchanges dynamically as crops developed. However, none of the reviewed studies integrated a growth model for both yield estimation and dynamic crop heat exchanges.

Regarding model selection, a key takeaway is that 55% of the studies using a growth model adopted the mechanistic model developed by Van Henten (1994). This two-state variables

model is based on a carbon balance, in which the net carbon assimilation rate results from the carbon fixed through photosynthesis, minus the respiration losses for maintenance and growth. The assimilated carbon is then partitioned into structural (leaves, stems, roots) and non-structural (carbohydrates) dry matter. Non-structural dry weight serves as stored energy that can be mobilized to support growth and metabolism at later stages. Mechanistic models are especially valuable for energy and yield analysis, as they are less constrained than empirical models, making them ideal, for instance, to develop energy-efficient solutions that balance energy and yield. However, the applicability of Van Henten's model, initially validated for semi-closed greenhouse systems, to CEA-HD spaces remains uncertain.

1.3.3 CO_2 exchange

When exposed to PAR, crops perform photosynthesis, which involves converting assimilated CO_2 and water into carbohydrates and oxygen. To promote this process, it is recommended to maintain CO_2 concentrations in CEA spaces between 400 ppm and 2000 ppm using a CO_2 enrichment system, with an optimal concentration of 1000 ppm (Kozai, 2018). It is also recommended that these CO_2-enriched spaces at 1000 ppm be airtight (Kozai et al., 2015) to avoid CO_2 dilution. Therefore, HVAC&D systems should operate in recirculation mode when the space is enriched in CO_2.

From an energy perspective, modelling the CO_2 assimilation rate could be valuable for evaluating energy efficiency strategies in CEA-HD systems. Air recirculation, while necessary to avoid CO_2 dilution, is energy-intensive. Consequently, the use of outdoor air ventilation is gaining attention as a means to reduce energy consumption (Decardi-Nelson & You, 2024; Eaton et al., 2023; Song et al., 2023). However, this can either reduce crop productivity or result in substantial CO_2 wastage if CO_2 injection continues during ventilation, as reported by Decardi-Nelson and You (2024).

Beyond ventilation strategies, modelling CO_2 assimilation could also be relevant for developing synergies that improve overall system performance through heat and mass

exchange between CEA-HD spaces and adjacent spaces, buildings, or district energy systems. Opportunities include reusing CO_2-rich air from occupied spaces (Ledesma et al., 2022), recovering low-grade waste heat from the CEA-HD space (Blom et al., 2023), or sourcing CO_2 from industrial processes or combustion heating (Wang et al., 2022).

Of the 12 studies reviewed in this section, only Graamans et al. (2018) and Keyvan and Roshandel (2024) have integrated CO_2 modelling for a resource use analysis and an economic analysis, respectively. Keyvan and Roshandel (2024) used a function proposed by Graamans et al. (2018), which estimates the assimilation rate based on biomass dry weight accumulation using two factors (Equation (1.7)). The first factor is the CO_2 fixation efficiency, for which a value of 70% was used. The second accounts for the weight loss occurring during the conversion of CO_2 to carbohydrates, using a molecular weight ratio of 0.68 (Van Henten, 1994).

$$\dot{m}_{CO2} = \frac{n}{68\% \cdot 70\%} \cdot \frac{dDW_{tot}}{dt} \tag{1.7}$$

where:

$\dot{m}_{CO2}$ is the CO_2 assimilation rate, kg·hr^{-1}

n is the number of crops, plants

$\frac{dDW_{tot}}{dt}$ is the total dry weight accumulation rate, kg·plant^{-1}·hr^{-1}

Empirical models can be used to estimate the CO_2 assimilation rate based on the net photosynthetic rate. For instance, Okayama et al. (2008) proposed a plant-scale empirical model specifically tailored for controlled environment agriculture with high density (CEA-HD), using airspeed as the sole input variable (Equation (1.8)).

$$P_{cell} = 1.4 \cdot (1 - e^{-12.8s}) + 1.52 \tag{1.8}$$

where :

P_{cell} is the cell net photosynthetic rate, μmol·s^{-1}; and

s is the airflow speed, $m \cdot s^{-1}$

Separately, Jung et al. (2016) developed a canopy-scale empirical model for CEA-HD, based on two key variables: days after transplant (DAT) and ambient CO_2 concentration. This model is valid for DAT values ranging from 0 to 28 days and CO_2 concentrations between 70 and 1200 ppm. Notably, the lower bound of 70 ppm corresponds to the CO_2 compensation point, where net photosynthesis is zero (i.e., gross photosynthesis equals respiration). The model is expressed in Equation (1.9).

$$P_{canopy} = \frac{21.812 \cdot e^{-0.057DAT} \cdot e^{-0.050DAT} \cdot [CO_2]}{57.4 \cdot e^{-0.057DAT} + 0.38 \cdot e^{-0.050DAT} \cdot [CO_2]} - 18.608 \cdot e^{-0.056DAT} \quad (1.9)$$

where:

P_{canopy} is the net photosynthetic rate, $\mu mol \cdot m^{-2} \cdot s^{-1}$;

DAT is the days after transplant, days; and

$[CO_2]$ is the air CO_2 concentration in ppm.

The corresponding CO_2 assimilation rate based on the canopy net photosynthesis rate can then be estimated using Equation (1.10).

$$\dot{m}_{CO2}(t) = M_{CO2} \cdot P_{canopy} \cdot A_v \quad (1.10)$$

where:

$\dot{m}_{CO}$ is the CO_2 assimilation rate, $kg \cdot s^{-1}$;

M_{CO} is the CO_2 molar mass, $kg \cdot \mu mol^{-1}$;

P_{canopy} is the net photosynthetic rate, $\mu mol \cdot m^{-2} \cdot s^{-1}$;

A_v is the total leaf area in the space, m^2;

1.4 Literature gaps

Given the potential for improvement in SEC and productivity of existing facilities, models are essential for developing solutions that balance energy and yield in CEA-HD spaces. However, due to disparities in SEC values estimated by current models and inconsistencies in modelling approaches, it remains unclear whether these models can effectively support comprehensive energy and yield analysis. One major limitation is the widespread use of constant heat exchanges from crops, which restricts model adaptability and confines the analysis to a specific growth management method. The estimation of short-wave radiation absorbed by crops was also limited by the use of a variable, the CAC, which is constrained to a particular crop planting density. In fact, energy and yield analysis would require a model capable of operating under different growing conditions, growth management methods, and crop spacing configurations. When it comes to lighting heat gains, some studies did not distinguish between radiative and convective heat gains, while others considered specific heat fractions. These heat fractions can vary across different fixtures, and the impact of this variability on the energy load remains unclear. It was also uncertain whether light interception was accounted for in all studies, despite its importance in fulfilling the law of conservation of energy. Moreover, the impact of neglecting light interception when estimating lighting heat gains has not been quantified. Concerning heat storage in hydroponic solution, it was excluded from all studies, despite the potential impact remaining unquantified. Lastly, it is unclear whether the most adopted growth model is suitable for CEA-HD applications.

CHAPTER 2

OBJECTIVES AND METHODOLOGY

2.1 Objectives and specific objectives

The main objective of this thesis is to develop a modelling approach adapted to CEA-HD spaces for energy and yield analysis. The developed approach includes a thermal space and crop model to support analysis for a wide range of growing conditions that can be used to grow lettuces in CEA-HD spaces. The main objective relies on the following specific objectives:

(1) Exploring the impact of different modelling approaches on energy loads. The focus is on often neglected elements and, thus, assesses the impact of these simplifications. The elements are:
   a. Thermal storage in hydroponic solution
   b. Light interception
   c. Crop growth
   d. Variation in light heat fractions ($f_{conv}/f_{LW}/f_{SW}$) across LED lights

(2) Developing a dynamic crop model adjusted to cultivation in CEA-HD spaces. The developed model is integrated into a BPS tool as a component and includes an energy balance and a growth model.

(3) Assessing the impact of growing conditions on both energy and yield through a case study. The selected growing conditions are:
   a. Temperature
   b. Vapour pressure deficit (VPD)
   c. Photosynthetic photon flux density (PPFD)
   d. Photoperiod

2.2 Methodology

This section provides an overview of the general methodology of this research and summarizes the main characteristics of the articles.

2.2.1 Overview

This research focuses on CEA-HD facilities featuring vertically stacked hydroponic production systems for lettuce cultivation relying exclusively on electric lighting. A single case study is used for the whole research: the Controlled Environment Test Bench located in École de Technologie Supérieure (ÉTS). The test bench, also referred to as the BE2C, includes a three-tier hydroponic production system with a 2.8 m^2 footprint and a cultivation area of 7.5 m^2. The modelling is carried out using TRNSYS 18 simulation software (Klein & al., 2017) due to its versatility, which is well-suited for exploratory research and development of custom components. The overall methodology follows a structured, four-step process, as illustrated in Figure 2.1. Figure 2.1 also highlights key contributions of this research: the development of new TRNSYS components (available on the GitHub repository of the Thermal and Building Sciences Laboratory) and the publication of four peer-reviewed articles.

(1) The first step involved developing a basic CEA-HD space model in TRNSYS, consisting of a model of the test bench as a thermal zone, coupled with an existing crop model, a crop energy balance (Talbot & Monfet, 2020). The latter is available in the "lettuces-steady-state" folder on GitHub and referred to as *Type 209*. This model is based on the validated algorithm by Graamans et al. (2017), where the LAI and CAC are defined as fixed parameters, meaning crop size and coverage remain constant over the simulation period.

(2) The basic model was then used to fulfill the first specific objective of evaluating how different modelling approaches affect energy loads. The impact of thermal storage in the hydroponic solution and light interception on energy loads was assessed and

documented in *Article #1* (CHAPTER 3). It required building a custom component for the hydroponic solution and integrating it into the base model. Subsequently, the impact of dynamic crop growth and lighting heat fractions was assessed and documented in *Article #2* (CHAPTER 4). For this purpose, *Type 209* required some modification; LAI and CAC were changed from parameters to variable inputs. This allowed for feeding the energy balance with time series for LAI and CAC to simulate crop growth. This version, referred to as *Type 210*, is available in the "lettuces-dynamic" GitHub folder.

(3) To meet the second specific objective, the base model was used as a foundation but required deep modifications to improve its versatility, resulting in *Type 211*. This component integrates a dynamic lettuce growth model and other changes, such as dynamic air properties, a light interception sub-model compatible with various planting densities and the capability to simulate both solar and electric lighting as energy inputs to the crop energy balance. The growth model was calibrated for different growing conditions for its use in CEA-HD spaces, and this work is documented in *Article #3* (CHAPTER 5).

(4) Finally, using the developed modelling framework, a set of 180 simulation scenarios was automated to analyze how different growing conditions can influence both energy loads and yield. Scenarios were generated by combining different temperatures, VPD, PPFD and photoperiod. The analysis and findings are presented in *Article #4* (CHAPTER 6).

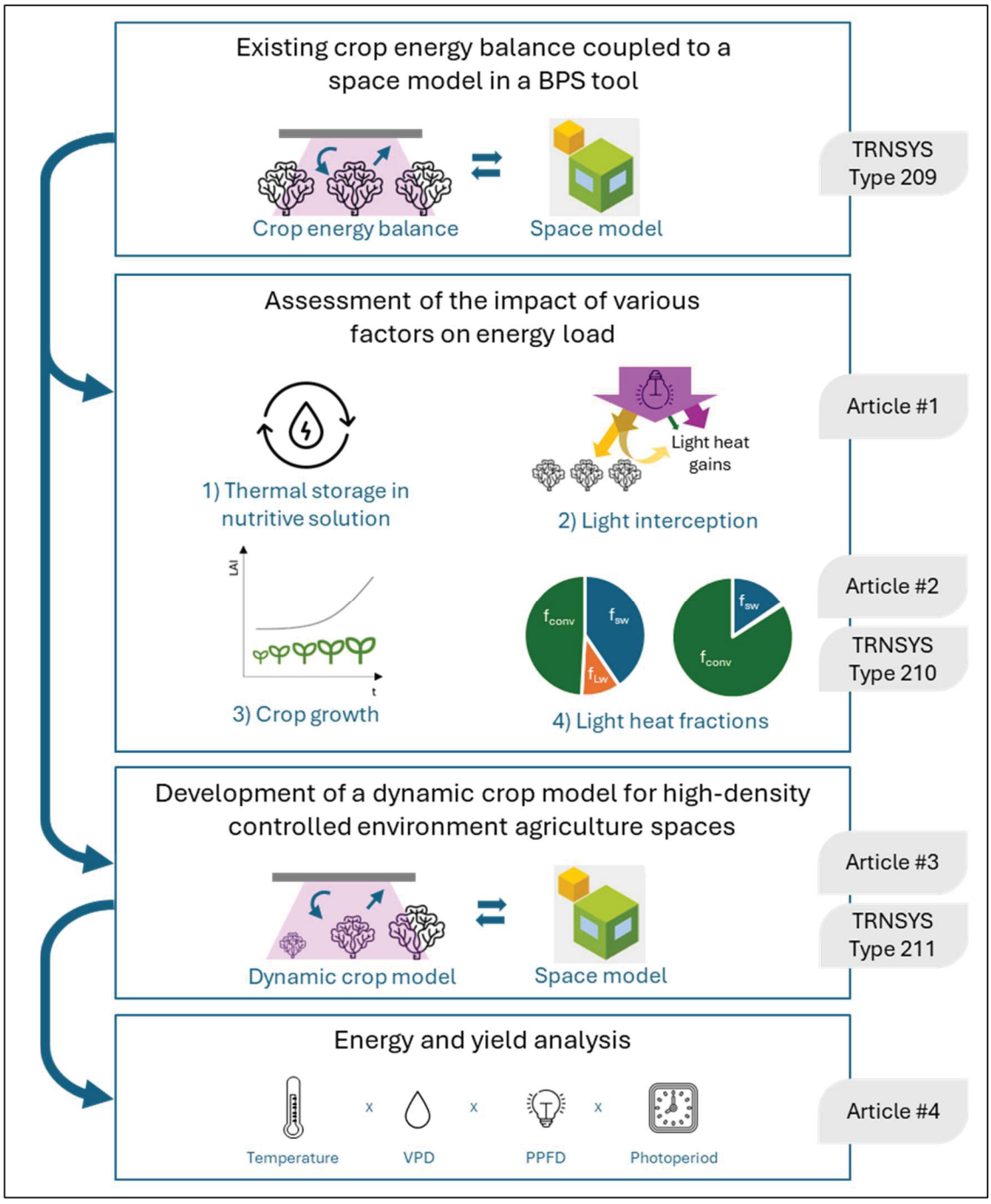

Figure 2.1 Methodology overview

2.2.2 Structure overview of the article-based thesis

This section outlines the structure of the four articles that form the outcome of this thesis, along with the TRNSYS components available on GitHub. Together, these articles address the main research objective, which is to develop a modelling approach adapted to CEA-HD spaces for energy and yield analysis. Table 2.1 summarizes, for each article, the main information and the specific research objective addressed.

Table 2.1 Overview of the structure of the article-based thesis

#	Title	Published in	Year	Spec. objective
1	*Impact of Modelling Thermal Phenomena in a High-Density Controlled Environment Agriculture (CEA-HD) Space*	Proceedings of Building Simulation 2021: 17th Conference of IBPSA, Bruges, Belgium	2021	1
2	*Estimated energy demand and sensible heat ratio of a controlled-environment agriculture space for a growth cycle*	ASHRAE Transactions, Vol. 127, Issue 2, Pages 211-219	2021	1
3	*Development of a crop growth model for the energy analysis of controlled agriculture environment spaces*	Biosystems Engineering, Vol. 238, Pages 38-50	2024	2
4	*Analysing the influence of growing conditions on both energy load and crop yield of a controlled environment agriculture space*	Applied Energy, Vol. 368, Pages 123406	2024	3

CHAPTER 3

IMPACT OF MODELLING THERMAL PHENOMENA IN A HIGH-DENSITY CONTROLLED ENVIRONMENT AGRICULTURE (CEA-HD) SPACE

Marie-Hélène Talbot[a], Danielle Monfet[a], Timothé Lalonde[a], Didier Haillot[a]

[a]École de Technologie Supérieure,
1100 Notre-Dame Ouest, Montréal, Québec, Canada H3C 1K3

Paper published in the *Proceedings of Building Simulation 2021: 17th Conference of IBPSA*, September 2021

Abstract

There is a rising interest in controlled environment agriculture (CEA) to address food security issues. Modelling of indoor high-density CEA (CEA-HD) spaces is relatively recent and often some of the thermal phenomena, such as the effect of light interception by crops leaves and the thermal storage capacity of the hydroponic solution, are assumed to be negligible. In this study, the impacts of those thermal phenomena on the energy demand and consumption of a small-scale CEA-HD space, modelled in a BPS tool, are quantified. Both phenomena are modelled and compared to a base case, for which none of the phenomena were considered. For a specific size of crops, the effect of light interception by crops leaves led to a reduction of 35% of both peak sensible cooling demand and annual consumption. The thermal storage in the hydroponic solution led to a reduction of 46% and 76% of the peak sensible heating demand and annual consumption, respectively.

Key Innovations

- Modelling of the effect of light interception by crops leaves and its influence on the space lighting heat gains, which showed a 35% reduction of the peak sensible cooling demand of an indoor CEA-HD space for a specific size of crops;

- Modelling of the thermal storage in the hydroponic solution, which showed a reduction of 76% in annual sensible heating consumption and a small reduction of 9% in annual sensible cooling consumption.

Practical implications

Based on the findings of this study, a simulation practitioner should consider the effect of light interception by crops leaves when modelling a CEA-HD space. Depending on the purpose of the simulation, the thermal storage in the hydroponic could also be considered and assumptions should be chosen with care. The proposed modelling approach can also be used to compare the performance of different HVAC systems and the energy performance of CEA-HD space.

3.1 Introduction

The integration of an indoor high-density controlled environment agriculture (CEA-HD) space to the urban environment could contribute to local food security all over the globe (Armanda et al., 2019). In extreme climates, outdoor conditions are not suitable to year-round agriculture and protected agriculture is essential to grow food locally (McCartney & Lefsrud, 2018). CEA-HD spaces are indoor spaces for which crops are grown vertically in electrically lit beds. Indoor CEA-HD leads to higher yield than agriculture in fields; however, they often have high energy demand mostly due to sensible cooling and dehumidification requirements (Graamans et al., 2018).

Modelling indoor CEA-HD spaces, where crops considered as internal heat gains/losses, is fairly new and a common approach is still missing (Waldron, 2018). Several interactions need to be considered when modelling an indoor CEA-HD space to predict the space energy demand. The CEA-HD space energy demand is mainly influenced by the heat gains/losses induced by crops and the heat gains from lighting (Talbot & Monfet, 2020). During photosynthesis, when the lights are on and cause convective and radiative heat gains, the crops induce an evaporative cooling effect (sensible heat loss combined with a latent heat gain)

caused by crop transpiration. Along with these two main thermal phenomena, additional thermal phenomena might occur in a CEA-HD space that are not always considered when the space is modelled.

The first phenomenon impacts the space radiative heat gains from lights within the space. Crops leaves intercept and absorb a part of the photosynthetic active radiation (PAR) emitted by lights and convert it into latent energy through crop photosynthesis. The portion of the PAR intercepted and absorbed by crops depends on the leaf's coverage of the cultivated area. Thus, the radiative energy intercepted and absorbed by crops reduces the space radiative heat gain from lighting. Modelling a CEA space using a building performance simulation (BPS) tool has been completed by Benis et al. (2017a), Golzar et al. (2018), Graamans et al. (2018), Harbick and Albright (2016), Kokogiannakis and Cooper (2015), Nadal et al. (2017),Ward et al. (2015), Zhang and Schulman (2017), and Zhang and Kacira (2020b). However, except for the study completed by Kokogiannakis and Cooper (2015), none have mentioned the effect of light interception by crops leaves and its impact on the space energy demand, which has not been quantified yet. The second phenomenon assesses the possible thermal storage occurring if a hydroponic production system is used.

In this study, the impacts of these two different thermal phenomena on energy demand and consumption are assessed independently and simultaneously. The modelling of these phenomena supports the identification of the acceptable simplifications to be made when modelling an indoor CEA-HD space.

3.2 Overall approach

To assess the impact of different thermal phenomena on the energy demand of an indoor CEA-HD space, a steady-state lettuce model is coupled to the space model in TRNSYS (Klein & al., 2017), a BPS tool.

The impact of each phenomenon on energy demand is assessed independently over a single day. Thus, a total of four cases are included:

1) Base case: The indoor CEA-HD space is modelled without detailed models of the selected thermal phenomena, i.e., they are considered to be negligible.
2) Light interception (LI) case: The effect of light interception by crops leaves on the space lighting heat gains is considered.
3) Thermal storage (TS) case: The thermal storage in the recirculating hydroponic solution is considered.
4) Combined case: The impacts of these two different thermal phenomena on energy demand and consumption are assessed simultaneously.

For each case, a description of the models used is provided including the main inputs and assumptions.

3.3 Base model

The base model includes a space model and a crops model. At every simulation time step, the space indoor conditions are used as inputs to the crops model to estimate the rates of heat gains/losses induced by the crops. These rates are then included as additional internal heat gains/losses to the space model as illustrated in Figure 3.1.

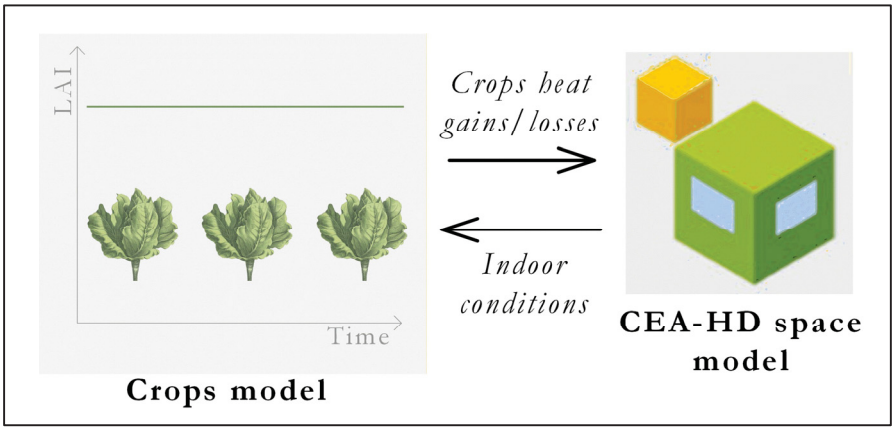

Figure 3.1 Base case model

The modelled indoor CEA-HD space is a 3.02m x 2.44m x 1.97m space located in a building maintained at an indoor temperature of 20°C. In this CEA-HD space, the crops are grown using a nutrient film technique (NFT) hydroponic system that has a 2.8 m2 footprint with a total of 30 growing channels equally distributed over three tiers with a vertical spacing of 46.5 cm, as illustrated in Figure 3.2. The production system can grow 27 lettuces/$m^2_{cultivated}$.

CEA-HD space model. The CEA-HD space is modelled with walls, floor and ceiling having an overall U-value of 0.12 W/(K·m^2), a thermal capacity of 1000 J/(kg·K), a density of 113.17 kg/m^3, and are covered with water-repellent panels to minimize migration of water vapour through the surfaces. The space is enriched in CO_2 to enhance crops growth and is airtight to avoid the dilution of the CO_2. Moreover, a forced air circulation system ensures the air is well-mixed and that there is sufficient air velocity over the leaves to facilitate gas exchange.

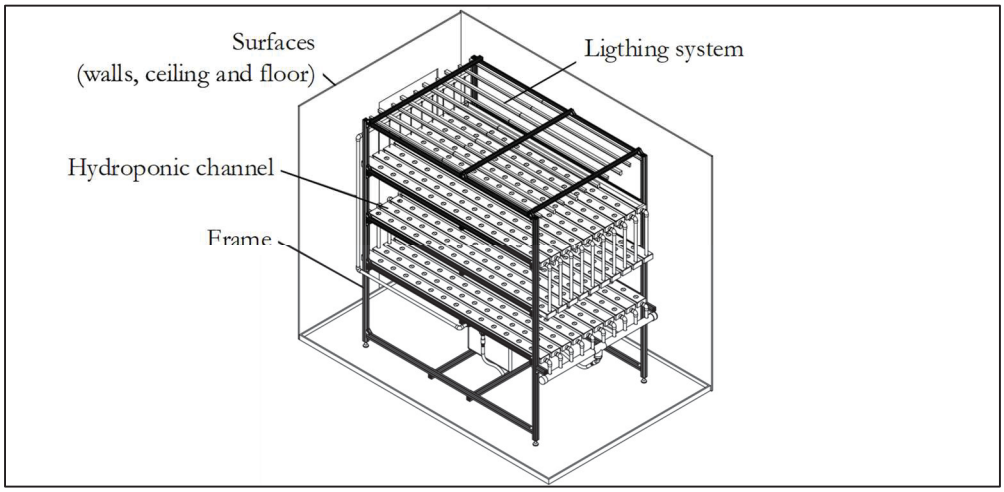

Figure 3.2 CEA-HD space

The indoor conditions and growing parameters are summarized in Table 3.1. Indoor conditions alternate between two sets of conditions that are optimal for crop growth when (1) photosynthesis occurs during the photoperiod (when the lights are on) and (2) respiration occurs during the dark period (when the lights are off).

Table 3.1 Growing conditions

Indoor conditions (photoperiod/dark period)	
Temperature	21°C / 18°C
Humidity	70% / 74%
Vapour pressure deficit	0.75 kPa / 0.54 kPa
Lighting	
Type of lamps	LED
Electric power input	144.2 W·m-2cultivated
PPFD	288.5 µmol·s-1·m-2cultivated
Photoperiod	14 hours
Heat fractions (f_{conv} / f_{LW} / f_{SW})	0.43 / 0.17 / 0.40
CO_2	700-1000 ppm

Crops model. The heat gains/losses induced by crops are modelled using a single energy balance between the crops and their environment and are computed as additional internal gains/losses to the space model. They are estimated using a steady-state lettuce model (Graamans et al., 2018) that is fully integrated to the BPS tool (Talbot & Monfet, 2020). Several factors influence the heat gains/losses induced by crops and one of them is the size of the crops that is often estimated using the Leaf Area Index (*LAI*), which is the total leaf area (*LA*) multiplied by the number of plants per unit of cultivated area (Equation (3.1)).

$$LAI = LA \cdot \frac{Number\ of\ plants}{Cultivated\ area} \tag{3.1}$$

Thus, the value of *LAI* varies with the crops stage of growth and density.

3.3.1 Light interception (LI) model

The light interception model considers the effect of light interception by crops leaves, i.e., that not all the lighting radiative energy leads to a heat gain since part of that radiative energy is intercepted and absorbed by the crops. The effect of light interception varies according to the surface covered by the crops which is influenced by the leaf area, the crop density (number of crops per unit of cultivated area), and the leaf absorption coefficient of PAR (α_{pl}). The surface covered by the crops is estimated using the Cultivation Area Cover (*CAC*), which is the

percentage of the cultivated area that is covered by the leaves. The *CAC* can be found empirically based on *LAI* (Tei et al., 1996). The leaf absorption coefficient is a parameter that is crop-specific and was set to 0.95 in this study. As illustrated in Figure 3.3, the light interception model is similar to the base case model except for one additional input, the *CAC* from the crops model, that is used by the space model.

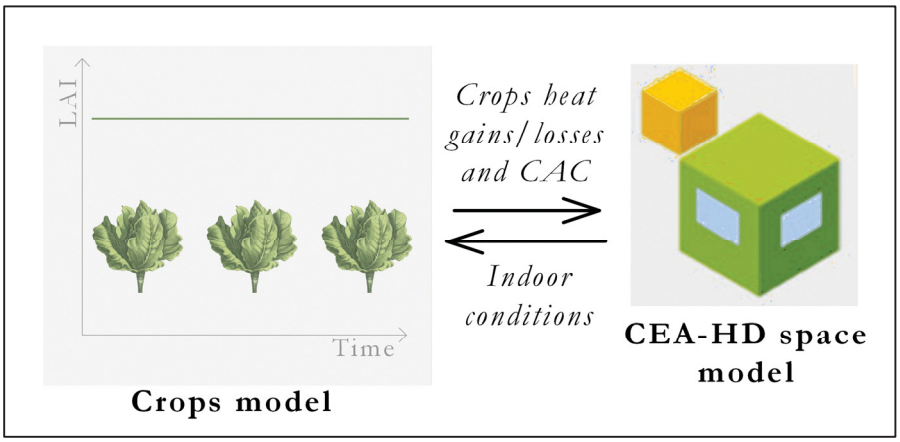

Figure 3.3 Light interception model

The indoor-face heat balance for each surface is computed according to the heat balance (HB) method (ASHRAE, 2013b) using Equation (3.2). The short-wave radiation flux to an indoor surface (walls, ceiling or floor) from lights (q''_{SW}) is equal to the electric power input of the lights (q''_{light}) multiplied by the short-wave radiative heat fraction (f_{SW}), which corresponds to the lights' efficiency. When the effect of light interception by crops leaves is considered, q''_{SW} is reduced and can be calculated according to Equation (3.3).

$$q''_{LWX} + q''_{SW} + q''_{LWS} + q''_{ki} + q''_{conv} = 0 \tag{3.2}$$

$$q''_{SW} = q''_{light} \cdot f_{SW} \cdot \left(1 - CAC \cdot \alpha_{pl}\right) \tag{3.3}$$

where,

q''_{LWX} is the net long-wave radiation flux exchange between surfaces [W/m^2];

q''_{SW} is the short-wave radiation flux to surface from lights [W/m^2];

q''_{LWS} is the long-wave radiation from equipment in zone [W/m^2];
q''_{ki} is the conductive flux through wall [W/m^2];
q''_{conv} is the convective heat flux to zone air [W/m^2];
q''_{light} is the electric power input of the lights [W/m^2];
f_{SW} is the short-wave radiative heat fraction of lights [-];
CAC is the cultivation area cover [%];
α_{pl} is the leaf absorption coefficient of PAR [-].

The effect of light interception by crops leaves is assessed for three different *LAI*:

- *LAI* = 0: Optimal indoor conditions are maintained, but crops have not grown leaves yet. Thus, there is no light interception by the crop's leaves.
- *LAI* = 2.1: Crops are grown according to a diversified stage growth method, which allows continuous harvesting, and thus, a mean value of 2.1 is maintained.
- *LAI* = 3.55: Crops reach a maximum value, and they are all grown according to a single stage growth method, which allows harvesting a larger production at the end of the growth cycle. This value corresponds to a harvested lettuce head of 243 g.

3.3.2 Thermal storage (TS) model

Thermal storage occurs in the hydroponic solution. In the studied CEA-HD, the hydroponic solution is pumped from a tank on the ground to the top tier at a flowrate of 0.67 L/s and distributed equally to the ten channels of this tier. At the end of each channel, the hydroponic solution drops into the corresponding channel placed in the mid-tier and then into the corresponding channel placed at the bottom tier. At the bottom tier, the hydroponic solution is returned to the tank using a single pipe. The thermal storage in the hydroponic solution is considered by estimating the heat exchange (gain or loss) between the hydroponic solution and the space at each time step based on the indoor air temperature. The heat exchange is then included in the space model as an input (Figure 3.4).

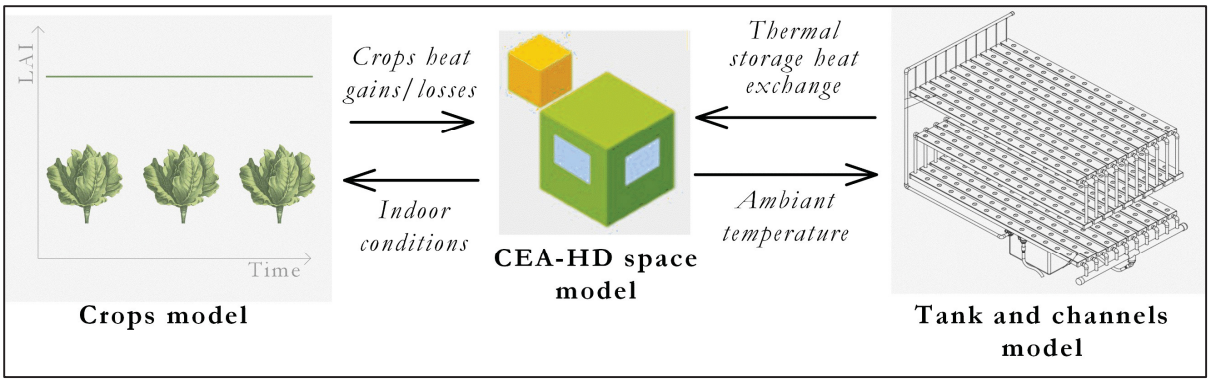

Figure 3.4 Thermal storage model

Two components that hold the hydroponic solution in a closed-loop are modelled: a cylindrical tank of 0.07 m^3 with a 0.359 m height and the channels, which are 15.6 cm wide, 2.2 m long with a maximum solution depth of 3.8 cm. It is assumed that the hydroponic solution has the thermal properties of water and the outside convective coefficient (h_o) is set to 7.22 W/(m^2·K). In the model, the following are neglected: the heat exchanged between the supply and return pipes and the space; the radiative heat exchanged between the components and the space; the impact of the roots on any possible flow turbulence in the channels; and any possible heat exchanges between the roots and the solution.

Other assumptions for the different components are listed below:

- For the tank: the bottom is insulated and the heat released by the pump to the solution is neglected. The tank is modelled using TRNSYS Type 531, which is a constant volume storage tank for which the solution held is divided into five isothermal nodes. For this application, the inlet flow stream is located at the top of the tank and the outlet flow stream at the bottom.
- For the channels: they are rectangular and there is an air gap between the hydroponic solution and the channel cover, as illustrated in Figure 3.5, this is considered to create a barrier to heat exchange and evaporation with the space. Thus, the channels are modelled using a modified version of TRNSYS Type 31 for circular pipes to account for that last particularity. Type 31 is a component used to model circular or rectangular pipes. It is a plug flow model that breaks the pipe into segments of fluid. The heat exchange with the environment and the fluid internal energy can be estimated at each time step with this component. The diameter

input is set to an equivalent diameter corresponding to the volume of the solution in the channels.

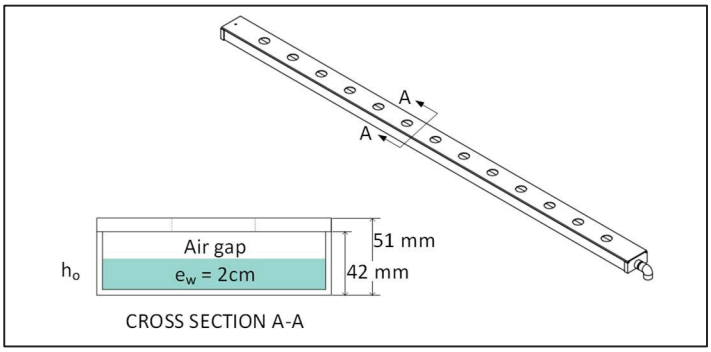

Figure 3.5 Channel cross-section detail

Three different hydroponic solution depths (e_s) in the channels of 1 cm, 2 cm and 3 cm are considered which respectively correspond to a total mass of 0.08 kg, 0.15 kg and 0.23 kg. The Reynolds number of the channels flow was also verified to ensure it is below 2100 as it has been targeted as the maximum Reynolds number to optimally grow crops using a NFT production system (Guzmán-Valdivia et al., 2019).

3.3.3 Combined model

One additional simulation is completed where all studied phenomena are included in the model.

3.4 Results

Results are presented in terms of sensible and latent energy demands for a single day for the four different cases. The simulation is completed with a timestep of 1/6 hour (10 minutes). The single day results are obtained after a 2-day warm-up period. Additionally, the impact on the annual energy demand and consumption is compared at a *LAI* of 2.1.

3.4.1 Effect of light interception by crops leaves

The sensible energy demand of the space when the effect of light interception by crops leaves for different *LAI* is considered is presented in Figure 3.6.

As expected, for a *LAI* of 0 and during the dark period, the effect of light interception is null. For a *LAI* of 2.1, the peak sensible cooling demand during the photoperiod is about 35% lower when the effect of light interception is considered. For larger crops (*LAI* of 3.55), the peak sensible cooling demand during the photoperiod is about 53% lower when the effect of light interception is considered.

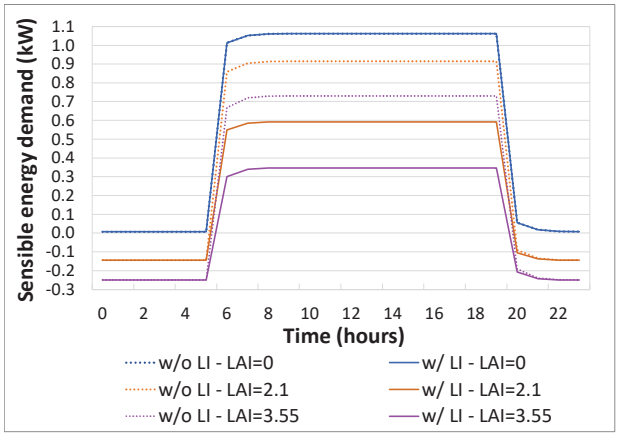

Figure 3.6 Sensible energy demand without and with the effect of light interception by crops leaves for different LAI

3.4.2 Thermal storage in the hydroponic solution

The sensible energy demand of the space when thermal storage (TS) in the hydroponic solution is considered for different solution depths is presented in Figure 3.7. When the TS phenomenon is considered, the energy demand increases gradually when the space is going from the dark period to the photoperiod and vice versa. It also lowers the sensible cooling and heating peak demands. As illustrated in Figure 7, the sensible cooling and heating peak demands are lowered

by 2% (e_s = 1 cm) to 4% (e_s = 3 cm) and by 25% (e_s = 1 cm) to 44% (e_s = 3 cm), respectively when the TS phenomenon is considered. The impact of the TS phenomenon is more significant on the peak sensible heating demand than on the peak sensible cooling demand.

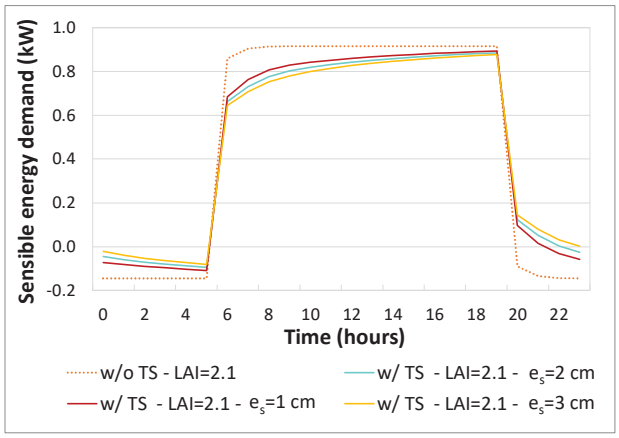

Figure 3.7 Sensible energy demand without and with the hydroponic solution thermal storage for different solution depths at LAI = 2.1

The hydroponic solution temperature in the thermal storage system also varies throughout the day and depends on the depth of the solution (Figure 3.8*).* As expected, the temperature of the hydroponic solution fluctuates between 18°C and 21°C, which are the photoperiod and dark period temperature setpoints, respectively.

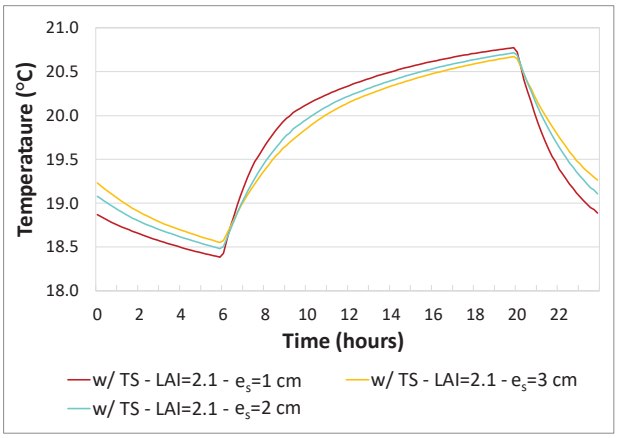

Figure 3.8 Temperature of the hydroponic solution in the thermal storage system for different solution depths at LAI=2.1

3.4.3 Combined phenomena

The sensible energy demand of the space when the effect of light interception by crops leaves and thermal storage in the hydroponic solution is considered for a *LAI* of 2.1 and a hydroponic solution depth of 2 cm is presented in Figure 3.9 as an example. The combination of the two phenomena led to more important reduction of the sensible cooling and heating energy demands. When both phenomena are considered, the sensible cooling and heating peak demands are lowered from 38% (e_s = 1 cm) to 39% (e_s = 3 cm) and from 31% (e_s = 1 cm) to 46% (e_s = 3 cm) compared to the base case, respectively.

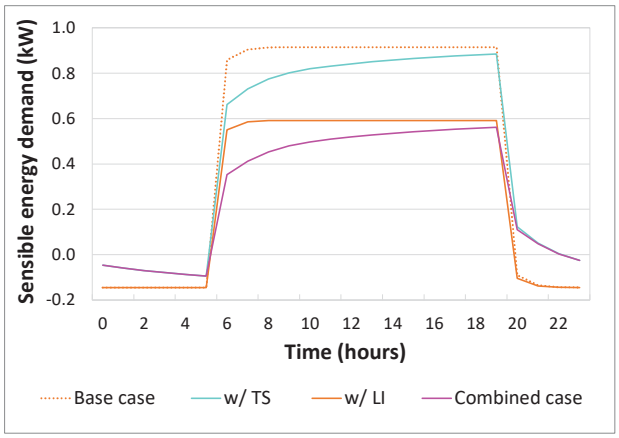

Figure 3.9 Sensible energy demand with the combined effect of the phenomena at LAI = 2.1 and solution depth of 2 cm

3.4.4 Annual overview

The peak sensible energy demand and annual consumption of the space for every case are detailed in Table 3.2, including the relative reduction compared to the base case. The total energy demand and consumption include the main energy uses of the space: lighting, sensible cooling, sensible heating, and dehumidification. For the total energy consumption, the energy use distribution is illustrated for each case in Figure 3.10. To verify the results, the annual consumption per cultivated area per end use of the base case is compared to those obtained by Graamans et al. (2018), which are for a much larger CEA-HD space having a cultivated area of 50,000 m^2. The end energy use distribution is similar, with around half of the energy use attributed to lighting. In terms of cooling and dehumidification, even if the same crops model with a fixed *LAI* value of 2.1 is used in both studies, the energy consumption is different since the setpoints, lights heat fractions, photoperiod and external gains/losses are not the same in both studies.

Table 3.2 Annual sensible and total energy demand and consumption with LAI = 2.1

	Base case	LI case	TS case			Combined case		
			e_s = 1 cm	e_s = 2 cm	e_s = 3 cm	e_s = 1 cm	e_s = 2 cm	e_s = 3 cm
Cooling								
Peak demand (W)	**915**	592	893	885	877	571	562	555
Reduction (%)	**-**	35%	2%	3%	4%	38%	39%	39%
Consumption (kWh)	**4650**	3008	4350	4283	4235	2702	2634	2586
Reduction (%)	**-**	35%	6%	8%	9%	42%	43%	44%
Heating								
Peak demand (W)	**145**	145	108	94	82	100	82	79
Reduction (%)	**-**	0%	25%	35%	44%	31%	44%	46%
Consumption (kWh)	**504**	510	234	169	121	235	169	121
Reduction (%)	**-**	-1%	54%	66%	76%	53%	66%	76%
Total								
Peak demand (W)	**2368**	2045	2346	2338	2330	2024	2015	2008
Reduction (%)	**-**	14%	1%	1%	2%	15%	15%	15%
Consumption (kWh)	**13 497**	11 870	12 928	12 795	12 701	11 289	11 156	11 061
Reduction (%)	-	12%	4%	5%	6%	16%	17%	18%

The TS phenomenon has a larger relative impact on the energy consumption than on the energy demand. The reduction reaches 76% for the sensible heating consumption compared to the base case. The largest reduction on the total energy demand (6%) and total energy consumption of the space (18%) occurs when the effect of light interception by crops leaves and the TS phenomenon with a solution depth of 3 cm are considered. Overall, the effect of light interception by crops leaves is the phenomenon that influences the most the energy use distribution of the space by reducing the sensible cooling consumption portion from 34% to 26%. This also influences the portion of the most important energy use of the space, the electrical consumption by lighting, which increases from 44% to 50%.

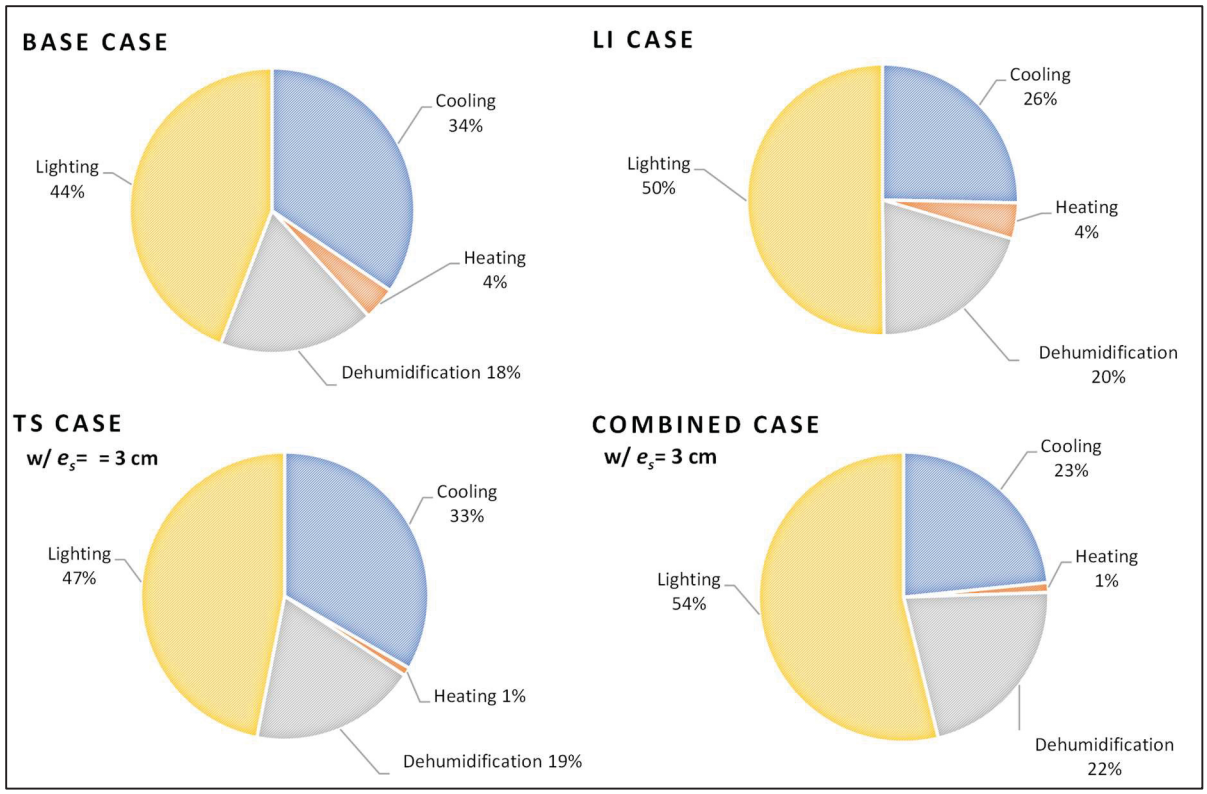

Figure 3.10 Energy use distribution of the consumption for each case with LAI = 2.1

3.5 Discussion and conclusion

The results of this study have provided a closer examination of the magnitude of the impacts of different phenomena on a small-scale indoor CEA-HD space. The results demonstrated that both thermal phenomena reduced the predicted sensible energy demand.

The effect of light interception by crops leaves is particularly important when estimating the sensible cooling energy demand of the space during photoperiod. Based on the results of this study, it would be recommended to include it to any indoor CEA-HD model, especially since it can easily be modelled by a simulation practitioner without much manipulations. The impact of the effect of light interception by crops leaves would be more important with the use of more efficient LED lights than those used in this study (f_{SW} = 40%) since a larger portion of the light-electric power input would be converted into PAR and intercepted by crops. Thus, as lights get more efficient, it is most likely that the impact of this phenomenon would increase

in scale. However, the principal limitation of the LI model is the empirical relation used to estimate the *CAC* based on *LAI* since it only applies to a density of 27 lettuces/$m^2_{cultivated}$.

For the TS phenomenon, the impact on the sensible cooling energy demand is lower than the effect of light interception by crops leaves; however, it impacts more importantly the sensible heating and cooling consumption. Modelling thermal storage in a NFT hydroponic system requires a deep understanding of the installed growing system to correctly select the outside convection coefficient between the channels and the space, and this is not a trivial task. An arbitrary value of 7.22 W/(m^2·K) was used in this study and since results showed how the TS phenomenon influence the space energy demand and consumption, a deeper fluid analysis to determine more precisely the outside convective coefficient would be a beneficial contribution to the research field. Depending on the purpose of the simulation, the practitioner could decide to consider or not the TS phenomenon. For example, to complete operating strategies analysis, a detailed portrait of CEA-HD space energy demand is essential, and the TS phenomenon should be modelled. On the contrary, if the practitioner decides to neglect it, the magnitude of the error induced could be estimated based on this study.

Since the small-scale CEA-HD space used in this study is an existing test bench that will be in operation soon, upcoming work will consist of validating the proposed models using experimental data. The study has targeted two thermal phenomena with a potential impact on space energy demand and have quantified them, which had not been done previously. The findings of this study support the development of improved modelling practices of indoor CEA-HD spaces, have identified variables to be tuned to calibrate indoor CEA-HD models and have provided an approach to predict space energy demand to depict reality more faithfully.

Aknowledgement

The authors would like to acknowledge the contribution of Olivier Boudreau-Rousseau for the 3D modelling of the CEA-HD space. The work was supported by the Fonds de recherche du Québec – Nature et technologies (Quebec, Canada), PhD scholarship for the first author.

CHAPTER 4

ESTIMATED ENERGY DEMAND AND SENSIBLE HEAT RATIO FOR A CONTROLLED ENVIRONMENT AGRICULTURE SPACE FOR A GROWTH CYCLE

Marie-Hélène Talbot[a], Danielle Monfet[a]

[a]École de Technologie Supérieure,
1100 Notre-Dame Ouest, Montréal, Québec, Canada H3C 1K3

Paper published in *2021 ASHRAE Transactions*, June 2021

Abstract heading

Growing food in controlled-environment agriculture (CEA) spaces have made year-round food production possible in cold climate and urban areas. However, designing and operating heating, ventilation and air conditioning (HVAC) systems required to maintain the indoor growth conditions (temperature, humidity, carbon dioxide (CO_2) concentration and light intensity) is still challenging since the sensible heat ratio (SHR) can significantly vary between the photoperiod and the dark period as well as throughout the growth cycle. In this study, the energy demand and the SHR of a small high-density CEA (CEA-HD) space is estimated for a growth cycle using a building performance simulation (BPS) tool. The results are presented for two types of light-emitting diode (LED) lamps as well as for two different crops (lettuces) models, an existing steady-state lettuce model and a modified version of that existing model that includes a crop growth model (dynamic model). For the LED lamps, the impact on the energy demand is assessed for different heat fractions (short-wave radiative / long wave radiative /convective) for high electrical efficiency (HEE) and low electrical efficiency (LEE) lamps. The results showed that the energy demand is influenced significantly by the heat fractions of the LED lamps and the stage of growth of the crops. The sensible cooling demand

is more important in the second part of the growth cycle for the LEE LED lamps, which have a higher convective heat fraction. This is explained by the fact that as the crops grow, the leaves absorb (and convert) more short-wave radiation thus, lowering the lamps heat gains in the space. Also, the SHR of the space during photoperiod in the second part of the growth cycle is 70% (HEE lamps) and 47% (LEE lamps) lower than the SHR in the first part of the cycle. The use of a crop growth model is more suitable to predict the sensible and latent energy demand of a CEA space in operation, while a steady-state model could be appropriate to complete load calculation.

4.1 Introduction

Controlled-environment agriculture (CEA) offers many advantages, including yields ranging from fifteen (greenhouse) to nearly one hundred (high density spaces) times more than field cultivation and the ability to produce year-round, even in harsh conditions (Kozai et al., 2015). This higher yield is possible by maintaining specific indoor environmental conditions - temperature, humidity, CO_2 concentration, light intensity (spectrum and duration) - to enhance crop growth. Different types of production systems can be held in a CEA space; however, this study focuses on high-density CEA (CEA-HD) spaces where crops are stacked vertically in multi-tier hydroponic growing beds under electrical lighting.

In CEA-HD spaces, the indoor conditions for crop growth are maintained using HVAC and other systems. However, designing and operating HVAC systems for CEA-HD spaces are challenging and the design and operating criteria to be considered are sparse (Jonlin & Lewellen, 2017). The main challenge lies in the difficulties of maintaining the temperature and humidity setpoints, without any major fluctuations, using a single HVAC system for very different sensible heat ratios (SHR), which is the sensible heat demand divided by the total heat demand, that occurs in a CEA-HD space. If the humidity setpoint is not maintained, it could increase crop transpiration (when the relative humidity is too low) or it could lead to proliferation of fungi (when the relative humidity is too high). Since CEA-HD spaces are usually airtight, their energy demand is driven by two main internal sources: the gains from

lighting and the gains/losses induced by the crops (Talbot & Monfet, 2020). Heat gains from lighting are radiative (long-wave and short-wave) and convective, while crops induce evaporative cooling through transpiration (Davis & Hirmer, 2015). The contribution from internal sources to the CEA-HD spaces leads to high sensible cooling and latent cooling (dehumidification) demands (Graamans et al., 2018; Lalonde et al., 2019). However, estimating the horticultural lighting heat gains and heat gains/losses induced by the crops is not simple for the following reasons:

- the heat fractions of the horticultural LED lights, which correspond to the distribution of the heat that is generated by lamps into radiative (short-wave and long-wave) and convective heat gains, are required and usually not specified by the lamp manufacturers;
- a model based on an energy balance between the crops and the indoor environment, including a crop growth model, is required.

Building performance simulation (BPS) tools can support the design and allow the analysis of many scenarios. During the design phase, they can be used to complete load calculation by considering the heat gains/losses induced by the crops (Talbot & Monfet, 2020). They can also support the analysis of different operating strategies and their impact on HVAC systems performance by considering the variation in the SHR of the space when the lights are turned on and off as well as the changes that occur with crop growth. However, modelling CEA spaces that consider the gains/losses induced by the crops is still relatively recent and a concerted modelling approach is still missing (Waldron, 2018). Furthermore, a steady-state model is often used to estimate the impact of crops on the energy demand of a CEA-HD space, which overlooks the impacts induced by crop growth.

In this paper, the impacts on the estimated energy demand and SHR of the heat fractions of light-emitting diode (LED) lamps and crop growth for a small-scale CEA-HD space are assessed. This is achieved by estimating the energy demand and the SHR of the small-scale CEA-HD space for a growth cycle using a building performance simulation (BPS) tool, TRNSYS (Klein & al., 2017). The results are presented for two types of LED lamps with different heat fractions as well as for two different crops (lettuces) models, an existing steady-

state lettuce model and a modified version of this first one that includes a crop growth model (dynamic model). The results illustrate some of the challenges met during the operation of a CEA-HD space and propose an approach that leads to better predictions of the SHR to support the design process.

4.2 Methodology

The energy demand and SHR of the small-scale CEA-HD space are estimated and the impact of two variables – the heat fractions of LED lamps (high electrical efficiency (HEE) and low electrical efficiency (LEE)) and crops model (steady-state and crop growth) – are assessed. A total of four simulations are completed as illustrated in Table 4.1.

Table 4.1 Combination of the studied variables

Heat fractions of LED lamps / Crop model	1 - HEE	2 – LEE
A- Steady-state	Simulation HEE/S	Simulation LEE/S
B- Growth	Simulation HEE/G	Simulation LEE/G

For the four simulations, the small-scale CEA-HD is modelled and includes a lettuce model coded as a TRNSYS component. For Simulations HEE/S & LEE/S, the steady-state lettuce model used is based on the algorithm proposed by Graamans et al. (2017), while for Simulations HEE/G & LEE/G, a dynamic lettuce model that includes a growth model (Shimizu et al., 2008) is used as illustrated in Figure 4.1. At every simulation time step, the CEA-HD indoor conditions are used in the crop model to estimate the rates of heat gains/losses induced by the crops. These rates are then integrated as additional internal gains/losses to the CEA-HD model.

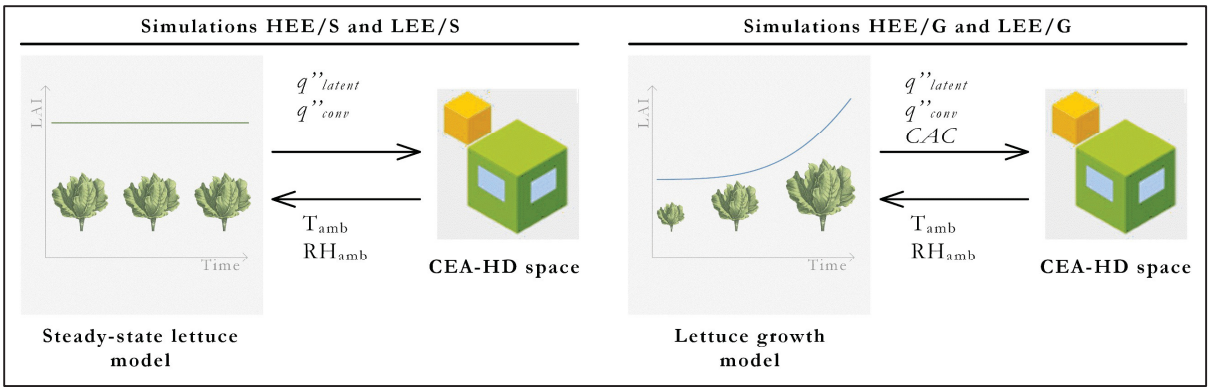

Figure 4.1 Overview of the modelling approach used for Simulations HEE/S & LEE/S (to the left) and Simulations HEE/G & LEE/G (to the right)

The modelled CEA-HD space is a 3.02m x 2.44m x 1.97m (9'11"x 8' x 6'6") space located in a building maintained at an ambient temperature of 20°C (68°F). A vertical hydroponic stacking system with a 2.8 m2 (30.1 ft^2) footprint and three tiers with 46.5 cm (18 in) vertical spacing is installed in the space as illustrated in Figure 4.2. The walls, floor and ceiling of the CEA-HD space have an overall U-value of 0.12 W/(K·m^2) (0.02 BTU/(hr·°F·ft2)), a thermal capacity of 1000 J/(kg·K) (0.239 BTU/lb·°F), a density of 113.17 kg/m3 (7.06 lb/ft^3) and are covered with water-repellent panels to minimize migration of water vapour through the surfaces. The space is enriched in CO_2 to enhance crops growth and is airtight to avoid the dilution of the CO_2. Moreover, a forced air circulation system ensures the air is well-mixed and a sufficient air velocity over the leaves to facilitate gas exchange. The indoor conditions and growing parameters are summarized in Table 4.2. Indoor conditions alternate between two sets of conditions that are optimal for crop growth when (1) photosynthesis occurs during the photoperiod (when the lights are on) and (2) respiration occurs during the dark period (when the lights are off).

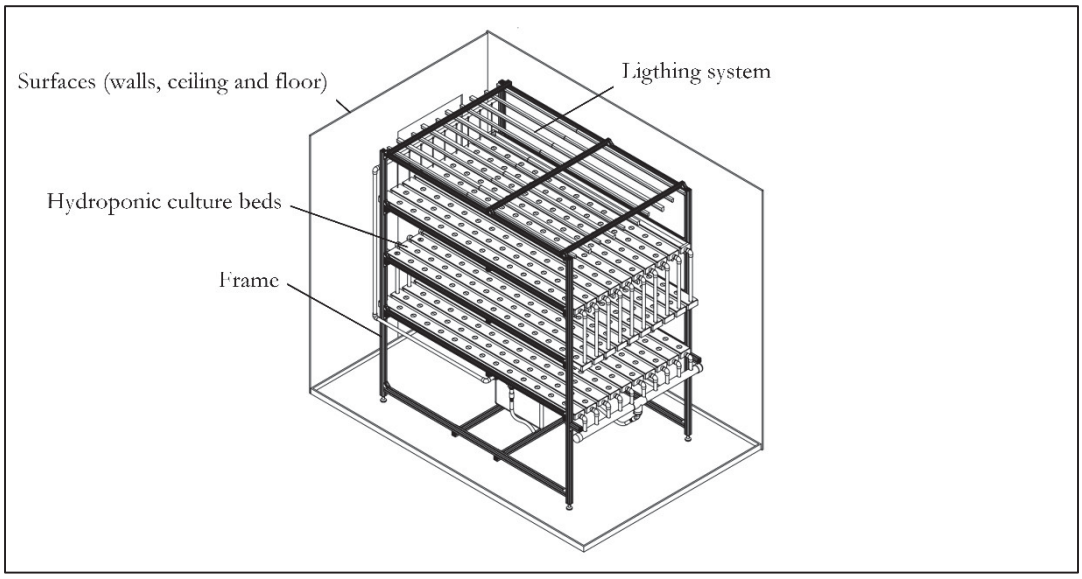

Figure 4.2 Small-scale CEA-HD space

Table 4.2 Indoor environmental conditions and growing parameters

Temperature (photoperiod/dark period)	21°C/18°C (69.8°F/64.4°F)
Relative humidity (photoperiod/dark period)	70%/74%
Lighting	
Type of lamps	LED
Electric power input	144.2 W/m^2
Photoperiod	14 hours
CO_2	700 – 1000 ppm

4.2.1 Heat fractions of the LED lamps

Most horticultural LED lamps manufacturers specify the electric power input (W), the photosynthetic photon flux (PPF) (µmol/s) and the efficacy (µmol/J), which is the ratio between the PPF (umol/s) and the electric power input (W). Some also specify the electric efficiency (or short-wave heat fraction), which is the ratio of the short-wave radiant power to the electric power input. The electric efficiency can be calculated by dividing the efficacy by the maximum efficacy, which depends on the LED specific spectrum (Kusuma et al., 2020). For the studied CEA-HD space, only the total electric power input of the installed LED lamps is available. Thus, the impact of two different types of LED lamps (HEE and LEE) is assessed.

The heat fractions (short-wave radiative / long-wave radiative / convective) for the HEE (Simulations HEE/S or /G) and LEE (Simulations LEE/S or /G) LED lamps are based on experimental values for regular LED lamps (Liu et al., 2017) and are respectively 0.405/0.104/0.491 and 0.154/0.005/0.841.

4.2.2 Crop models

Heat gains/losses induced by crops can be modelled using a single energy balance between the crops and their environment (Figure 4.3), while the size of the crops can be estimated using the Leaf Area Index (LAI), which is the leaves area of a single crop (LA) multiplied by the number of crops per unit of cultivated area. For the steady-state model, the model used is one that has previously been validated in an electrically lit CEA space (Graamans et al., 2018) and is fully integrated to the BPS tool (Talbot & Monfet, 2020). For this model, the LAI value must be estimated, which is arbitrary and varies according to the growth management method. In this study, the LAI is set to 2.1, which is based on crops being grown using a diversified stage crop growth management method (Graamans et al., 2018).

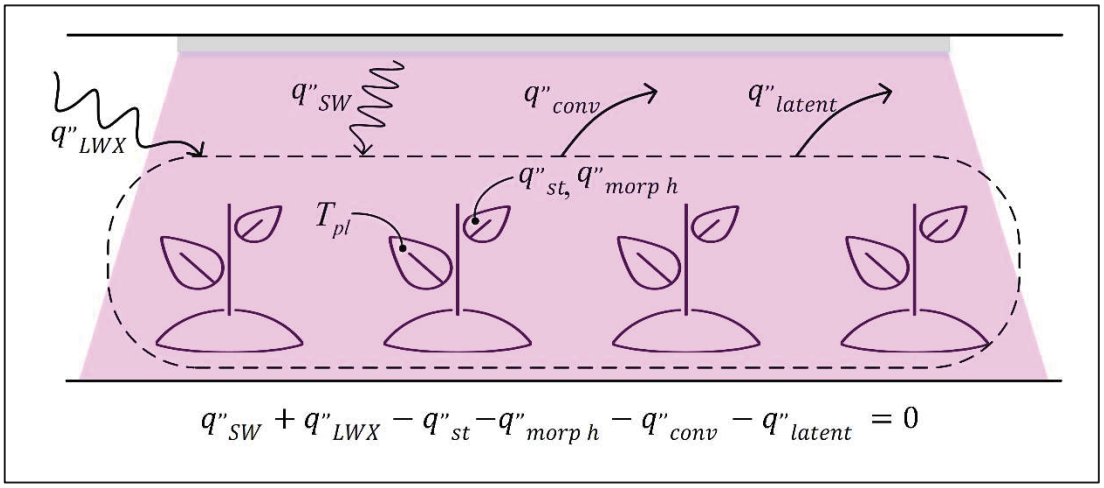

Figure 4.3 Crop energy balance: control volume and equation
Adapted from Talbot and Monfet (2020, p.1449)

The crop growth model is a modified version of the steady-state model. It is based on the model proposed by Shimizu et al. (2008) that calculates the fresh weight of lettuces head hourly until it is harvested. In this case, the LAI is determined from the fresh weight at each time step using the Specific Leaf Area (SLA) and the crops density (number of plants per unit of cultivated area). In this study, the fresh weight of a lettuce head is set to 243 g (0.54 lb) at its harvest of 30 days for a crop density of 27 lettuces/m^2 (2.5 lettuces/ft^2). As crops grow, the cultivation area cover (CAC) increases, which is the percentage of the cultivated area that is covered by the leaves. The CAC values are estimated according to the correlation proposed by Tei, Scaife, and Aikman (1996), which is a function of LAI and only valid for a density of 27 plants per unit of cultivated area. Table 4.3 presents an overview of the growth parameters used to complete the analysis.

Table 4.3 Studied growth parameters

Simulation	**LAI**	**CAC**
Steady-state (simulations HEE/S & LEE/S)	LAI = 2.1	CAC = 0.81
Growth (simulations HEE/G & LEE/G)	LAI = f (SLA, LA, density,time, FW)	CAC = f (LAI)

4.3 Results and discussion

The estimated energy (sensible and latent) demand and the SHR of the small-scale CEA-HD are illustrated in Figure 4.4 and Figure 4.5. A positive and negative sensible demand means that the space has, respectively, a sensible cooling demand and a sensible heating demand. A positive and negative latent demand means that the space has, respectively, a dehumidification demand and a humidification demand. Depending on the magnitude of the demands, it might be more economical to let the indoor conditions float around the indoor setpoints. The estimated energy demands are mainly influenced by the gains from lighting and gains/losses induced by the crops. The impact of external sources (conduction through envelope) is minimal.

4.3.1 Impact of heat fractions of the LED lamps

The impact of the LED lamps heat fractions is assessed by comparing the results for HEE and LEE lamps as illustrated in Figure 4.4 and Figure 4.5 by full lines and dotted lines, respectively. During photoperiods, for the steady-state crop model, less sensible cooling demand (-23%) and more dehumidification demand (+37%) are needed when HEE lamps are used than for LEE lamps. For the HEE lamps, the part of the lights electric power input that is short-wave radiation and captured by crops and converted into latent energy through photosynthesis is higher. Consequently, the lighting sensible heat gains are lower and latent heat gains/losses induced by crops are higher for HEE lamps compared to LEE lamps. Similarly, the SHR during photoperiod is lower for HEE lamps compared to LEE lamps. During the dark periods, the heat fractions of the LED lamps have no influence since the lights are off.

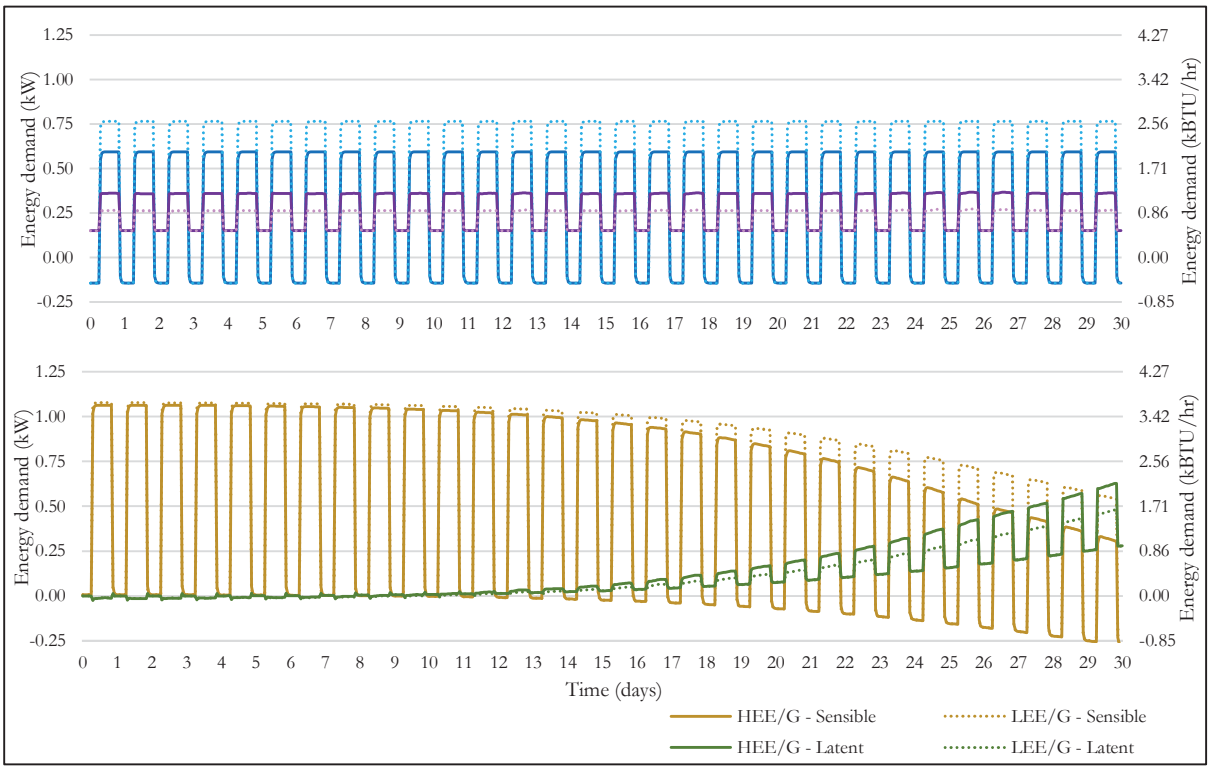

Figure 4.4 Estimated sensible and latent energy demand of a small-scale CEA-HD with HEE and LEE LED lamps using a steady-state crop model and a crop growth model

During photoperiods, for the crop growth model, the difference between using HEE or LEE lamps is minimal for the first 15 days of the growth cycle: the sensible cooling demand is 1% to 4% higher when LEE lamps are used compared to HEE lamps. In the first part of the growth cycle, the leaves of the crops are small (maximum LAI value of 0.3) and the gains/losses induced by the crops are low compared to the lighting heat gains. Thus, for this portion of the growth cycle, it is the lighting heat gains that drive the energy demand, which depends on the heat fractions of the LED lamps. During the last 15 days of the growth cycle, the leaves of the crops grow exponentially, and the sensible cooling demand is lower (from -4% to -43%) when HEE lamps are used compared to LEE lamps. This is explained by the increase of CAC as the leaves of the crops are getting larger (maximum LAI of 3.5), leading to more short-wave radiation being captured by the leaves and converted into latent energy. A similar trend is noticed for the variation in the SHR of the space. During the first 15 days of the growth cycle, not much difference is noticed. However, in the second part of the growth cycle, the difference is more important. On the last day of the cycle, the SHR is 38% lower when HEE lamps are used compared to LEE lamps, which is explained by the difference in the heat fractions of the LED lamps.

4.3.2 Impact of crop growth

The impact of crop growth is assessed by comparing the results for the steady-state model and the crop growth model as illustrated in Figure 4.4 by the blue and purple lines (steady-state) and the yellow and green lines (growth) and in by the orange lines (steady-state) and the cyan lines (growth). Several significant differences are noticed when a steady-state crop model versus a crop growth model is used to estimate the energy demand and SHR of a CEA-HD space. When a steady-state crop model is used (simulations HEE/S or LEE/S), the estimated sensible and latent energy demand and SHR are the same one day after another. During photoperiods, the estimated SHR is 0.6. During dark periods, when the lights are off, the gains/losses induced by the crops drive the space energy demand leading to dehumidification being needed as well as heating to balance the cooling effect of the crops.

However, when a crop growth model is used (simulations HEE/G or LEE/G), the changes in demand are influenced by a combination of factors. First, the energy demand during photoperiod and dark period varies hourly as the crops grow instead of being constant. For simulation HEE/G, there is a sensible cooling demand as well as a negative latent demand, meaning humidification is required to maintain the indoor air conditions during the photoperiods of the first 8 days. Past the 8-day mark, there is still a sensible cooling demand but the latent energy is now positive; thus, dehumidification is required. As the crops grow, the sensible cooling demand decreases and the dehumidification demand increases. These changes lead to a SHR that changes significantly with the crop growth. For example, the mean SHR on the 9th day of the growth cycle is 0.99, while being 0.33 for HEE lamps and 0.53 for LEE lamps on the last day of the growth cycle (30th day). This variation in SHR over the production cycle, as well as on a daily basis, is particularly challenging to be handle by a single HVAC system. When the designed HVAC system is not able to operate at lower SHR value, a stand-alone dehumidification system is needed. During dark periods, for the first 13 days, the dehumidification demand is under 10 W (34 BTU/hr) and the sensible cooling demand is very low ±10 W (34 BTU/hr): for the first 10 days cooling is required, while for the next three days, sensible heating is required. Then, as the crops grow, the sensible heating and dehumidification demand increases.

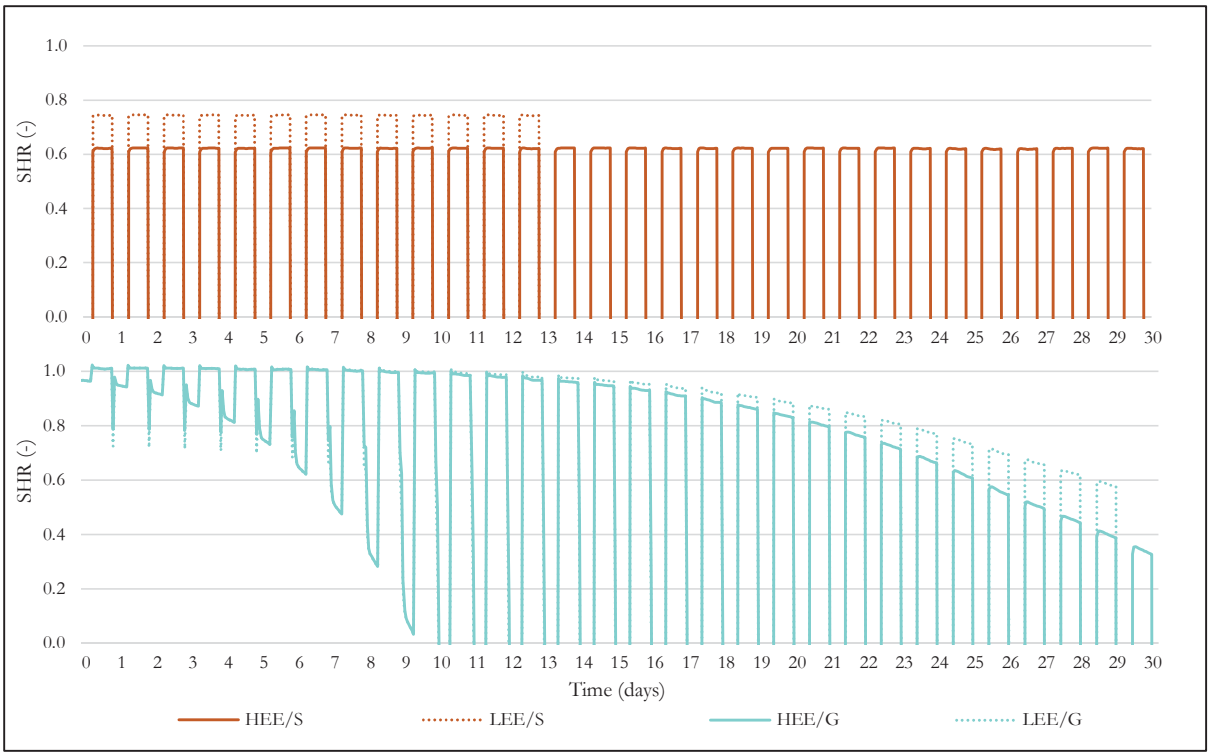

Figure 4.5 Sensible heat ratio of a small-scale CEA-HD with HEE and LEE LED lamps using a steady-state crop model and a crop growth model

The use of a steady-state crop model is a convenient simplification, but depending on the purpose of the analysis completed, might not be appropriate. For load calculation, the use of a steady-state model combined with the right design conditions and parameters is appropriate. However, the use of a growth crop model is more appropriate to dress a more detailed portrait of the energy demand of the CEA-HD space and support the analysis of different operating strategies as it represents the reality more faithfully.

The main limitation of the current study lies with the crop growth model selected to complete the analysis. First, the fresh weight at the 30th day of the cycle has to be specified, which depends on the indoor environmental conditions. Second, the model is valid for photosynthetic photon flux density (PPFD) values between 140 and 200 µmol/(s·m^2), which was not the case for the LED lamps used in this study. The hypothetical heat fractions of the LED lamps were 292 µmol/(s·m^2) and 110 µmol/(s·m^2) for the HEE and LEE lamps, respectively. However, the

results still illustrated how different heat fractions of the LED lamps could influence the energy demand of a CEA-HD space.

4.4 Conclusion

In this paper, the impacts on the estimated energy demand and SHR of the heat fractions of LED lamps and crop growth for a small-scale CEA-HD space were assessed. The results obtained by modelling the small-scale CEA-HD space in a BPS tool showed that both the heat fractions of LED lamps and crop growth significantly influenced the energy demand and SHR of the space. The results highlighted that: (1) the heat fractions of horticultural LED lamps need to be specified by manufacturers and (2) crop growth needs to be considered when estimating the energy demand and the SHR of a CEA-HD space. The impact of the heat fractions of the LED lamps during the photoperiod was more significant in the second part of the growth cycle. In terms of crop model, the use of a steady-state crop model was compared to a more complicated approach that calculates the stage of growth according to a growth model. The use of a steady-state model to estimate energy demand showed differences in the obtained results compared to when a crop growth model was used. The modelling of CEA-HD space would be improved with more precise heat fractions of horticultural LED lamps and the use of a crop growth model. Even though a steady-state crop model with a static stage of growth is appropriate to complete load calculations, a modelling approach that can show how energy demand varies daily and throughout a growth cycle is of prime importance to address HVAC system operation issues.

Acknowledgements

The authors would like to acknowledge the Fonds de recherche du Québec – Nature et technologies (Quebec, Canada) who are funding one of the authors as a PhD candidate.

CHAPTER 5

DEVELOPMENT OF A GROWTH MODEL FOR THE ENERGY ANALYSIS OF CONTROLLED AGRICULTURE ENVIRONMENT SPACES

Marie-Hélène Talbot[a], Danielle Monfet[a]

[a]École de Technologie Supérieure,
1100 Notre-Dame Ouest, Montréal, Québec, Canada H3C 1K3

Paper published in *Biosystems Engineering*, February 2024

Abstract

In controlled environment agriculture spaces, the conditions fluctuate between photoperiod and dark period, with crops growing continuously. As crops grow, their impact on the energy demand and energy use, often estimated using a building performance simulation tool, becomes more prominent. In this paper, a dynamic crop model integrated into a building performance simulation tool is proposed to estimate the yield and heat gain/loss from crops by combining a growth model and an energy balance model of the crops. The developed growth model is an adjusted version of a greenhouse lettuce growth model modified for high-density controlled environment agriculture applications by calibrating the sensitive parameters for several indoor environment conditions (temperature, lighting, etc.) using an experimental growth dataset. The yield, the energy demand and the energy use were assessed for a case study modelled in TRNSYS. The results obtained using the greenhouse and developed growth models were compared to those generated with the experimental growth dataset. Depending on the indoor environment conditions, the difference in specific energy use estimated using the experimental growth dataset and the developed model varied between 0.1% and 3.5%, indicating that the model led to an acceptable level of accuracy. The dynamic crop model estimates yield and heat gain/loss from crops for various indoor environment conditions, which are essential for carrying out energy, financial, and environmental analyses.

Keywords: Controlled environment agriculture, Crop growth, Heat gain/loss from crops, TRNSYS, Energy use

Highlights

- Existing crop growth model overestimates growth in controlled agriculture spaces.
- A calibrated grey-box mechanistic crop model is proposed.
- Crop growth and dynamic heat exchanges are integrated to a building simulation tool.
- The model is applicable to various indoor environment conditions.
- This approach supports analyses that balance both yield and energy consumption.

5.1 Introduction

Controlled environment agriculture (CEA), such as stand-alone agricultural building (greenhouse, plant factory, vertical farm, container farm) or building-integrated agriculture (BIA) (rooftop greenhouse, BIA space with electric and natural lighting), is a promising strategy for year-round crop production. When the crops are stacked vertically, these spaces can be classified as high-density CEA spaces, also known as indoor plant environments without sunlight or vertical farms. These are suitable for local production in cold climates and dense urban areas. High-density CEA spaces enhance crop growth by maintaining specific indoor environmental conditions – temperature, humidity, carbon dioxide (CO_2) concentration, lighting intensity, spectrum, and duration. Protecting the crops from the outdoors while providing optimal growing conditions improves the yield significantly. Still, it also leads to high energy consumption, primarily due to lighting, cooling and dehumidification.

Various indoor environment conditions and novel growing approaches are constantly explored to enhance yield without jeopardising nutritional quality. For example, under high photosynthetically active radiation (PAR) levels and optimal nutrient uptake, the cultivation cycle to obtain 250 g lettuce head can be as low as 18 days (Carotti et al., 2021). However, when searching for the best growing conditions, the impact of the explored conditions on

energy consumption is rarely assessed, as the focus is mostly on yield and quality. Consequently, designing and operating CEA spaces that balance yield and energy consumption is challenging. To address those issues, energy modelling can be used to support the analysis of complex thermal processes of CEA operation, such as evaluating different energy-efficient operation strategies (Iddio et al., 2020). To enhance the energy analysis of CEA spaces by estimating yield and energy consumption, the modelling of a CEA space, often completed using a building performance simulation (BPS) tool, must incorporate the heat exchanges between the crops and their environment, the heat/gain from crops, as the crops grow (El Ghoumari et al., 2005).

A limited number of studies have considered yield and crops as additional internal gain/loss in a BPS tool, and their characteristics, including the different approaches, are compiled in Table 5.1.

Benis et al. (2017b), Graamans et al. (2018), and Zhang and Kacira (2020b) selected a mechanistic growth model to assess yield but calculated the heat gain/loss from crops independently using a fixed leaf area index (LAI) or fixed evaporation rate. The LAI is a dimensionless variable defined as the total one-sided area of photosynthetic tissue per unit of ground surface area (Watson, 1947). Ward et al. (2015), Jans-Singh et al. (2021), and Talbot et al. (2022) selected a mechanistic growth model to estimate dynamic heat gain/loss from crops. On the other hand, Talbot and Monfet (2021), Ledesma et al. (2022), Yeo et al. (2022), and Song et al. (2023) chose an empirical growth model to estimate dynamic heat gain/loss from crops.

Thus, energy analysis completed using a BPS tool must include modelling crop growth and the heat exchanges between crops and their environment. Furthermore, it must also consider the impact of light interception by crops on lighting heat gain. An overview of modelling approaches for each of these phenomena is provided in sections 5.1.1 to 5.1.3.

Table 5.1 Characteristics of studies that incorporated crops as an additional internal gain/loss in a BPS tool and growth model to model a CEA space

Reference	BPS tool	Space Type[1]	Crop Type	Type of growth model	Dynamic heat gain/loss from crops
Ward et al. (2015)	TRNSYS	RTGH	Tomato	Mechanistic model (Vanthoor et al., 2011)	☑
Benis et al. (2017b)	EnergyPlus	RTGH BELO BENL	Tomato	Mechanistic model (Vanthoor et al., 2011)	
Graamans et al. (2018)	EnergyPlus	GH PF	Lettuce	Mechanistic model (Van Henten, 1994)	
Zhang and Kacira (2020b)	EnergyPlus	PF	Lettuce	Mechanistic model (Van Henten, 1994)	
Talbot and Monfet (2021)	TRNSYS	BELO	Lettuce	Empirical model (Shimizu et al., 2008)	☑
Jans-Singh et al. (2021)	EnergyPlus	BENL	Lettuce	Mechanistic model (adaptation of Vanthoor et al. (2011) to lettuce)	☑
Ledesma et al. (2022)	EnergyPlus	RTGH	Lettuce	Empirical model based on data from Fraile-Robayo et al. (2017)	☑
Talbot et al. (2022)	TRNSYS	CF	Lettuce	Mechanistic model (Van Henten, 1994)	☑
Yeo et al. (2022)	TRNSYS	RTGH	Tomato	Empirical model discretised in seven stages of growth	☑
Song et al. (2023)	EnergyPlus	CF	Lettuce	Empirical model	☑

[1] Stand-alone spaces | PF: Plant factory, CF: Container farm, GH: Stand-alone greenhouse
Building integrated agriculture (BIA) spaces | BELO: BIA space with electric lighting only, BENL: BIA space with electric and natural lighting, RTGH: Rooftop greenhouse

5.1.1 Modelling the crop growth

Crop growth is influenced by air temperature, light intensity and CO_2 concentration. As crops grow, physiological variables such as root and shoot dry weights, water mass and leaf area change over time. The fluctuation of those variables can be predicted using either empirical or mechanistic models. The different models predict growth from a transplant to a harvest size for lettuces. Empirical models use one or many functions that are developed through data fitting. Those functions are easy to implement, but their application is generally limited. They can be bound to one set of growing conditions or a range of growing conditions. Shimizu et al. (2008) have developed a growth model applicable to lettuces growing at a wide range of CO_2

concentrations (400 and 1200 ppm) and a narrow range of lighting intensities (140–200 μmol $m^{-2}·s^{-1}$), but with all of the other conditions being fixed. Hang et al. (2019) have developed a growth model that can use different air temperatures and lighting intensities as inputs, but that was validated over a limited set of conditions, such as low CO_2 concentration. Growth models can also be discretized into sub-models corresponding to a stage of growth (Yeo et al., 2022). On the other hand, mechanistic plant growth models are algorithms that model plant physiological processes such as light interception, photosynthesis rate and respiration loss. They are generally more robust than empirical models. However, in some cases, they use parameters from the literature that do not match the specific growing conditions, potentially leading to "erroneous predictions" (Both, 1995). Many mechanistic models, such as those proposed by Critten (1991), Van Henten (1994), Pearson et al. (1997) and Zhang et al. (2008), are extended versions of the model proposed by Sweeney et al. (1981) for which two outputs, the structural dry weight and the non-structural dry weight, are calculated to assess the total dry weight. Another category of mechanistic models is based on a balance of carbon flows, such as the NICOLET model (Seginer et al., 1998) or an adaptation to lettuce by Jans-Singh et al. (2021) of a tomato yield model (Vanthoor et al., 2011). More recently, artificial intelligence approaches, such as machine learning (Cohen et al., 2022) and fuzzy logic and neural networks (Chang et al., 2021), have also been used to predict crop growth.

Three of the studies in Table 5.1 selected the mechanistic growth model proposed and validated by Van Henten (1994) to model lettuce growth in a CEA space. This model is based on principles from plant physiology and parameters selected from the literature. It estimates the total dry weight (structural and non-structural) of lettuces (*Lactuca sativa L.*) as a function of air temperature, solar irradiance and CO_2 concentration. The model was validated experimentally for two cultivars in a semi-controlled greenhouse, and the indoor conditions were monitored for 56 days. Over this period, the air temperature varied between 7 ◦C and 24°C (mean value of 12°C), the mean daily light integral (DLI), which is the number of photosynthetically active photons delivered to a specific area over 24 h, was 5 $mol·m^{-2}·d^{-1}$ and the CO_2 concentration varied between 347 ppm and 776 ppm (mean value of 464 ppm). In high-density CEA spaces, air temperature, DLI and CO_2 concentration are maintained at a

higher level than the one used to validate the model. Thus, it is unclear if this model suits high-density CEA applications. Graamans et al. (2018) commented that the model might underestimate dry matter production for higher temperatures, which are usually maintained in those spaces compared to a semi-controlled greenhouse.

5.1.2 Modelling heat gain/loss from crops

Different approaches have been proposed to model heat gain/loss from crops, i.e., the latent heat gain and the sensible heat gain/loss, in BPS tools. These include using a fixed evaporation rate, fixed LAI or a dynamic LAI, as reported in Table 5.2. Using a fixed stage of growth is appropriate for sizing the heating, ventilation and air conditioning (HVAC) equipment or for modelling crops that are growing according to a diversified stage growth management method (Talbot & Monfet, 2020). Still, it is not sufficiently precise to establish the energy use as the crops grow.

Table 5.2 Approaches to estimate heat gain/loss from crops in BPS tool

Approach	**Reference**
1) Fixed evaporation rate	Harbick and Albright (2016) Zhang and Kacira (2020b)
2) Fixed leaf area index	Kokogiannakis and Cooper (2015) Benis et al. (2017b) Nadal et al. (2017) Graamans et al. (2018) Lalonde et al. (2019) Baglivo et al. (2020)
3) Dynamic leaf area index that varies according to growing conditions in a transient modelling approach	Ward et al. (2015) Jans-Singh et al. (2021) Talbot and Monfet (2021) Ledesma et al. (2022) Talbot et al. (2022) Yeo et al. (2022) Song et al. (2023)

5.1.3 Modelling light interception

Modelling light interception has two functions: (1) determining the useful fraction of the PAR emitted by lights absorbed by crops, which influences both the heat gain/loss from crops and growth and (2) determining the lighting heat gain. A few studies incorporated the impact of light interception on lighting heat gain (Kokogiannakis & Cooper, 2015; Liebman-Pelaez et al., 2021; Talbot & Monfet, 2020), and one incorporated it as a dynamic variable that varies with growth (Talbot & Monfet, 2021). Light interception is a thermal phenomenon that cannot be neglected to comply with the law of energy conservation.

The previous sections have highlighted the different approaches used to model crops and how they were integrated into BPS tools. The proposed approaches to model growth and heat gain/loss from crops lack integration, suitability to CEA applications and versatility across several indoor conditions. In this paper, a dynamic crop model that can predict the growth and heat gain/loss from crops for several indoor environment conditions, integrated into a BPS tool, is proposed. It is a grey-box model parametrised using an experimental growth dataset from the literature that predicts yield and heat gain/loss from crops for several indoor environment conditions. It is intended to be part of a versatile and transient approach developed in the TRNSYS software (Klein & al., 2017) that aims to improve CEA space energy, financial and environmental analyses. This study focuses on developing a lettuce model because it is one of CEA's most commonly cultivated species (Agritecture & WayBeyond, 2021) and can be grown in vertical stacks.

5.2 Methods

This section presents the developed model, its parametrisation and calibration using an experimental growth dataset available in the literature, and its implementation for energy analysis. The implementation is verified by comparing the use of the experimental growth dataset versus the outputs of the dynamic crop model to estimate the yield, the energy demand, and the energy use over a cultivation cycle combined into two indicators: the specific energy

demand for lighting, cooling, dehumidification and heating as well as the specific energy use. These are estimated by dividing the maximum energy demand per category and the energy used by the shoot fresh weight harvested over one cultivation cycle. The energy demand includes the electric energy demand for lighting as well as the rate of energy that the space requires to maintain the indoor environment at desired conditions for cooling, dehumidification, and heating. In this context, the energy use is the integral of the energy demand (lighting, cooling, dehumidification and heating) over one cultivation cycle. The energy demand is influenced by the heat gains/losses from external sources (conduction through building envelope, solar heat gain through fenestration, ventilation and infiltration) and internal sources (occupants, lighting, equipment and crops). As such, the energy demand does not include the impact of any HVAC equipment, such as the sensible heat gain of a dehumidifier located in the space or the latent heat removal associated with the sensible cooling process or the efficiency of the equipment.

5.2.1 Dynamic crop model

The dynamic crop model developed in this study combines two submodels, the growth model and the energy balance model, with intermediary variables being exchanged between the two sub-models (Figure 5.1). The growth model estimates, at every timestep, the total (shoot and root) plant dry weight (DW_{tot}). The shoot fresh weight (FW_{sht}) and the LAI are estimated using the total plant dry weight. The shoot fresh weight is used to estimate yield, while the LAI is used to estimate the heat gain/loss from crops and the PAR not absorbed by crops, two variables transferred to the thermal zone model. The heat gain/loss from crops are incorporated as additional internal gains/losses at the airnode energy balance solved according to the heat balance method, while the PAR not absorbed by crops is used to estimate the lighting heat gain.

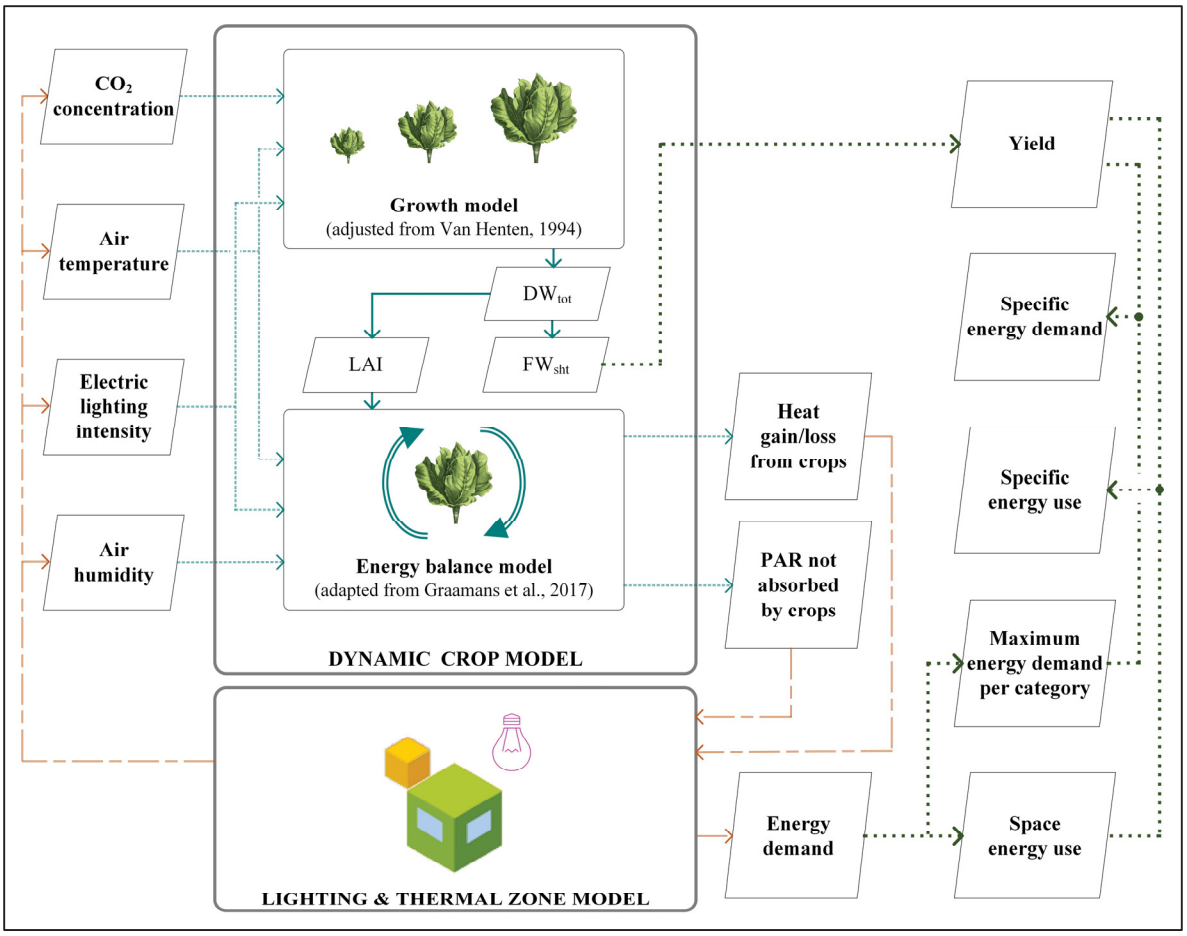

Figure 5.1 Overview of the dynamic crop model developed as a TRNSYS component

5.2.1.1 Growth model

The adjusted growth model is an adaptation of the algorithm proposed by Van Henten (1994) coded according to the equations and parameters summarised in Table-A I-1 and Table-A I-2. This model was developed to be used solely with solar PAR. Thus, it is first modified, as expressed by Equation (5.1), to account for both PAR sources (solar and electric lighting) to make it suitable for CEA applications.

$$PAR = c_{sol_{to}PAR} \cdot q''_{sol} + c_{PPFD_{to}PAR} \cdot PPFD \quad (5.1)$$

Where PAR is the total photosynthetic active radiation that includes both solar and electric lighting ($W \cdot m^{-2}_{cultivated}$); $c_{PPFD_{to}PAR}$ is the fraction of the total solar spectrum that is PAR, set to a value of 0.44; $c_{PPFD_{to}PAR}$ is the conversion factor from PPFD to the equivalent solar PAR, set to a value of 0.217 $W \cdot m^{-2}_{cultivated} \cdot (\mu mol \cdot m^{-2} \cdot s^{-1})^{-1}$ (Dorais, 2003); and $PPFD$ is the photosynthetic photon flux density from electric lighting ($\mu mol \cdot m^{-2} \cdot s^{-1}$).

The growth model is then parametrised by (1) modifying some parameters according to recent literature or to be more suitable to high-density CEA applications and (2) calibrating the parameters of the growth model that were previously identified as sensitive (Van Henten & Van Straten, 1994) using an experimental growth dataset from Carotti et al. (2021) detailed in Table 5.3.

Table 5.3 Experimental growth dataset used to parametrise the growth model
Taken from Carotti et al. (2021)

Conditions	**Low PPFD**			**Medium PPFD**			**High PPFD**		
PPFD, $\mu mol \cdot m^{-2} \cdot s^{-1}$	200			400			750		
DLI, $mol \cdot m^{-2} \cdot d^{-1}$	11.5			23.0			43.0		
$DW_{content}$ at harvest, %	2.6			3.8			4.2		
Air temperature, °C	20	24	28	20	24	28	20	24	28
Relative humidity (photoperiod/dark period), %	75/85	80/89	85/91	75/85	80/89	85/91	75/85	80/89	85/91
SLA, $cm^2 \cdot g_{DW}^{-1}$	360	436	400	295	300	314	244	272	250
Cultivation cycle, days	28.0	25.3	27.0	21.2	19.0	23.6	18.3	18.1	21.2

Carotti et al. (2021) reported the shoot fresh weight (FW_{sht}) and total dry weight (DW_{tot}) per plant for lettuce (*Lactuca sativa cv. Batavia Othilie*) growing in a CEA space under different PPFD and indoor air conditions with a planting crop density of 25 $plant \cdot m^{-2}$. Those conditions were reported for a root temperature of 28°C, a vapour pressure deficit (VPD) that alternated between 0.58 kPa and 0.34 kPa for the photoperiod and dark period, respectively, a CO_2 concentration of 1200 ppm and a photoperiod of 16 h. The growth model is calibrated from a transplant weight of 1.2 $g_{FW} \cdot plant^{-1}$ with a dry matter content estimated to be 5% (Puccinelli et al., 2022) to the moment the shoot fresh weight reaches a marketable weight of 250 $g_{FW} \cdot plant^{-1}$.

Four sensitive parameters (Van Henten & Van Straten, 1994), light use efficiency at very high CO_2 concentration (c_ε), yield factor (c_β), extinction coefficient (k_s) and saturation growth rate ($c_{gr,max}$), are calibrated using the growth experimental dataset. Calibration is used to match the output of a model with measured data by modifying its parameters. There is no consensus on the approach or criteria to use for the calibration of growth models. Lopez-Cruz et al. (2017) compared three calibration methods, a classic nonlinear least squares method and two Bayesian methods, to improve the prediction of lettuce dry weight with a growth model. Different criteria were used depending on the method, such as the sum of the square error and the root mean square error (RMSE). They concluded that the methods all performed similarly. Two techniques were employed sequentially by Ramirez et al. (2003) to calibrate a tomato growth model: least squares identification methods and a genetic algorithm. Due to the limited availability of information on the subject, it may be advisable to employ best practices for calibrating BPS models, as the developed growth model is integrated into this type of tool. The calibration of BPS models, specifically building energy models, can be automated or manual, depending on the number of parameters to calibrate. Automated calibration is characterised by programmed mathematical procedures or analytical approaches to complete the calibration procedure (Coakley et al., 2014), such as statistical methods (e.g., Bayesian approach) and evolutionary algorithms (e.g., genetic algorithm). Baba et al. (2022) reported that Bayesian approaches have been used to calibrate unknown input variables, while genetic algorithms have been used in several studies for the auto-calibration of energy consumption. They also concluded that genetic algorithms required fewer simulations to obtain a calibrated model. Thus, the variables c_ε, c_β, k_s, $c_{gr,max}$ are calibrated using a genetic algorithm that minimises the RMSE between the shoot fresh weight estimated with the growth model and the shoot fresh weight reported by Carotti et al. (2021). The shoot fresh weight estimated with the growth model is calculated according to equation (5.2) based on the total dry weight from the growth model. The parameters' bounds are listed in Table 5.4, and the genetic algorithm is limited to a maximum of 200 generations and a population size of 50.

$$FW_{sht}(t) = DW_{sht}(t)/DW_{content} = \left[(1 - c_\tau) \cdot DW_{tot}(t)\right] / DW_{content} \qquad (5.2)$$

Where FW_{sht} is the shoot fresh weight (g_{FW}·plant^{-1}); $DW_{content}$ is the dry matter content (g_{DW}·g_{FW}^{-1}); DW_{sht} is the shoot dry weight (g_{DW}·plant^{-1}); DW_{tot} is the total dry weight (g_{DW}·plant^{-1}); and c_τ is the ratio of the root dry weight to the total dry weight.

Table 5.4 Bounds used for the calibration of the growth model sensible parameters

Parameter	Lower bound	Upper bound	Reference
c_ε, g·J^{-1}	3·10^{-6}	17·10^{-6}	Set heuristically
c_β	0.4	0.9	Lopez-Cruz et al. (2017)
k_s	0.66	0.9	Tei et al. (1996) and Van Henten (1994)
$c_{gr,max}$, s^{-1}	0.5·10^{-6}	5.0·10^{-6}	Set heuristically

Statistical criteria, such as the Coefficient of Variation of the Root Mean Square Error (CVRMSE) and the Maximum Absolute Difference (MAD), are also calculated, as proposed by Baba et al. (2022), to compare the obtained results.

5.2.1.2 Energy balance model

The energy balance model adapts the algorithm proposed by Graamans et al. (2017). The energy balance is defined by equation (5.3), where the latent and sensible gain/loss from crops are defined by equations (5.4) and (5.5) and the net radiation terms by equations (7) and (8), and where the thermal storage in the leaf and stems is considered negligible (Stanghellini, 1987). Every term of the energy balance equation varies with leaf growth, which is considered using the LAI. The LAI, as defined by equation (5.6), is proportional to the leaf area per crop (LA) and the planting crop density (PCD), (Kozai, 2016). The system of equations is solved using the modified secant method, which has been adapted to calculate moist air properties dynamically.

$$q''_{plt,sol} + q''_{plt,SW} - q''_{plt,conv} - q''_{plt,latent} = 0 \quad (5.3)$$

$$q''_{plt,latent} = LAI \cdot \lambda \frac{\chi_s - \chi_a}{r_s + r_a} \quad (5.4)$$

$$q''_{plt,conv} = LAI \cdot \rho_{a,i} \cdot c_{p_{a,i}} \frac{T_{plt} - T_{a,i}}{r_a} \quad (5.5)$$

$$LAI = PCD \cdot LA \quad (5.6)$$

Where the net radiation flux absorbed by the crops can be from solar radiation ($q''_{plt,sol}$) and/or the short-wave radiation from electric lighting ($q''_{plt,SW}$) (W·m$^{-2}_{\text{cultivated}}$); $q''_{plt,latent}$ is the latent heat flux from crops (W·m$^{-2}_{\text{cultivated}}$); $q''_{plt,conv}$ is the convective heat flux (gain or loss) from crops (W·m$^{-2}_{\text{cultivated}}$); LAI is the Leaf Area Index (m$^2_{\text{leaves}}$·m$^{-2}_{\text{cultivated}}$); λ is the heat of vaporisation of water (kJ·kg^{-1}); χ_s is the vapour concentration at the canopy level (g·m^{-3}); χ_a is the air vapour concentration (g·m^{-3}); r_s is the stomatal resistance (s·m^{-1}); $r_a$is the aerodynamic resistance (s·m^{-1}); $\rho_{a,i}$ is the indoor air density (kg·m^{-3}); $c_{p_{a,i}}$ is the specific heat of the indoor air (J·(kg·°C)$^{-1}$); T_{plt} is the leaves temperature (°C); $T_{a,i}$ is the indoor air temperature (°C); LA is the leaf area per plant (m$^2_{\text{leaves}}$·plant^{-1}); and PCD is the planting crop density (plant·m$^{-2}_{\text{cultivated}}$).

The absorbed PAR ($q''_{sol,plt}$ and $q''_{SW,plt}$), often referred to as net radiation, is the primary input flux to the energy balance of the crops (equation (5.3)) and represents a portion of the transmitted solar radiation (equation (5.7)) or PAR emitted by lights (equation (5.8)) depending on the light interception. The light interception fraction (i.e., $1 - e^{-k_s \cdot LAI}$) is assessed using extinction coefficients as proposed by Katsoulas and Stanghellini (2019) since it can be applied to various planting crop densities.

$$q''_{plt,sol} = (1 - e^{-k_{s,sol} LAI}) \cdot q''_{sol} \quad (5.7)$$

$$q''_{plt,SW} = \left(1 - e^{-k_{s,el} LAI}\right) \cdot q''_{el,SW} \quad (5.8)$$

Where $k_{s,sol}$ and $k_{s,el}$ are the extinction coefficients associated with solar radiation and PAR from electric lighting; q''_{sol} is the transmitted solar radiation flux ($W \cdot m^{-2}_{cultivated}$); and $q''_{el,SW}$ is the short-wave radiation flux from electric lighting ($W \cdot m^{-2}_{cultivated}$).

5.2.1.3 Light interception modelling

The electric lighting power input (q''_{el}) splits in three: the convective heat gain ($q''_{el,conv}$), the long-wave radiation heat gain ($q''_{el,LW}$), and the short-wave radiation ($q''_{el,SW}$), often referred to as the photosynthetic active radiation (PAR). The energy distribution depends on the lighting heat fractions (convective (f_{conv})/ radiative long-wave (f_{LW})/radiative short-wave (f_{SW})) which are specific to the lights model. Only a fraction of the short-wave radiation is intercepted and absorbed by crops ($q''_{plt,SW}$), while the rest is contributing to the lighting heat gain ($q''_{zone,SW}$) as illustrated in Figure 5.2. As the leaf coverage over the cultivated area expands, the light interception increases, thereby increasing the radiation absorbed by crops and decreasing lighting heat gain. Light interception is influenced by factors such as cultivated crops, planting crop density and light source.

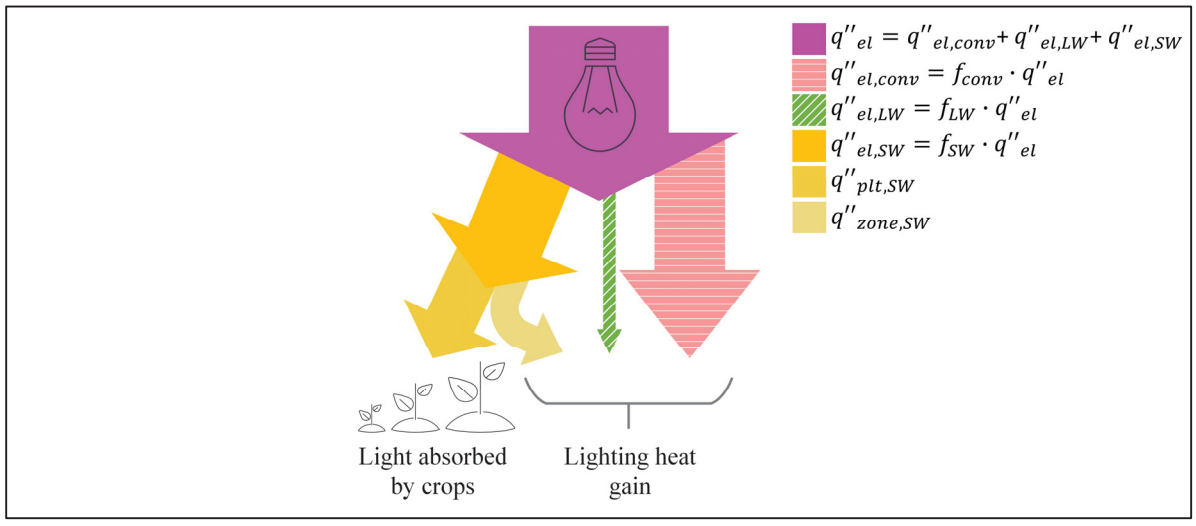

Figure 5.2 Energy distribution of the electric lighting power input

5.2.2 Space model

The modelled space is a 3.02m x 2.44m x 1.97m room located in a building maintained at an ambient temperature of 20°C, and the simulation timestep is 10 minutes. A vertical hydroponic stacking system with a 2.8 m^2 footprint and three tiers with 46.5 cm vertical spacing is installed in the space, as illustrated in Figure 5.3. The walls, floor and ceiling have an overall U-value of 0.12 $W \cdot (K \cdot m^2)^{-1}$, a thermal capacity of 1000 $J \cdot (kg \cdot K)^{-1}$, and a density of 113.17 $kg \cdot m^{-3}$. They are covered with water-repellent panels to minimise the migration of water vapour through the surfaces. The space is enriched in CO_2 to enhance crop growth and is airtight to avoid the dilution of the CO_2. Moreover, it is assumed that the air is well-mixed and air velocity over the leaves is sufficient to facilitate gas exchange. Indoor conditions alternate between two states: (1) photosynthesis state that occurs during the photoperiod (when the lights are on) and (2) respiration state that occurs during the dark period (when the lights are off). The three tiers are lit with electric lighting, and their heat fractions are assumed to be 0.52/0.11/0.37 (f_{SW}/ f_{LW}/f_{conv}) as illustrated in Figure 5.2.

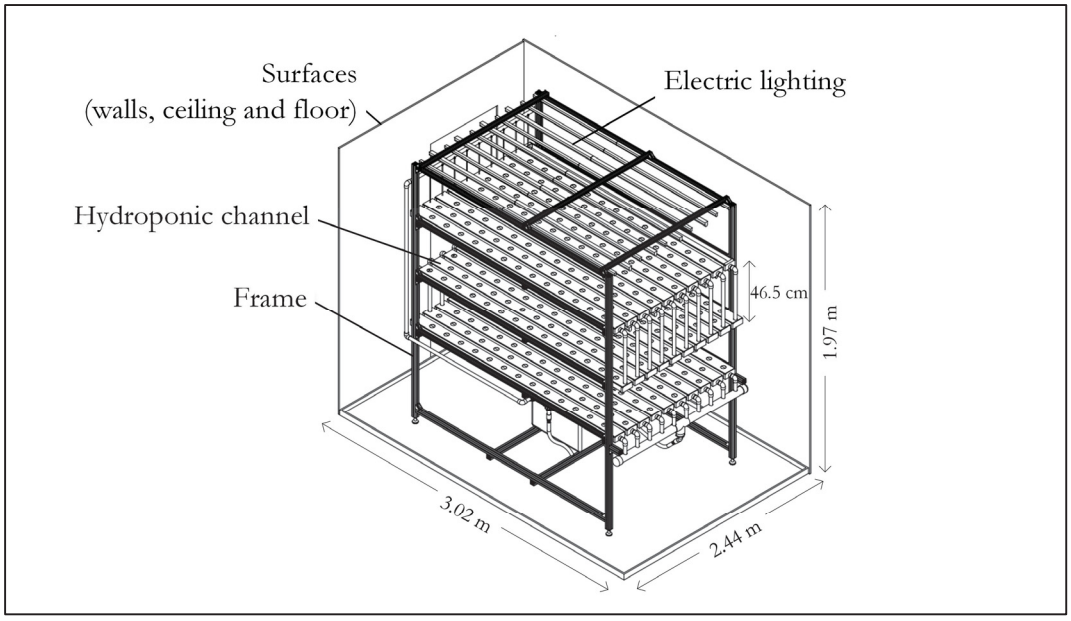

Figure 5.3 Small-scale high-density CEA space

5.2.3 Modelling verification

Two different verifications are proposed to ensure the crop model is implemented correctly. First, the reliability of the growth model to predict yields for other lighting intensities that are not part of the experimental growth dataset, specifically at 300 and 500 $\mu mol \cdot m^{-2} \cdot s^{-1}$. It is completed by assessing yields at 200, 300, 400 and 500 $\mu mol \cdot m^{-2} \cdot s^{-1}$ and the anticipated result is a linear rise in annual yield between 200 and 500 $\mu mol \cdot m^{-2} \cdot s^{-1}$ as previously established by Jin, Ji, et al. (2023). For lighting intensities of 300 and 500 $\mu mol \cdot m^{-2} \cdot s^{-1}$, the values of the sensible parameters are determined through interpolation, drawing upon the calibrated values.

Second, to ensure the implementation of the energy balance is accurate, the proposed energy modelling approach is then verified by comparing the estimated energy use per category with those reported by Graamans et al. (2018). This verification is solely for implementing the energy balance model, as the results are for a fixed LAI of 2.1 with a light interception fraction of 0.81. The indoor environment conditions are adjusted to match those reported in Table 5.5, with a planting crop density of 17.6 $plant \cdot m^{-2}$. Additionally, the cultivated area is increased to 10.2 m^2 to maintain the same ratio of cultivated area over the volume specified in Graamans et al. (2018). For this verification, two alterations are also introduced to the proposed energy modelling approach: (1) the impact of light interception on lighting heat gain is neglected, and (2) moisture removal associated with the sensible cooling process, with a sensible heat ratio of 0.7, is added. The latest is included because the software DesignBuilder accounts for moisture removal when computing the cooling energy demand of the space. The comparison is completed for the energy use by category for lighting, cooling and dehumidification, as detailed in section 5.3.4.

Table 5.5 Indoor environment conditions of the CEA modelled by Graamans et al. (2018)
Taken from Graamans et al. (2018)

Indoor environment conditions	**Values**
PPFD, μmol·m^{-2}·s^{-1}	500
DLI, mol·m^{-2}·d^{-1}	28.8
Heating setpoint (photoperiod/dark period), °C	24/24
Cooling setpoint (photoperiod/dark period), °C	30/30
Minimum relative humidity (photoperiod/dark period), %	65/65
Maximum relative humidity (photoperiod/dark period), %	90/90

5.3 Results

The results are presented for the case study, the small-scale CEA-HD space, for two versions of the developed crop model: (1) with the initial growth model (section 5.3.2) and (2) with the adjusted growth model (section 5.3.3) following the proposed modifications and calibration of the most sensitive parameters using a genetic algorithm. Before these results, the approach undertaken to establish the heat gain/loss from crops using the experimental growth dataset (Table 5.3) is detailed (section 5.3.1). The results from the verification of the models are presented in section 5.3.4.

5.3.1 Heat gain/loss from crops using the experimental growth dataset

The procedure used to assess the specific demand and the specific energy use based on the heat/gain loss from crops using the experimental growth data set is similar to the one illustrated in Figure 5.1. However, instead of modelling growth, the growth dataset is used. The dataset by Carotti et al. (2021) reported the shoot fresh weight (FW_{sht}) and total dry weight (DW_{tot}) per plant for lettuce as well as the Specific Leaf Area (SLA) and the dry matter content ($DW_{content}$) instead of the LAI. Thus, the LAI is estimated using the measured shoot fresh weight and dry matter content according to Equations (5.9) and (5.10). Equation (5.9) estimates the LAI based on the planting crop density, the SLA and the leaf dry weight (DW_{leaf}). Equation (5.10) estimates the leaf dry weight based on the leaves to shoot dry weight ratio (DW_{leaf}/DW_{sht}), the shoot fresh weight and the dry matter content.

$$LAI = PCD \cdot LA = PCD \cdot \left[SLA \cdot DW_{leaf}\right] \tag{5.9}$$

$$DW_{leaf} = \frac{DW_{leaf}}{DW_{sht}} \cdot DW_{sht} = \frac{DW_{leaf}}{DW_{sht}} \cdot FW_{sht} \cdot DW_{content} \tag{5.10}$$

Where SLA is the Specific Leaf area ($m^2 \cdot g_{DW}^{-1}$); DW_{leaf} is the dry leaf weight ($g_{DW} \cdot m^{-2}_{cultivated}$); and DW_{leaf}/DW_{sht} is the leaves to shoot dry weight ratio. It was estimated heuristically based on Carotti et al. (2021) to a value of 0.92.

As an example, the impact of the crops growing on the energy demand for cooling, heating and dehumidification at Medium PPFD/24°C is illustrated in Figure 5.4. As crops grow, the cooling energy demand decreases while the dehumidification energy demand increases during the photoperiods. During the dark periods, additional heating and dehumidification are required towards the end of the cultivation cycle, while the cooling energy demand remains minimal.

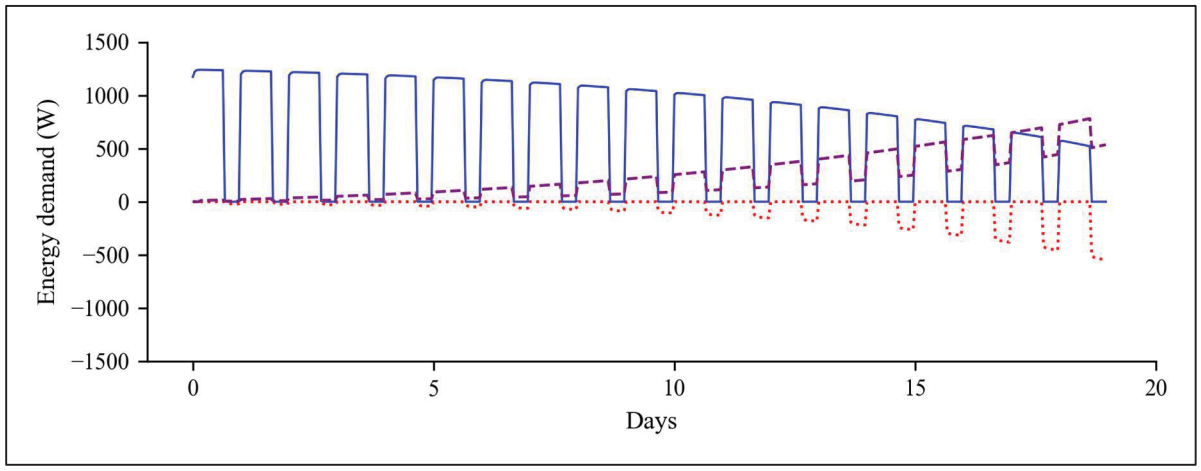

Figure 5.4 Energy demand at Medium PPFD @24°C over a cultivation cycle for cooling (solid line), heating (dotted line) and dehumidification (dashed line) using the experimental growth dataset

5.3.2 Performance of the initial growth model

The specific energy demand for lighting, cooling, dehumidification and heating and the specific energy use are presented in Figure 5.5 and Figure 5.6 when yield and heat gain/loss from crops are estimated using the experimental growth dataset reported by Carotti et al. (2021) versus the initial growth model. The two indicators are estimated over a cultivation cycle, i.e., from a transplant weight of 1.2 g_{FW}·plant^{-1} to a marketable weight of 250 g_{FW}·plant^{-1}. The LAI and cultivation cycle calculated using the experimental growth dataset versus the initial growth model are presented in Figure 5.7.

As expected, the lighting specific energy demand is not influenced by crop growth while the cooling specific energy demand is slightly influenced by crop growth due to light interception. On the other hand, the dehumidification demand and heating demand depend on the heat gain/loss from crops, which increase as the crops grow. The initial growth model overestimates the specific energy demand for dehumidification and heating, which can be attributed to an overestimation of the LAI, as illustrated in Figure 5.7.

The specific energy use is underestimated for most conditions when the initial growth model is used, with a maximum difference of 22.0% (High PPFD@28°C). This is explained by the shorter cultivation cycle estimated with the initial growth model. However, for some conditions, this is offset by overestimated energy demand for dehumidification and heating, leading to low differences in the specific energy use.

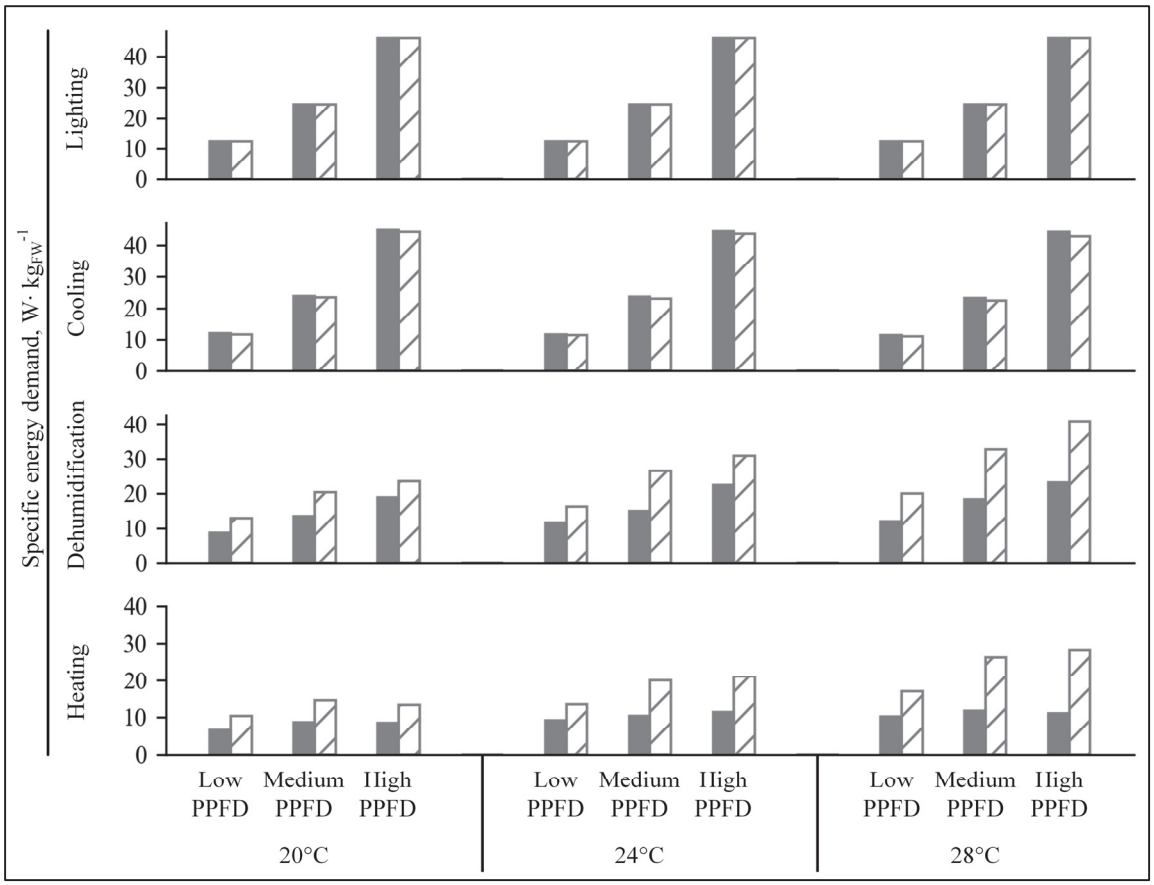

Figure 5.5 Specific energy demand estimated using the experimental growth dataset from Carotti et al. (2021) (solid bars) and the initial growth model from Van Henten (1994) (hatched bars) over one cultivation cycle

As illustrated in Figure 5.7, the initial growth model overestimates the growth rate for all the conditions, leading to an overly short cultivation cycle. The predicted cultivation cycle is consistently shortened by 2.2% (Medium PPFD@24°C) to 28.2% (High PPFD@28°C). The estimation of the maximum LAI is also overestimated by the initial growth model from 51% (Low PPFD@24°C) to 142% (High PPFD@28°C).

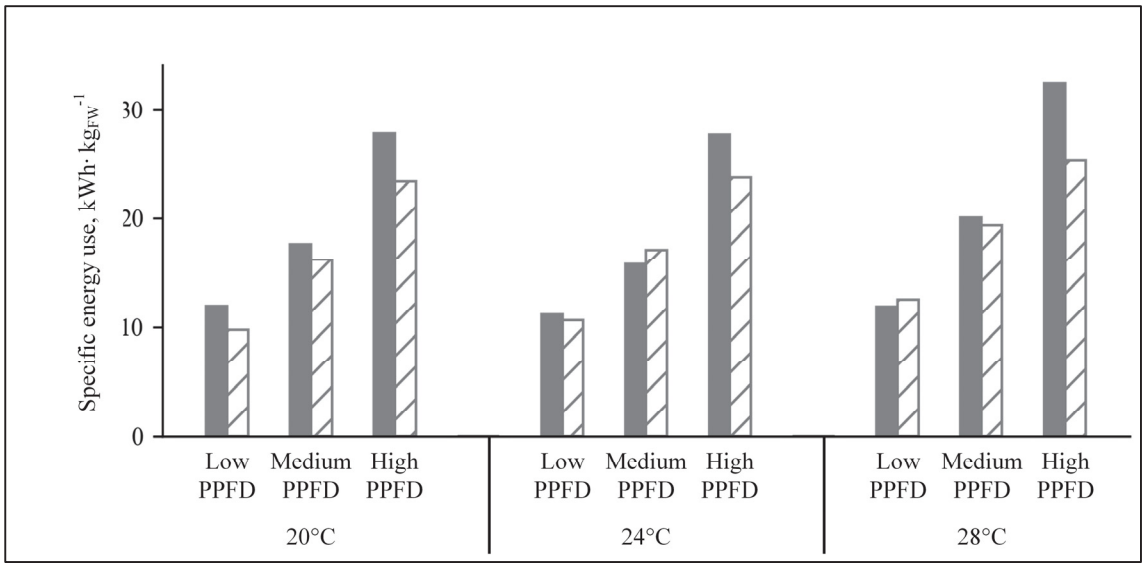

Figure 5.6 Specific energy use estimated using the experimental growth dataset from Carotti et al. (2021) (solid bars) and the initial growth model from Van Henten (1994) (hatched bars) over one cultivation cycle

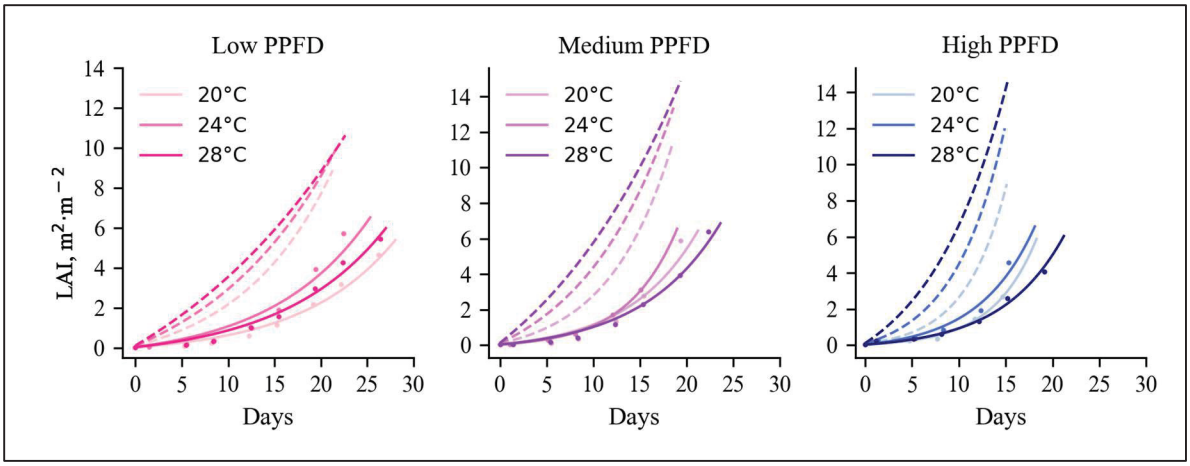

Figure 5.7 LAI estimated using the experimental dataset from Carotti et al. (2021) (solid lines) and the initial growth model from Van Henten (1994) (dashed lines) over one cultivation cycle

The results showed that the initial growth model did not perform well in a high-density CEA application. It overestimates the LAI and the growth rate. As a result, it significantly overestimates the specific energy demand for dehumidification and heating and the annual yield. The influence on specific energy use is lessened but underestimated for most conditions.

Thus, the model needs to be adjusted to better estimate the specific energy demand for dehumidification and heating and the specific energy use of a high-density CEA space.

5.3.3 Performance of the adjusted growth model

To improve the model, some parameters are modified according to recent literature or to be more suitable to high-density CEA application as listed in the last column of Table-A I-2. The boundary conductance (g_{bnd}) and stomatal conductance (g_{stm}) are modified (Table-A I-2) according to Graamans et al. (2017). Additionally, as highlighted in section 5.3.2 and illustrated in Figure 5.7, the LAI estimated using the initial growth model showed substantial differences compared to values derived from the experimental growth dataset. As such, the equation that calculates the LAI (Equation (I-6i)) is modified to Equation (I-6m) to use the specific leaf area (SLA) instead of the structural leaf ratio (c_{lar}) since the SLA is available in recent literature (e.g., Carotti et al. (2021)).

The calibration of the most sensitive parameters of the modified growth model leads to the parametrisation of the growth model shown in Figure 5.8, with the corresponding statistical criteria tabulated in Table 5.6.

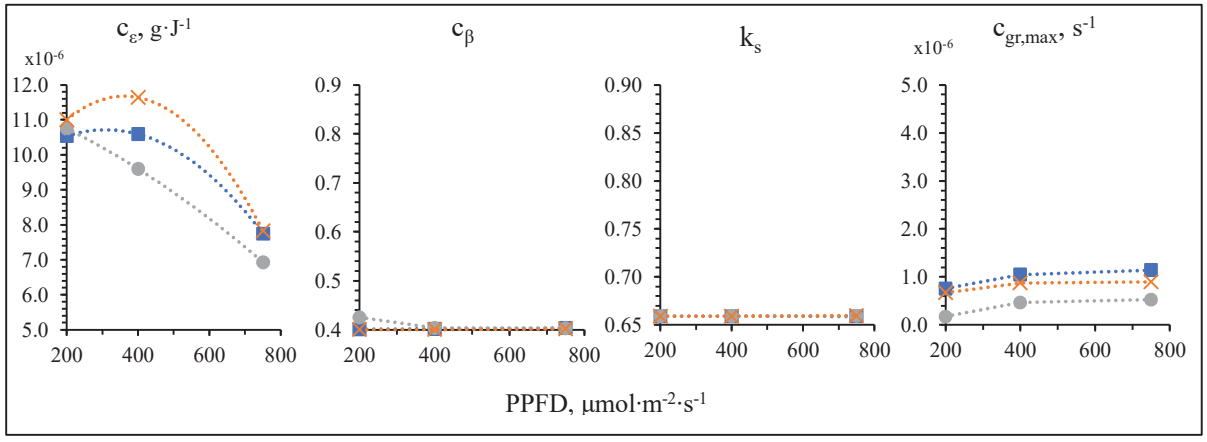

Figure 5.8 Calibrated sensible parameters for ■ 20°C, × 24°C, and ● 28°C

Table 5.6 Statistical criteria of the calibration minimising the RMSE of the fresh weight per plant.

	Low PPFD (200 µmol·m^{-2}·s^{-1})			**Medium PPFD (400 µmol·m^{-2}·s^{-1})**			**High PPFD (750 µmol·m^{-2}·s^{-1})**		
	20°C	**24°C**	**28°C**	**20°C**	**24°C**	**28°C**	**20°C**	**24°C**	**28°C**
RMSE, g_{FW}·plant^{-1}	2.1	8.8	6.6	12.2	12.3	18.2	16.2	16.0	14.5
CVRMSE, %	2.3	10.1	6.3	13.9	18.1	18.7	10.6	18.2	17.2
MAD, g_{FW}·plant^{-1}	2.9	15.9	14.1	19.2	19.9	35.2	17.9	31.3	26.4

The relative differences between the results obtained with the initial and adjusted growth model, compared to the results derived from the experimental growth dataset (Carotti et al., 2021), are presented in Table 5.7. The differences are reduced to less than 5.2% and 10.4% for the specific energy demand for dehumidification and heating and to 3.5 % for the specific energy use, compared to differences that ranged up to 79.4% and 153.5% for the specific energy demand for dehumidification and heating and 22.0% for the specific energy use with the initial growth model. The difference is reduced to less than 3.5% compared to differences that ranged up to 28.2%.

Table 5.7 Relative differences for the specific energy demand, specific energy use and cultivation cycle using the growth models (initial & adjusted) compared to the results derived from an experimental growth dataset

Conditions		Relative difference, %							
		Dehumidification specific energy demand		Heating specific energy demand		Specific energy use		Cultivation cycle	
		Initial	Adjusted	Initial	Adjusted	Initial	Adjusted	Initial	Adjusted
Low PPFD	20°C	49.3	0.5	60.4	1.4	18.2	1.0	24.0	1.2
	24°C	40.7	0.3	47.8	1.3	4.9	0.9	14.9	3.1
	28°C	65.4	2.5	66.8	4.1	5.3	0.5	16.2	1.7
Medium PPFD	20°C	49.8	0.0	68.3	1.7	8.4	1.6	12.8	3.5
	24°C	77.7	5.2	91.3	0.0	8.7	3.5	2.2	0.7
	28°C	79.4	0.1	122.3	8.0	3.5	1.5	18.0	3.4
High PPFD	20°C	24.5	0.0	57.1	3.2	15.9	1.2	14.9	0.2
	24°C	38.3	0.0	83.3	2.6	14.3	2.4	17.7	4.1
	28°C	76.5	2.0	153.5	10.4	22.0	0.1	28.2	1.2

5.3.4 Verification of the modelling approach

The results obtained with the adjusted growth model provide additional insight into establishing the energy performance of high-density CEA spaces. The results of two different verifications are presented. First, the ability of the growth model to predict yields for lighting intensities that were not included in the experimental growth dataset described in Table 5.3 is completed. The estimated yields for 200, 300, 400 and 500 $\mu mol \cdot m^{-2} \cdot s^{-1}$ are depicted in Figure 5.9. As expected, the figure illustrates linear correlations between predicted yield and lighting intensity. The R-square values obtained range from 0.8645 to 0.9201, demonstrating a satisfactory level of robustness of the model.

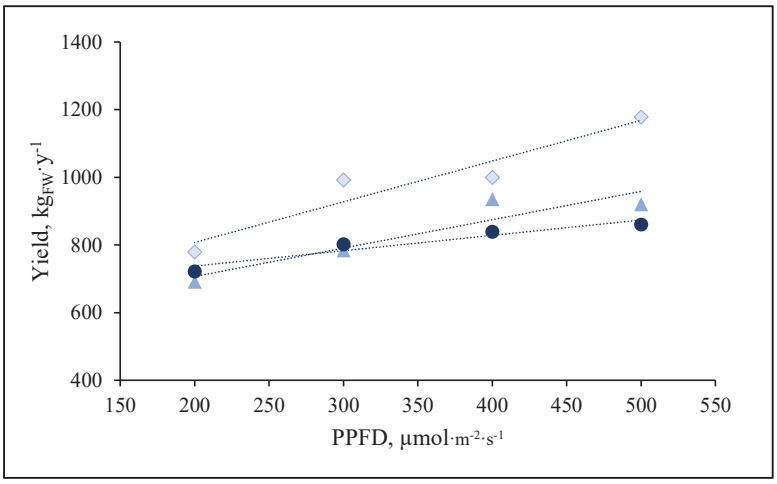

Figure 5.9 Estimated yield with the adjusted growth model for different lighting intensity for ▲ 20°C, ◇24°C, and ● 28°C

Second, to ensure that the implementation of the energy balance is accurate, a comparison of the estimated energy use by category with those reported by Graamans et al. (2018) is completed. As such, the model and the energy modelling approach are altered according to the information listed in section 5.2.3. As previously stated, this is solely for implementing the energy balance model as the results are for a fixed LAI of 2.1, a light interception fraction of 0.81 without considering its impact on the zone heat gain, crop density of 17.6 plant·m^{-2}, cultivated area of 10.2 m^2, PPFD of 500 µmol·m^{-2}·s^{-1}, DLI of 28.8 mol·m^{-2}·d^{-1}, temperature between 24-30°C, relative humidity between 65-90%, and a sensible heat ratio of 0.7. The comparison is completed over the lighting, cooling and dehumidification energy use intensity, as illustrated in Figure 5.10. Upon altering the proposed modelling approach, which only applies to the results presented in Figure 5.10, it is observed that the discrepancies for the cooling and dehumidification are 5% and 1%, confirming the proper implementation of the energy modelling approach.

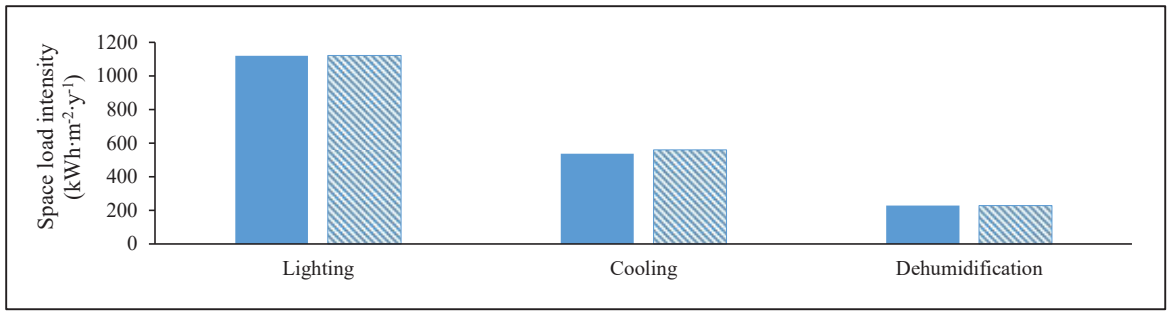

Figure 5.10 Comparison of the energy use intensity estimated by Graamans et al. (2018) (solid bars) and the ones from the current study as a verification step (hatched bars)

5.4 Discussion

The results obtained from this study are not easily comparable to data available in the literature since the specific energy use is rarely reported, unlike the specific energy consumption, which is based on the consumption of the HVAC equipment and lighting. Since several parameters influence the HVAC equipment design and performance, estimating their energy consumption adds a layer of complexity for comparative analyses. For example, Weidner et al. (2021) compared the specific energy consumption of various high-density CEA spaces modelled reported in the literature. The authors noted a significant disparity in specific energy consumption, ranging from approximately 3.2 to 59.1 $kWh \cdot kg_{FW}^{-1}$, which can be partially explained by important differences regarding the HVAC equipment design and performances. The disparity can also be attributed to differences in maintained indoor environment conditions, cultivation methods, location, envelope characteristics and energy modelling approach.

Graamans et al. (2018) are some of the few researchers who have reported specific energy use. Their model estimated yield using the growth model developed by Van Henten (1994) with specific energy use ranging from 1420 to 1489 $MJ \cdot kg_{DW}^{-1}$, depending on the location. This corresponds to a specific energy use of 15.5–15.6 $kWh \cdot kg_{FW}^{-1}$ for a dry matter content of 3.9%, which aligns with the results shown in Table 5.6. However, it is important to highlight that this comparison has limitations mainly due to (1) disparities in the modelling parameters, such as

the indoor environment conditions and possibly the weight of crops at transplant and harvest, and (2) the modelling approach. The main distinction in indoor environment conditions is the use of floating setpoints for indoor air temperature and relative humidity rather than tightly controlling them to a fixed value. As for the modelling approach, Graamans et al. (2018) did not use a growth model to estimate crops heat gain/loss; the LAI was set to a constant value over the simulation period. As specified in section 3.4, the impact of light interception on lighting heat gain was also neglected, and moisture removal associated with the sensible cooling process was included. When the latter (moisture removal) is factored into estimating the energy demand, it allows for the direct sizing of the dehumidification system based on the dehumidification energy demand. Conversely, omitting moisture removal might necessitate an intermediary step to size the dehumidification system using the dehumidification energy demand. However, this approach provides a comprehensive understanding of the space energy requirements for the proper sizing of the HVAC system since it supports calculating the space sensible heat ratio (SHR). As an example of the usefulness of this approach, it becomes apparent that towards the end of the cultivation cycle, the dehumidification energy demand increases, leading to a reduction of the SHR of the space. Consequently, selecting a cooling system that can deliver a low SHR would be better since it would be most efficient. Another example is if a heat recovery loop is used to cool LED lights. This type of cooling system does not contribute to any moisture removal from the air. As such, moisture removal associated with the sensible cooling process should not be included in the energy modelling approach.

It is important to underline some of the limitations of the developed crop model. One key parameter in the growth model, the dry matter content, has a significant influence over two main outputs: yield and heat gain/loss from crops. In the developed growth model, the dry weight is first estimated to subsequently derive the fresh weight and the LAI using the dry matter content. However, in comparison to data available in the literature, the dry matter contents used in this study (2.6, 3.8 and 4.2%, as specified in Table 5.3) are lower than those reported by Meinen et al. (2018), which ranged from 5.8% to 8.4% for the same variety (*'Othilie'*). Thus, the results obtained in this study, such as the specific energy demand and specific energy use, could be limited to *'Othilie'* lettuces with relatively low dry matter content.

Furthermore, the developed growth model exhibits additional limitations, such as being tailored for a harvest weight equal to or smaller than 250g_{FW} per plant, constrained to well-irrigated crops with adequate nutrients, specific to the indoor conditions that fall into the range of the experimental dataset used and specific to *'Othilie'* variety cultivated by Carotti et al. (2021). To perform energy analysis with indoor conditions that do not fall into the range of the experimental dataset used and/or other variety of lettuces, the sensible parameters could be calibrated using the approach proposed in this study for another experimental growth dataset and specific model parameters, such as the SLA and the dry matter content, should be adjusted. The developed crop model is tailored for high-density CEA applications and is part of a versatile approach. The model was developed to model spaces with solar and/or electric lighting for various planting crop densities and photoperiods. Dynamic moisture air properties also included in the model to support future calibrations under less common indoor air conditions. The next step would entail applying the same approach used in this study to other CEA applications, such as a closed greenhouse with electric lighting. This would require verifying and adjusting the growth model, if necessary. Additionally, the methodology developed in this study could potentially be applied to adapt the crop model to other leafy greens, such as kale and spinach.

5.5 Conclusion

In this paper, a grey-box growth model was developed to estimate the yield, the energy demand and the energy use of high-density controlled environment agriculture (CEA) spaces. The model builds upon an existing lettuce growth model, initially developed for greenhouses by Van Henten (1994) and adjusted by modifying specific parameters and calibrating the most sensitive ones. The calibrations were completed using an experimental growth dataset containing nine sets of indoor environment conditions for lettuce grown in a high-density CEA space. Two indicators were used to assess the model performance: specific energy demand and specific energy use. Before the proposed modifications and calibration, the initial model overestimated the leaf area index, which led to higher specific energy demand for heating and dehumidification. It also overestimated the growth rate, leading to underestimating the specific

energy use for most conditions. This initial assessment highlighted that the model must be adjusted for controlled environment agriculture applications. Specific parameters were thus modified according to available values in the literature and better suited to high-density CEA applications, and four sensitive parameters were calibrated. The model calibration was completed over the shoot fresh weight using a genetic algorithm with an objective function that minimised the root mean square error. This resulted in a parametrisation of four sensitive parameters (c_ε, c_β, k_s, $c_{gr,max}$), using nine sets of conditions. The dynamic crop model was developed as a grey-box model, incorporating the heat exchanges of crops as they grow to a high-density CEA space modelled in the TRNSYS software. Moreover, the dynamic crop model can be used for energy analysis of indoor environment conditions that fall within the range of conditions used in this study by interpolating the sensitive parameters. The calibration approach could be used to parametrise the model for other cultivars and indoor conditions. This contribution allows, through a transient approach, the estimation of yield, energy demand and energy use considering crop growth for a wide range of indoor environment conditions commonly selected to grow lettuce in CEA spaces. These are essential to complete energy, financial and environmental analyses and to support optimisation of the trade-off between crop growth and energy requirements.

Data availability

The dynamic crop model developed in this paper is available as a TRNSYS component on GitHub. For access, consult the GitHub page of the Laboratory of Thermal and Building Science of ETS Montreal.

Declaration of generative AI and AI-assisted technologies in the writing process

While preparing this work, the authors used ChatGPT (GPT-3.5) to improve the language and readability of a few sentences (less than 10% of the text). After using this tool/service, the authors reviewed and edited the content as needed and took full responsibility for the content of the publication.

Declaration of competing interest

The authors declare that they have no known competing financial interests or personal relationships that could have appeared to influence the work reported in this paper.

Acknowledgements

This work was supported by the Fonds de recherche du Quebec – Nature et technologies (Quebec, Canada), PhD scholarship for the first co-author, as well as NSERC research grants RGPIN-2020-04576 and ALLRP 561361-21.

CHAPTER 6

ANALYSING THE INFLUENCE OF GROWING CONDITIONS ON BOTH ENERGY LOAD AND CROP YIELD FOR A CONTROLLED ENVIRONMENT AGRICULTURE SPACE

Marie-Hélène Talbot[a], Danielle Monfet[a]

[a]École de Technologie Supérieure,
1100 Notre-Dame Ouest, Montréal, Québec, Canada H3C 1K3

Paper published in *Applied energy*, February 2024

Abstract

Controlled environment agriculture, such as vertical farming, consists of stacking crops in a controlled environment and is transforming agriculture by providing a highly productive solution for year-round production. However, vertical farms are also energy-intensive due to precise control of the growing conditions (temperature, humidity, carbon dioxide, and lighting). While many studies focus on optimising indoor conditions to enhance yield, the impact of those growing conditions on energy is often overlooked. This study aims to provide a comprehensive analysis, using a dynamic model, of the influence of growing conditions typically used to cultivate lettuces on energy and crop yield. Several combinations of air temperatures (20, 24 and 28°C), vapour pressure deficits (0.54 and 0.85 kPa), lighting intensities (200 to 700 $\mu mol \cdot m^{-2} \cdot s^{-1}$) and photoperiods (12 to 24 hours) are studied. The dynamic model, developed using a building performance simulation tool, supports the simultaneous assessment of energy load and crop yield. It includes a model of a small-scale vertical farm that integrates a dynamic crop model to estimate heat gains/losses from crops and crop growth rate according to growing conditions. The results indicated that the best compromise between energy load and yield is at an air temperature of 24°C. Moreover, lowering lighting intensity and extending the photoperiod positively impacted both energy load and yield. Certain growing conditions, such as lowering the vapour pressure deficit, can reduce the need for dehumidification. Additionally, for lighting intensities exceeding

500 μmol·m^{-2}·s^{-1}, although the energy load continued to increase linearly with the lighting intensity, the growth rate was limited, resulting in reduced production efficiency. These extensive results and thorough analyses offer valuable insights into the influence of the growing conditions on energy load and yield.

Keywords: Controlled Agriculture Environment (CEA); Vertical Farm; Energy Modelling; Energy Efficiency; Energy Load

Highlights

- Energy and yield of a vertical farm are modelled with TRNSYS for several conditions.
- The influence of temperature, VPD and PPFD were assessed for over 180 scenarios.
- An air temperature of 24 °C represents a better compromise compared to 20 °C or 28 °C.
- Lowering PPFD and extending photoperiod benefit both energy and yield.
- Changing the growing conditions can reduce the need for dehumidification.

6.1 Introduction

The vertical farming industry is experiencing rapid global expansion, with the market projected to surpass four times its 2022 value of USD 5.6 billion by 2030 (Shahbandeh, 2023). This remarkable growth is primarily attributed to advancements in light-emitting diode (LED) technology, which has become more affordable (Kozai, 2016). As a result, research in vertical farming, also known as plant factories, indoor farms, container farms, and indoor plant environments, has proliferated. The number of journal articles explicitly focusing on vertical farming has significantly increased, growing from less than 175 publications before 2015 to more than seven times that number as of October 2023.

Vertical farming is notorious for its high energy use, spurring a notable increase in energy efficiency, utilisation, and conservation research. Before 2015, only five publications focused on these aspects while reaching nearly fifteen times that number as of October 2023. The

energy consumption is mainly attributed to electric lighting and heating, ventilation and air conditioning (HVAC) systems (Graamans et al., 2018). It is driven by internal loads, mainly attributed to lighting and crops. It has been assessed that, if well insulated, vertical farms' energy consumption is "largely insensitive to location" (Eaton et al., 2023), which means that the outdoor environment has no significant impact on energy consumption. Thus, the main energy consumption for HVAC systems comes from cooling and dehumidification equipment, which are required to dissipate the heat generated by electric lighting and crop transpiration. The cooling and dehumidification equipment ensure the specified indoor air temperature and relative humidity are maintained (Talbot et al., 2021). The choice of indoor air conditions can substantially influence the energy consumption of the space; in buildings, increasing the cooling setpoint from 22.2°C to 25°C has been shown to lead to average savings in cooling energy up to 29% (Hoyt et al., 2015). In parallel, the choice of indoor conditions also influences growth rate.

The growth rate is affected by indoor air conditions, defined by the temperature, humidity, or vapour pressure deficit (VPD). It is also affected by lighting intensity and CO_2 concentration, which, above a specific limit, can reach a saturation point. The VPD, which is the difference between the theoretical pressure exerted by water vapour held in saturated air at a given temperature and the pressure exerted by the water vapour held in the air at the same given temperature, is particularly important. It requires maintaining the air temperature and the humidity level within an acceptable range. Failure to do so can lead to water stress or promote mould growth and diseases, substantially reducing the growth rate or resulting in complete crop loss. Recent crop research has been focused mainly on exploring innovative cultivation techniques and the impact of different indoor environmental conditions to increase yield without compromising nutritional quality. For each crop, and even among different cultivars, optimal growing conditions exist that enhance crop yield in terms of both quality and quantity. For instance, Carotti et al. (2021) investigated the impact of different photosynthetic photon flux densities (PPFD), indoor air conditions and root temperatures on lettuce growth. They maintained the CO_2 concentration at 1200 ppm, the VPD during the photoperiod and dark period at 0.58 kPa and 0.34 kPa, respectively and a photoperiod of 16 hours. Table 6.1

summarises the number of days per cultivation cycle and the production intensity (yield per unit of cultivated area) to produce a 250 g lettuce head of *Lactuca sativa cv. Batavia Othilie* for different indoor conditions. Depending on the PPFD level (200, 400, and 750 μmol $m^{-2}·s^{-1}$) and indoor air temperature (20, 24, and 28°C), the cultivation cycle varied between 18 and 28 days. According to the reported data, the yield increased with PPFD and temperature, with the highest yield at 24°C.

Table 6.1 Cultivation cycle and yield to produce 250g lettuce head with a photoperiod of 16 hours under different indoor air conditions
Taken from Carotti et al. (2021)

PPFD (μmol $m^{-2}·s^{-1}$)	200			400			750		
Temperature (°C)	20	24	28	20	24	28	20	24	28
Cultivation cycle (days)	28.0	25.3	27.0	21.2	19.0	23.6	18.3	18.1	21.2
Production intensity ($kg_{FW}·m^{-2}$)	81	90	84	108	120	97	125	126	108

The data reported by Carotti et al. (2021) are limited to a fixed CO_2 concentration and photoperiod duration. Other researchers have extensively investigated the impact of CO_2 enrichment, and it has been reported that it can improve productivity by 35% (Kozai et al., 2015). Jung et al. (2016) conducted an experiment on *Lactica sativa L.* growing in a vertical farm. Their results indicated that a saturation point is reached at a specific CO_2 concentration; beyond that threshold, increasing the CO_2 concentration no longer notably enhances productivity. This saturation point varies depending on factors such as the stage of growth and the growing conditions. Thus, setting the CO_2 concentration to 1200 ppm ensures that CO_2 is not limiting growth. Regarding the impact of photoperiod duration, Jin, Formiga Lopez, et al. (2023) have reported that crop yield increases linearly for PPFD below 500 $μmol·m^{-2}·s^{-1}$. Similar to CO_2 concentration, saturation can be reached beyond a certain threshold, depending on factors such as the growing conditions. The impact of different combinations of PPFD and photoperiod while maintaining a constant daily light integral (DLI) has also been investigated (Elkins & van Iersel, 2020; Kelly et al., 2020). It was found that for DLI exceeding 10.4 $mol·m^{-2}·d^{-1}$, extending the photoperiod and decreasing the PPFD led to improved yields.

Crop growth also influences the energy use associated with lighting and HVAC systems. As crops grow, their leaves expand, increasing the Photosynthetically Active Radiation (PAR)

intercepted and absorbed by crops. This rise in absorbed radiative energy, through photosynthesis, translates into increased crop transpiration, i.e., the latent heat gain from crops. Consequently, as the crops grow, the latent load increases (EPRI, 2018), which necessitates more dehumidification to remove the humidity generated by the crops (Holden et al., 2021). Moreover, depending on the growing conditions, the leaf temperature is often lower than the air temperature, resulting in the cooling of the air surrounding the crops, which is defined as the sensible heat loss from crops. During the dark period, crops continue to transpire and cool their surroundings, and this effect increases as the leaves expand during growth. Although the humidity setpoint is generally set high, reaching around 85% and 90% during the photoperiod and dark period, respectively (Carotti et al., 2021), dehumidification remains crucial to prevent condensation on colder surfaces, such as the crops leaves, and to mitigate mould growth and diseases. Those phenomena highlight how the choice of growing conditions influences the heat gains/losses from crops, thus indirectly impacting the energy consumption of the space.

Although the influence of growing conditions on yield is well-documented, their influence on both energy consumption and yield is not extensively studied. Consequently, only a few studies have reported energy consumption and yield specifically for lettuce cultivation in vertical farms. As such, Ohyama et al. (2018) and Blom et al. (2022) are among the few that have measured energy consumption of the lighting and HVAC equipment, as well as fresh yield. Conversely, several studies have estimated both the energy consumption and fresh yield of lettuces using energy modelling (Eaton et al., 2023; Graamans et al., 2018; Talbot et al., 2022; Zhang & Kacira, 2020a) or adopted a mixed approach using measured fresh yield combined with an energy model (Blom et al., 2023) or simplifications to estimate the energy consumption (Stanghellini & Katzin, 2023). The data for annual energy intensity, production intensity, and energy consumption per fresh yield, which can be referred to as the specific energy consumption (SEC), are provided in Table 6.2.

Table 6.2 Reported annual energy intensity, production intensity and SEC based on the energy consumption of lighting and HVAC equipment, cultivation area and fresh yield

Reference	Type of results [1]	$T_{a,i}$ [2], °C	$\varphi_{a,i}$ [2], %	PPFD, µmol·m^{-2}·s^{-1}	Photo period, hrs	Production intensity, kg·m^{-2}	Energy intensity, kWh·m^{-2} (%Light/%HVAC) [3]	SEC, kWh·kg^{-1} (MJ·kg^{-1})
Graamans et al. (2018)	M	24-30	65-90	500	16	126	1224-1249 (84-93/7-16)	15.5-15.6 (55.8-56.1)
Ohyama et al. (2018)	E	24	No setpoint	120/200	15	31	588 (N/A) [4]	18.7 (67.3)
Zhang and Kacira (2020a) - low DLI	M	24	No setpoint	226	16	57-58	416-439 (86-90/10-14)	7.1-7.7 (25.6-27.2)
Zhang and Kacira (2020a) - high DLI				260		63	484-527 (82-90/10-18)	7.7-8.3 (27.2-30.0)
Blom et al. (2022)	E	N/A [4]	N/A [4]	140	20	69	1020 (66/34)	14.8 (53.3)
Talbot et al. (2022)	M	21	70	434	12	61	1092 (52/48)	18.0 (64.8)
Blom et al. (2023)	M	24	79	200	16	79	418 (80/20)	5.3 (19.1)
Eaton et al. (2023) - reference	M	19-24	50-85	200	24	104	1259 (69/31)	12.2 (43.9)
Eaton et al. (2023) - optimised							640 (70/30)	6.2 (22.3)
Stanghellini and Katzin (2023)	M	24	80	200	16	91	400 (80/20)	4.4 (15.8)

[1] M: Modelling, E: Experimental
[2] $T_{a,i}$: Indoor air temperature | $\varphi_{a,i}$: Indoor ai relative humidity
[3] Percentage of electricity associated with electric lighting (%Light) and HVAC equipment (%HVAC)
[4] N/A: Not available

Various factors contribute to the observed disparities, including the growing conditions, the lighting and HVAC equipment design, particularly the photosynthetic photon efficacy (PPE) and the coefficient of performance (COP) of the cooling and dehumidification equipment. Moreover, the selected modelling approach and assumptions are also influential for the modelled results.

The energy intensity ranges from 400 kWh·m^{-2} to 1260 kWh·m^{-2}, being primarily influenced by the combination of PPFD (140 to 500 mol·m^{-2}·s^{-1}), photoperiod (12 to 24 hours) and PPE

(1.5 to 3.5 $\mu mol \cdot J^{-1}$). Furthermore, certain results are based on minimal or no dehumidification energy consumption, leading to lower energy intensity. For instance, Graamans et al. (2018) and Eaton et al. (2023) used floating humidity setpoints, while Zhang and Kacira (2020a) did not specify any humidity setpoint. Given the high energy requirement for dehumidification, a model that tightly controls temperature and humidity will likely exhibit higher energy intensity. This aligns with experimental findings. For example, Ohyama et al. (2018) reported a much lower energy intensity of 588 $kWh \cdot m^{-2}$ in their vertical farm compared to 1020 $kWh \cdot m^{-2}$ in the study by Blom et al. (2022), despite having similar PPFD and photoperiod. Indeed, Ohyama et al. (2018) had no humidity control and a PPE of 2.9 $\mu mol \cdot J^{-1}$, while Blom et al. (2022) results included the use of an independent dehumidification system and a low PPE of 1.5 $\mu mol \cdot J^{-1}$. The only exception among the studies reported in Table 6.2 is the model from Blom et al. (2023), which has a low energy intensity of 418 $kWh \cdot m^{-2}$. This is explained by the HVAC equipment that cools and dehumidifies indoor air, a single packaged air handling unit with an overall COP of 3.6. Single packaged air handling units are far more efficient than conventional systems, like split cooling units combined with independent dehumidifiers, as modelled by Talbot et al. (2022) and Eaton et al. (2023). Also, the annual energy intensity estimated by Blom et al. (2023) did not include the energy consumption during the dark photoperiod, for which dehumidification is usually needed.

The production intensity ranges from 31 $kg_{FW} \cdot m^{-2}$ to 126 $kg_{FW} \cdot m^{-2}$, primarily influenced by the crop growth rate, planting crop density and the weight of harvested lettuce head. The median production intensity reported is 66 $kg_{FW} \cdot m^{-2}$, which is relatively low, as it has the potential to reach at least 90 $kg_{FW} \cdot m^{-2}$ and theoretically go up to 190 $kg_{FW} \cdot m^{-2}$ (Blom et al., 2023) for a planting crop density of 25 $plants \cdot m^{-2}$, a harvested weight of 250 g, and given the growing conditions outlined by Carotti et al. (2021). The results suggest that the growing conditions used by Ohyama et al. (2018) and Blom et al. (2022) may have limited growth; notably, Blom et al. (2022) did not have any CO_2 enrichment system.

The energy consumption per fresh yield, the SEC, is the main indicator used to assess and improve energy efficiency. Most SEC reported in the literature are derived from energy

models, while a minority are based on experimental results or survey data from operational facilities (Sabeh et al., 2022). The SEC ranges from 4.4 to 18.7 $kWh \cdot kg_{FW}^{-1}$ of fresh weight, indicating a considerable variation, which is even more pronounced when considering various crops, with SEC ranging from 3.2 to 59.1 $kWh \cdot kg_{FW}^{-1}$ (Ahamed et al., 2023; Eaton et al., 2023; Weidner et al., 2021). Although SEC is a widely used indicator for assessing vertical farming energy efficiency, it may be insufficient. Two facilities could have similar SEC values yet have significantly different production intensities.

Amongst the studies that have reported numerical results in Table 6.2, differences in the modelling approach were observed. Regarding growth modelling, most studies used Van Henten's model, which has been validated for semi-closed greenhouses but might not be suitable for vertical farms in its original form (Graamans et al., 2018; Talbot & Monfet, 2024). Blom et al. (2023) did not model growth and instead relied on experimental data to estimate yield. This approach lacks the versatility to assess energy consumption and yield under different growing conditions, as it would require conducting experiments for each set of conditions. Regarding energy modelling, most studies assumed the heat gains/losses from crops remained constant, overlooking their variation as the lettuces grew. In most cases, the modelling approaches for energy and growth were decoupled. This means most of the study neglected the indirect influence of growing conditions and that the growth model was only used to estimate yield.

To balance energy consumption and yield in vertical farms, it is essential to grasp the influence of growing conditions on both energy consumption and yield. Given the many possible combinations of parameters, comparing existing studies and understanding how growing conditions influence energy consumption and yield is challenging for several reasons. Each study has focused on a specific set of conditions, while numerous combinations of growing conditions (e.g., air temperature, VPD, PPFD, photoperiod, CO_2 concentration) are possible. Moreover, the combinations selected generally resulted in low productivity intensity, which hinders understanding the influence of growing conditions on the energy efficiency of highly productive vertical farms. Additionally, some studies did not consider highly influential

factors, such as CO_2 enrichment, precise control of temperature and humidity, and the implementation of the dehumidification systems typically found in vertical farms. Furthermore, the energy consumption during the dark period must be included in the calculation, as it is not negligible. Comparing studies is also challenging due to significant variations in HVAC and lighting systems, including the type of equipment, the COP of the equipment, and lighting efficacies. Consequently, analysing the results from these studies and determining how the growing conditions influence energy efficiency in vertical farms is complex. Thus, for vertical farms, the influence of growing conditions on energy consumption and yield remains sparsely documented. Furthermore, ongoing research should aim to identify the best combination of growing conditions for vertical farms, including the corresponding impact on energy load, according to the space energy balance. This approach offers more insightful results than solely energy consumption assessment, which is influenced by the performance of HVAC equipment (Weidner et al., 2021). Clear conclusions remain elusive, necessitating further research to simultaneously investigate the influence of the growing conditions on energy load and yield, which requires a dynamic modelling approach tailored for vertical farms.

This study aims to bridge this gap by completing a comprehensive parametric analysis of growing conditions and their influence on energy load and yield of a small-scale vertical farm, a high-density controlled environment agriculture (CEA) space. The selected growing conditions cover many real-world possibilities, including combinations that result in high productivity intensities. The analysis uses a transient modelling approach that integrates a dynamic crop model adapted to vertical farming applications to estimate (1) the heat exchanges between the crops and their environment while crops grow and (2) yield. The objective is to gain a deeper understanding of the energy requirements and their sensitivity to growing conditions, all while considering the influence of these growing conditions on crop yield.

6.2 Methodology

This paper aims to evaluate the influence of growing conditions on the energy load and yield of high-density CEA spaces. The selected approach estimates the energy load and yield using a crop growth model for growing scenarios using a high-density CEA space model created in a building performance simulation (BPS) tool. The scenarios result from all possible combinations of several growing conditions, and the energy load is calculated based on the space energy demand, excluding HVAC equipment.

The design and operation of high-density CEA spaces are challenging and require complex HVAC equipment to meet the grower's operation requirements. High-density CEA spaces, commonly referred to as vertical farms, are usually airtight and thus include two main sources/sinks of heat: the gains from lighting and the gains/losses from crops (Talbot & Monfet, 2020). Lights and crops induce significant loads, leading to high energy loads in electricity, cooling and dehumidification. Energy modelling can assist the design and operation of energy-efficient CEA spaces. Two different approaches are proposed in the literature. The first one consists of using programming software (e.g., MATLAB), and the second one is using BPS tools (e.g., EnergyPlus, TRNSYS, etc.). BPS tools offer many advantages since they are used for different building applications. These advantages include meteorological data availabilities for several weather stations that are easy to use as inputs, thermal exchanges that are modelled according to well-established formulations, and extensive libraries of equipment. Creating a building model with a BPS tool is thus much faster and less prone to errors than developing a new script written from scratch in programming software. Hence, several researchers prefer using a BPS tool to model agricultural spaces such as greenhouses, plant factories or building integrated agricultural spaces to assess the space energy demand and HVAC energy end use (Ahamed et al., 2023). Co-simulation is sometimes chosen to model the space and crops using two tools (Jans-Singh et al., 2021).

Crops have been included in models of agricultural spaces to estimate energy load and crop yield to improve the analysis of CEA spaces. This involves modelling the heat exchanges of

crops with their environment, referred to as the “airnode” in most BPS tools, including latent heat gains, sensible heat gains or losses and light interception. Figure 6.1 illustrates some heat exchanges in a vertical farm, highlighting the close interaction between lighting and crops. Lighting influences the magnitude of the heat gains/losses from crops, and as the crops grow, the heat gains from lighting decrease due to light interception.

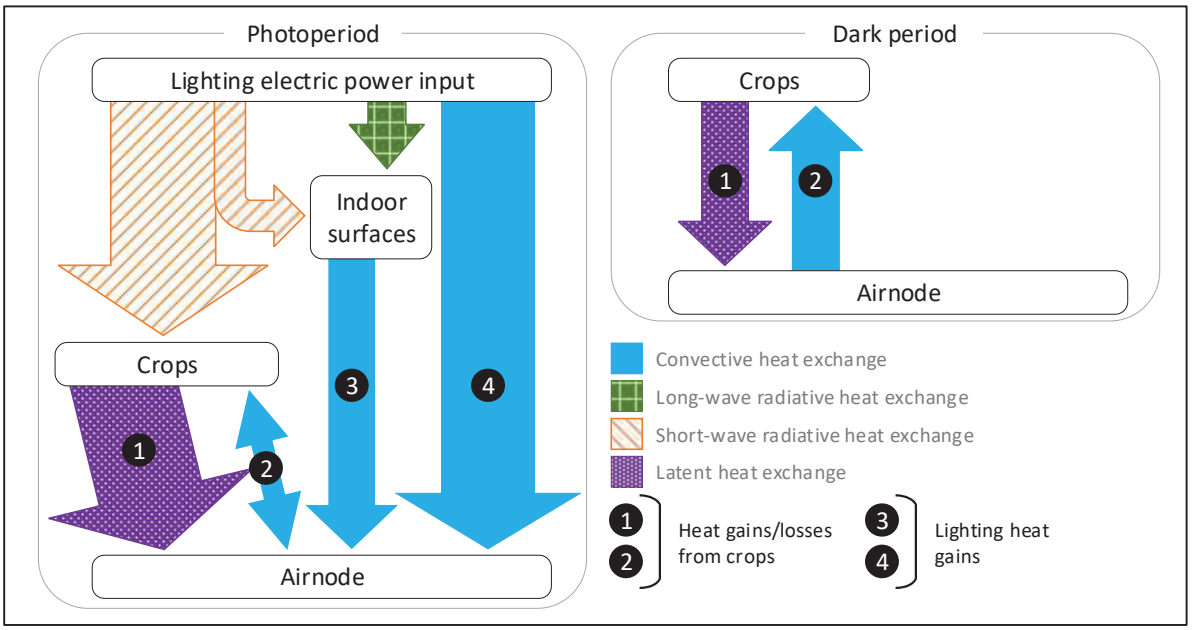

Figure 6.1 Visualisation of the heat exchanges that occur between lights, crops, indoor surfaces and the airnode within a CEA space

Thus, several thermal phenomena must be modelled to estimate the load, which includes the electric energy demand for lighting as well as the rate of sensible and latent heat to be removed or added to maintain a constant room air temperature and humidity level.

6.2.1 Description of the model

The high-density CEA space model, the vertical farm, was created in TRNSYS (Klein & al., 2017) and included three main components: electric lighting, crops, and a thermal zone. Figure 6.2 illustrates the interactions between these components and the flow of variables between them and also provides a visual representation of the model's inputs and outputs. The dynamic

crop model includes an energy balance and a growth model to estimate the heat exchanges between crops and their environment as they grow (Talbot & Monfet, 2024). The high-density CEA model has been previously validated using numerical results from Graamans et al. (2018): the differences in energy load intensities were 0%, 5% and 1% for lighting, cooling and dehumidification, respectively (Talbot & Monfet, 2024).

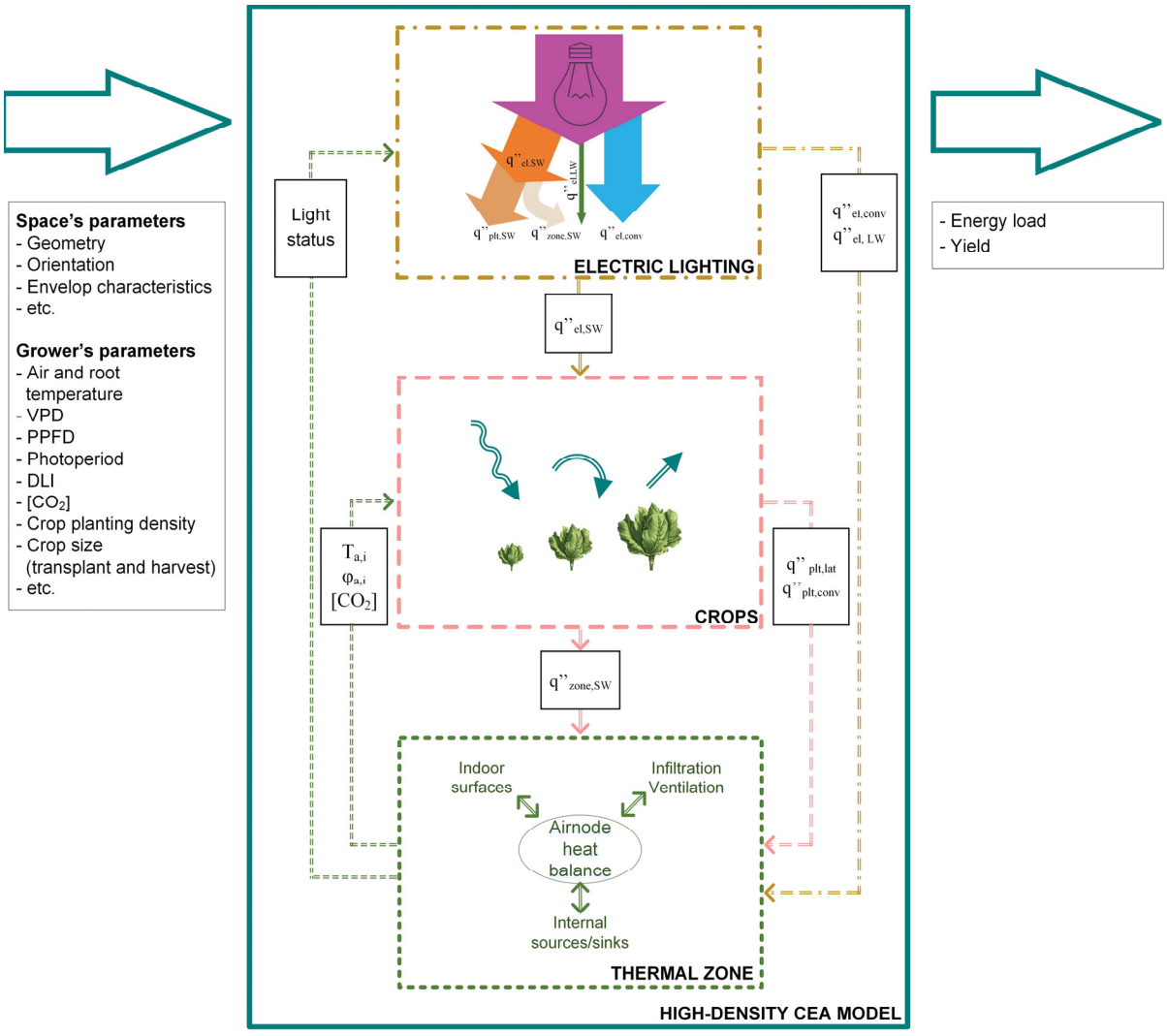

Figure 6.2 Overview of the model

The thermal zone model includes gains/losses from the electric lighting component and the crop model. The electric lighting component divides the associated heat gain in three main

gains, as also illustrated in Figure 6.1: the convective lighting heat gain ($q''_{el,conv}$), which is sent directly to the thermal zone; the long-wave lighting heat gain ($q''_{el,LW}$), which is treated as part of the radiative heat gain to the thermal zone; and the photosynthetic active radiation (short-wave radiation) from electric lighting ($q''_{el,SW}$), which is divided into two parts, one is absorbed by the crops ($q''_{plt,SW}$) and the other one is computed as a radiative heat gain to the thermal zone ($q''_{zone,SW}$). For the crop model, at every simulation time step, the indoor air conditions – air temperature ($T_{a,i}$), relative humidity ($\varphi_{a,i}$) and carbon dioxide concentration ([CO_2]) – and the photosynthetic active radiation (short-wave radiation) from electric lighting ($q''_{el,SW}$) are used as inputs to estimate the heat gains/losses from crops ($q''_{plt,lat}$ and $q''_{plt,conv}$). Those are considered additional internal heat gains/losses to the thermal zone. The model outputs the energy load, which is the sum of the lighting, cooling, dehumidification and heating loads. These correspond to the integral over time of the lighting power input, the rate of sensible heat removal, the rate of latent heat removal and the rate of sensible heat addition. These rates are calculated at each time step to maintain the specified indoor air conditions (temperature and relative humidity) at all times. Each component is further described in sections 6.2.1.1 to 6.2.1.3.

6.2.1.1 Thermal zone

In high-density CEA spaces, crops grow at high density –stacked vertically or horizontally – and only electric lighting is used. Figure 6.3 illustrates the modelled high-density CEA space, which is located in a building maintained at an ambient temperature of 20°C. The enclosure properties are listed in Table 6.3. The indoor surfaces are covered with water-repellent panels to minimise water vapour migration through the envelope. The space is enriched in CO_2 to enhance crop growth and is airtight to avoid the dilution of the CO_2. Moreover, it is assumed that the air is well-mixed and air velocity over the leaves is sufficient to facilitate gas exchange.

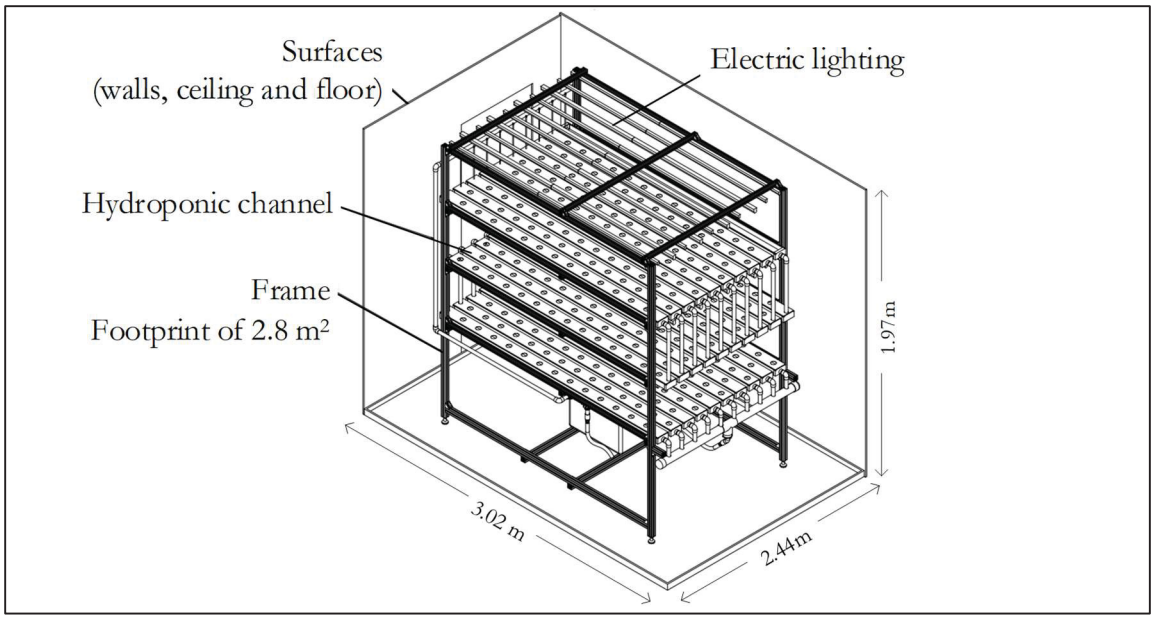

Figure 6.3 Small-scale high-density CEA space

Table 6.3 Characteristics of the envelope of the high-density CEA space

U-Value, $W \cdot (K \cdot m^2)^{-1}$	0.12
Thermal capacity, $J \cdot (kg \cdot K)^{-1}$	1000
Density, $kg \cdot m^{-3}$	113.17

6.2.1.2 Electric lighting

Growing conditions alternate between two states: (1) photosynthesis that occurs during the photoperiod (when the electric lighting is on) and (2) respiration that occurs during the dark period (when the electric lighting is off). The photoperiod is set to start at 00:00, i.e., the lighting is turned on at 00:00. As previously stated, the electric lighting power input (q''_{el}) is split in three: the convective heat gain ($q''_{el,conv}$), the long-wave radiation heat gain ($q''_{el,LW}$), and the short-wave radiation ($q''_{el,SW}$). The latter is divided into two: the radiation absorbed by crops ($q''_{plt,SW}$) and the radiation not absorbed by crops ($q''_{zone,SW}$), which is computed as a radiative heat gain to the thermal zone. Equations (6.1) to (6.5) define the electric lighting heat gains, while the main characteristics of the electric lighting are listed in Table 6.4.

$$q''_{el,conv} = f_{conv} \cdot q''_{el} \tag{6.1}$$

$$q''_{el,LW} = f_{LW} \cdot q''_{el} \tag{6.2}$$

$$q''_{el,SW} = f_{SW} \cdot q''_{el} \tag{6.3}$$

$$q''_{plt,SW} = \left(1 - e^{-k_{s,el}LAI}\right) \cdot q''_{el,SW} \tag{6.4}$$

$$q''_{zone,SW} = q''_{el,SW} - q''_{plt,SW} \tag{6.5}$$

Where q''_{el} is the electric lighting power input ($W \cdot m^{-2}_{cultivated}$); $q''_{el,conv}$ is the convective heat gain from electric lighting ($W \cdot m^{-2}_{cultivated}$); $q''_{el,LW}$ is the long-wave radiation heat gain from electric lighting ($W \cdot m^{-2}_{cultivated}$); $q''_{el,SW}$ is the short-wave radiation flux from electric lighting ($W \cdot m^{-2}_{cultivated}$); $f_{conv}/f_{SW}/f_{LW}$ are the electric lighting heat fractions; $q''_{plt,SW}$ is the short-wave radiation flux absorbed by the crops from electric lighting ($W \cdot m^{-2}_{cultivated}$); $k_{s,el}$ is the extinction coefficient associated to PAR from electric lighting; and $q''_{zone,SW}$ is the short-wave radiation flux not absorbed by crops from electric lighting ($W \cdot m^{-2}_{cultivated}$). The extinction coefficient, which accounts for the light attenuation in the canopy, depends on the leaf optical properties, the geometry of the crops, and the wavelength of the light.

Table 6.4 Characteristics of the electric lighting

Lamp type	LED
Photosynthetic photon efficacy (PPE)	2.6 $\mu mol \cdot J^{-1}$
Heat fractions ($f_{conv}/f_{lw}/f_{sw}$)	0.37 / 0.11 / 0.52

6.2.1.3 Crops

The dynamic crop model combines an energy balance and a growth model to estimate the heat exchanges between crops and their environment as they grow. The energy balance is an

adaptation of the validated model proposed by Graamans et al. (2017), which was adjusted to enhance its versatility (Talbot & Monfet, 2024). The growth model is an adaptation of the one initially proposed by Van Henten (1994), which has been adjusted for high-density CEA application by Talbot and Monfet (2024). As such, certain equations of the original model were revised based on recent literature and four sensitive parameters were calibrated using the experimental dataset from Carotti et al. (2021). Calibration was conducted for nine sets of conditions based on fresh weight per plant, resulting in root mean square error (RMSE) ranging from 2.1 to 18.2 g_{FW}·plant^{-1}. It was demonstrated that this calibration led to relative differences in the energy load per fresh weight, the specific energy load, of 0.1% to 3.5% over a growth cycle compared to the specific energy load obtained from the experimental dataset. This last verification ensures that the calibrated model was suitable for energy analysis since it induces reasonable errors. Additionally, the growth model was assessed for its suitability under different lighting intensities compared to those used by Carotti et al. (2021), resulting in a satisfactory level of robustness with R-square ranging from 0.86 to 0.92. Details of the growth model and the values of the calibrated parameters are provided in Table-A II-1. The growth model estimates, at every timestep, the total (shoot and root) plant dry weight (DW_{tot}), the shoot fresh weight (FW_{sht}) and the leaf area index (LAI) for a root temperature equal to air temperature and a constant CO_2 concentration of 1200 ppm. The LAI is defined as the ratio of the total leaf area to the cultivated area and can be estimated by multiplying the crop's leaf area by the planting crop density. The LAI plays a crucial role in the energy balance as it significantly influences some of the heat exchanges within the space, such as:

- the portion of the PAR absorbed by crops ($q''_{plt,SW}$) and the associated radiative heat gain from electric lighting ($q''_{zone,SW}$) estimated according to equations (6.4) and (6.5), respectively;
- the heat gains/losses from crops as the leaves grow, more specifically the crops latent heat gain ($q''_{plt,lat}$) and crops sensible heat gain/loss ($q''_{plt,conv}$) estimated using equations (6.6) and (6.7), respectively.

$$q''_{plt,lat} = LAI \cdot \lambda \frac{\chi_s - \chi_a}{r_s + r_a} \tag{6.6}$$

$$q''_{plt,conv} = LAI \cdot \rho_{a,i} \cdot c_{p_{a,i}} \frac{T_{plt} - T_{a,i}}{r_a} \quad (6.7)$$

Where $q''_{plt,lat}$ is the crops latent heat gain ($W \cdot m^{-2}_{cultivated}$); $q''_{plt,conv}$ is the crops convective heat gain or loss; LAI is the Leaf Area Index ($m^2_{leaves} \cdot m^{-2}_{cultivated}$); λ is the heat of vaporisation of water ($kJ \cdot kg^{-1}$); χ_s is the vapour concentration at the canopy level ($g \cdot m^{-3}$); χ_a is the air vapour concentration ($g \cdot m^{-3}$); r_s is the stomatal resistance ($s \cdot m^{-1}$); $r_a$is the aerodynamic resistance ($s \cdot m^{-1}$); $\rho_{a,i}$ is the indoor air density ($kg \cdot m^{-3}$); $c_{p_{a,i}}$ is the specific heat of the indoor air ($J \cdot (kg \cdot K)^{-1}$); T_{plt} is the leaves temperature (°C); and $T_{a,i}$ is the indoor air temperature.

6.2.2 Growing conditions

The selected growing conditions cover various growing conditions, including different dry bulb air temperature setpoints, VPD setpoints and lighting intensities. Each combination of these growing conditions represents a scenario wherein the energy load of the space and crop yield is estimated. The CO_2 concentration and VPD during the dark period are set at 1200 ppm and 0.48 kPa for all growing conditions. Also, the root temperature is equal to the air temperature, the crop planting density is 25 $crops \cdot m^{-2}$, the transplant weight is fixed at 1.2 $g_{FW} \cdot plant^{-1}$, and the harvested weight is specified as the maximum marketable weight of 250 $g_{FW} \cdot plant^{-1}$.

6.2.2.1 Air temperature and vapour pressure deficit (VPD)

Air temperature influences energy load, heat gains/losses from crops and crop growth, while VPD influences energy load and heat gains/losses from crops. Table 6.5 tabulates the selected temperatures and their corresponding relative humidity for the photoperiod/dark period, which vary according to the VPD setpoint. The temperature range is set between 20°C (lower limit) and 28°C (upper limit) based on experimental data reported by Carotti et al. (2021).

Additionally, the VPD for the photoperiod and dark period, with a VPD range during the photoperiod of 0.54 kPa (lower limit) and 0.85 kPa (upper limit), are specified in Table 6.5.

Table 6.5 Air temperature and associated relative humidity for a constant VPD maintained during photoperiod/dark period of 0.54/0.48 kPa and 0.85/0.48 kPa

Air temperature, °C	**Relative humidity (photoperiod / dark period), %**	
	VPD of 0.54 / 0.48 kPa	**VPD of 0.85 / 0.48 kPa**
20	77 / 79	64 / 79
24	82 / 84	71 / 84
28	86 / 87	77 / 87

6.2.2.2 Photosynthetic photon flux density (PPFD)

PPFD influences energy load, heat gains/losses from crops, crop growth and lighting heat gains. Table 6.6 tabulates the selected PPFD and their corresponding DLI for photoperiods of 12-, 14-, 16-, 18- , 20- and 22-hours. The PPFD range of 200 to 700 $\mu mol \cdot m^{-2} \cdot s^{-1}$ is based on experimental data from Carotti et al. (2021). A photoperiod of 24 hours is not considered because both Pennisi et al. (2020) and Silva et al. (2022) suggested that the optimal photoperiod for lettuce might be shorter than 24 hours. Silva et al. (2022) observed that at a PPFD of 400 $\mu mol \cdot m^{-2} \cdot s^{-1}$, continuous light significantly hindered lettuce growth and led to the lowest lighting energy efficiency compared to photoperiods of 12 to 22 hours. Moreover, the number of scenarios is limited by the use of DLI ranging from 11.5 to 43.2 $mol \cdot m^{-2} \cdot day^{-1}$ as reported by Carotti et al. (2021).

The combination of all these growing conditions results in 180 scenarios, as illustrated in Figure 6.4.

Table 6.6 Resulting DLI (mol·m^{-2}·day^{-1}) values for PPFD of 200 to 700 µmol·m^{-2}·s^{-1} combined to a photoperiod of 12-, 14-, 16-, 18- , 20- and 22-hours

Photoperiod, hrs / PPFD, µmol·m^{-2}·s^{-1}	12	14	16	18	20	22
200	-	-	11.5	13.0	14.4	15.8
300	13.0	15.1	17.3	19.4	21.6	23.8
400	17.3	20.1	23.0	25.9	28.8	31.7
500	21.6	25.2	28.8	32.4	36.0	39.6
600	25.9	30.2	34.6	38.9	43.2	-
700	30.2	35.3	40.3	-	-	-

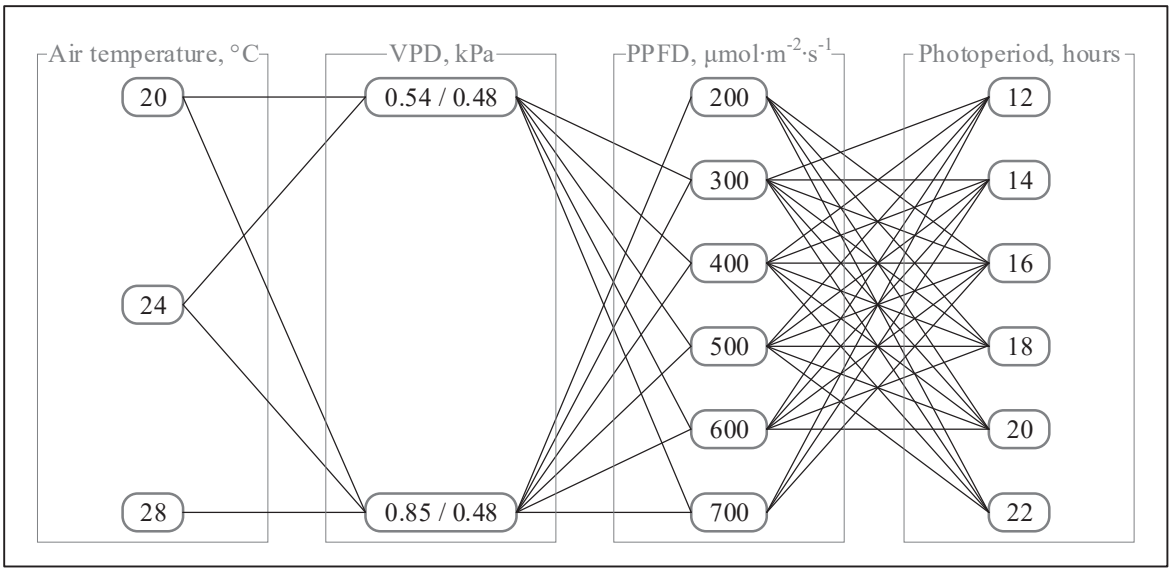

Figure 6.4 Representation of the 180 scenarios

6.3 Results

Annual simulations are completed for each of the 180 scenarios to compile data on the space energy demand, the associated energy load, the energy load per category and crop yield. Figure 6.5 displays the annual crop yield and energy load for all scenarios (Figure 6.4), with distinct symbols for photoperiods.

The results unveil disparities in annual energy load and crop yield, ranging from 35 to 98 GJ and 560 to 1,631 kg_{FW}, respectively. Moreover, the specific energy load, which assesses the efficiency of the production process, varied between 37.0 to 117.8 $MJ \cdot kg_{FW}^{-1}$. The results illustrate indoor environment conditions' significant influence on energy load and crop yield. The energy load increases linearly with crop yield as the duration of the photoperiod increases. Notably, the slope of this linear regression consistently steepens with higher PPFD, indicating that the trade-off between yield and energy load is declining at high PPFD.

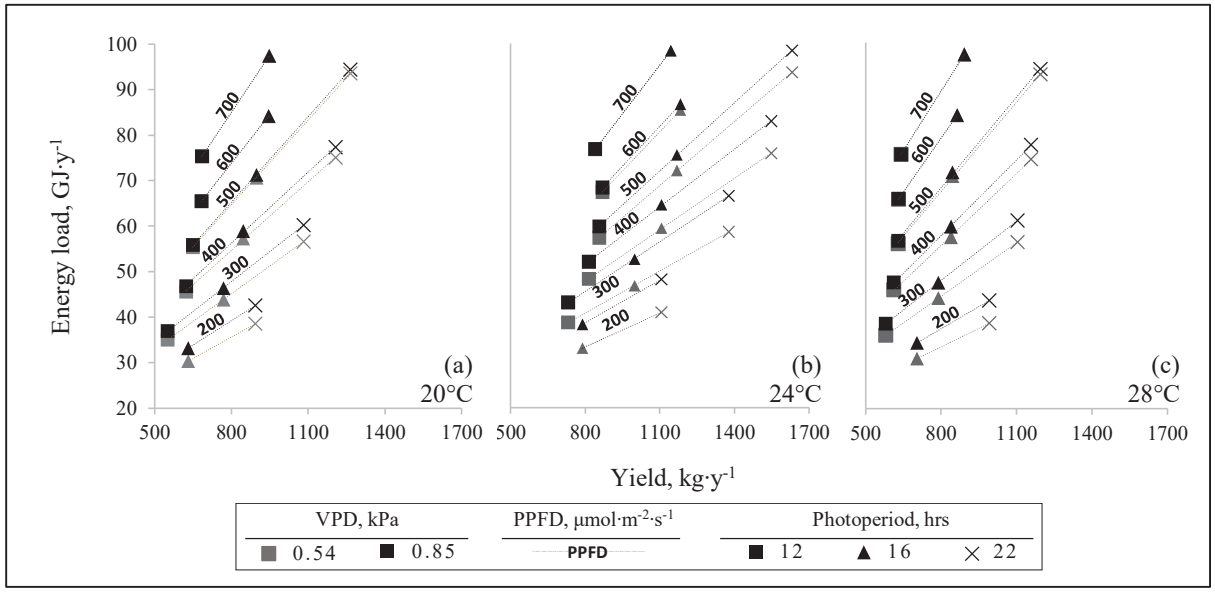

Figure 6.5 Annual energy load and yield for scenarios with a photoperiod of 12, 16 and 22 hours

The energy load per category averaged over the temperature for scenarios with a VPD of 0.54 kPa is illustrated in Figure 6.6. For those scenarios, the main energy load is for lighting, which accounts for 42-50% of the energy load. Meanwhile, cooling, dehumidification and heating contribute to 23-35%, 14-26% and 1-9% of the energy load, respectively.

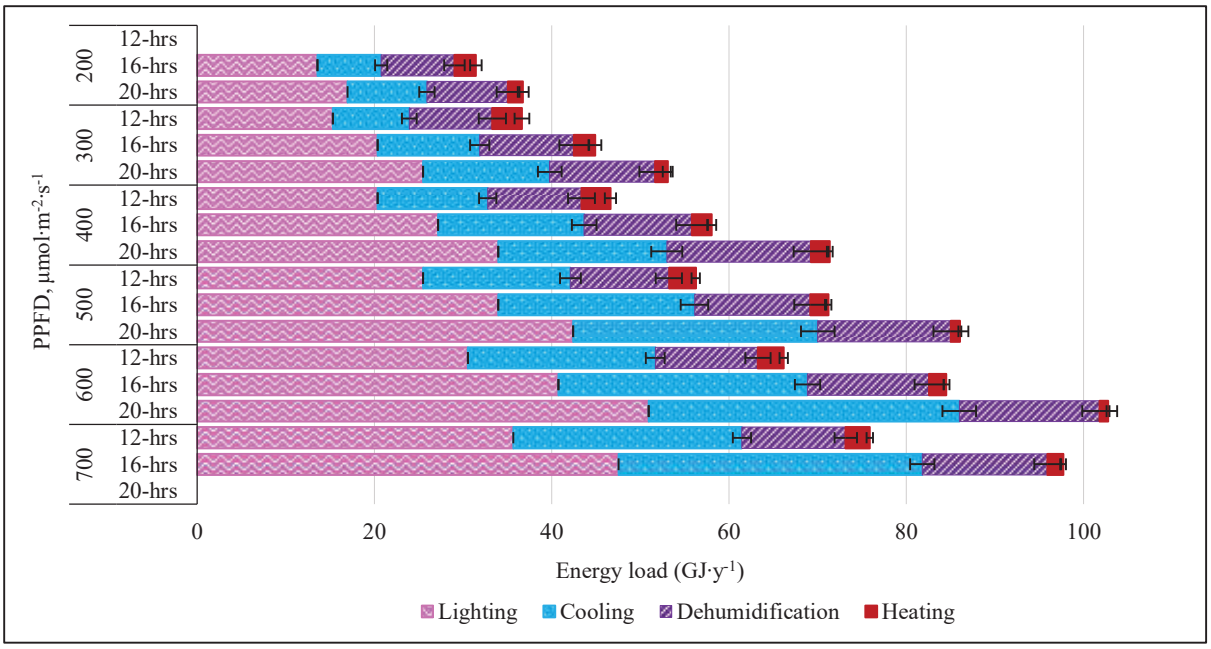

Figure 6.6 Energy load per category averaged over the temperature for scenarios with a VPD of 0.54 kPa

A separate analysis of the growing conditions is conducted to understand better the disparities observed in the results depicted in Figure 6.5. This analysis assesses the influences of each growing condition category on energy load and crop yield.

6.3.1 Air temperature

The influence on the energy load using lower (20°C) or higher temperature (28°C) setpoints, with 24°C as the reference, is illustrated in Figure 6.7.

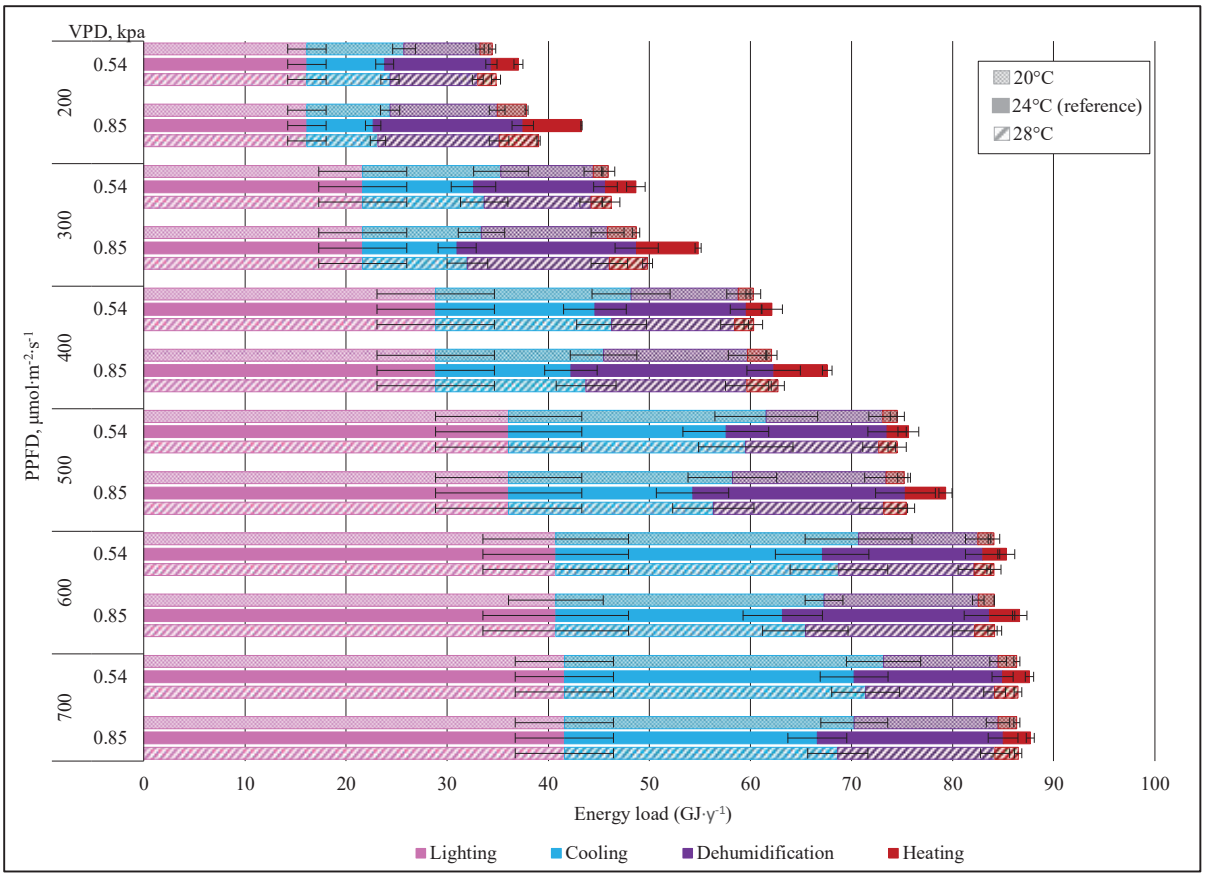

Figure 6.7 Energy load per category averaged over the photoperiod for scenarios with an air temperature of 20°C, 24°C and 28°C

The most significant reduction in energy load due solely to changes in air temperature occurs at the lowest PPFD, gradually decreasing with higher PPFD. Moreover, the reduction is more critical at high VPD than at low VPD. At a VPD of 0.85 kPa, when temperatures are set to 20°C and 28°C, the maximum reductions are 13% and 10%. When PPFD reaches 500 and 700 $\mu mol \cdot m^{-2} \cdot s^{-1}$, reductions below 2% are observed, whether under low or high VPD. This highlights that for high PPFD, the influence of the air temperature on energy load becomes less significant, i.e., the energy load is driven by the lighting and the required cooling rather than dehumidification.

Regarding the energy load per category, lowering the air temperature to 20°C increases the cooling load. The overall decrease in energy load is attributed to lower dehumidification and

heating loads. This is explained by lower heat gains/losses from crops at 20°C. The heat gains/losses from crops peak at 24°C, leading also to a reduction in energy load when the air temperature is raised to 28°C. When the air temperature is raised to 28°C, one would expect a decrease in cooling load due to the higher air temperature. Surprisingly, the results show an increase in cooling load. This is attributed to the heat gains/losses from crops: the crops cool their surroundings to a lesser extent at 28°C than at 24°C, mitigating the reduction in cooling demand expected for a higher air temperature setpoint. This dampens the benefit of raising the temperature to reduce the cooling load. Considering all those complex interactions, a more significant reduction is consistently achieved when the air temperature changes to 20°C rather than 28°C. The scenarios at 24°C consistently exhibit the highest dehumidification load per fresh yield.

Crop yield is also reduced by changes in air temperature to 20°C or 28°C, ranging from 11% to 27%. The combined reduction in energy load and crop yield reduces specific energy load, as illustrated in Figure 6.8, ranging from 1% to 35%. Thus, when considering energy load and crop yield simultaneously, maintaining the temperature at 24°C is the best option, resulting in the lowest specific energy load, especially at high PPFD. It is worth noting that for scenarios at 200 $\mu mol \cdot m^{-2} \cdot s^{-1}$ and 0.85 kPa, a mere 1% increase is observed when the temperature changes to 28°C.

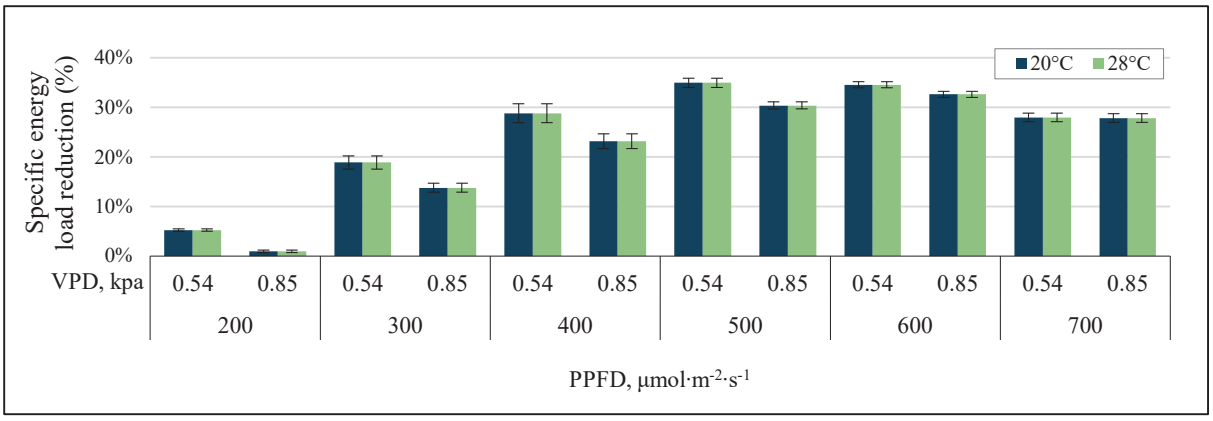

Figure 6.8 Reduction in specific energy load resulting from changes in temperature with a reference air temperature of 24°C

6.3.2 VPD

The influence of using a low VPD (0.54 kPa) on energy load, with a high VPD (0.85 kPa) being considered as the reference, is illustrated in Figure 6.9.

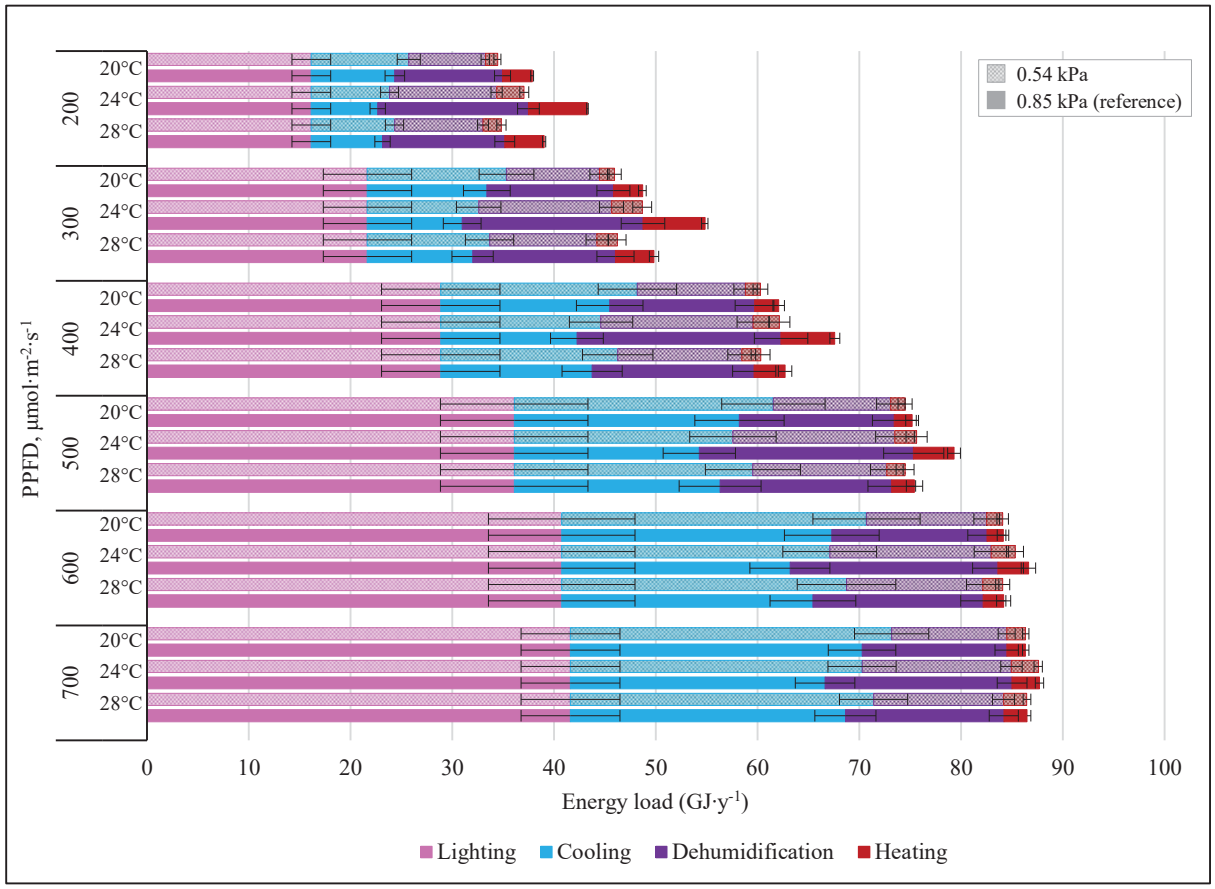

Figure 6.9 Energy load per category averaged over the photoperiod for scenarios with a VPD of 0.54 kPa and 0.85 kPa

Lowering the VPD leads to a higher reduction in energy load at lower PPFD. This reduction is more important at 24°C, reaching 14%, while it is 9% and 11% for air temperatures of 20°C and 28°C, respectively. Reductions of less than 2% are noted for PPFD exceeding 500 µmol·m^{-2}·s^{-1} at air temperatures of 20°C and 28°C and exceeding 600 µmol·m^{-2}·s^{-1} at 24°C, demonstrating that at high PPFD, the influence of VPD on the energy load becomes negligible. Regarding the energy load per category, lowering the VPD at low PPFD leads to higher relative humidity, which lowers the dehumidification load and heat gains/losses from crops. The latter

results in a slight increase in cooling load. As the PPFD rises, heat gains/losses from crops become more critical. At high PPFD, lowering the VPD reduces the dehumidification load but significantly increases the cooling load. At 700 $\mu mol \cdot m^{-2} \cdot s^{-1}$, the reduction in dehumidification load is entirely offset by the increase in cooling load.

Crop yield is not affected by lowering the VPD since it is assumed that VPDs of 0.54 kPa and 0.85 kPa do not induce water stress and, thus, do not limit crop growth.

6.3.3 PPFD

When maintaining a constant photoperiod, increasing the PPFD leads to higher lighting and cooling demands due to lighting, resulting in a substantial rise in energy load. The combined energy load for lighting and cooling increases from 50% to 87% with higher PPFD.

Figure 6.10 illustrates how energy load and crop yield vary with the PPFD for an air temperature of 24°C, VPD of 0.54 kPa, and photoperiods of 12 to 22 hours. The energy load increases linearly with the PPFD for each photoperiod. Likewise, crop yield increases linearly for PPFD below 500 $\mu mol \cdot m^{-2} \cdot s^{-1}$, which aligns with information reported by Jin, Formiga Lopez, et al. (2023), which was also corroborated in the development of the growth model by Talbot and Monfet (2024). However, beyond 500 $\mu mol \cdot m^{-2} \cdot s^{-1}$, other limiting factors come into play, diminishing production efficiency at high PPFD.

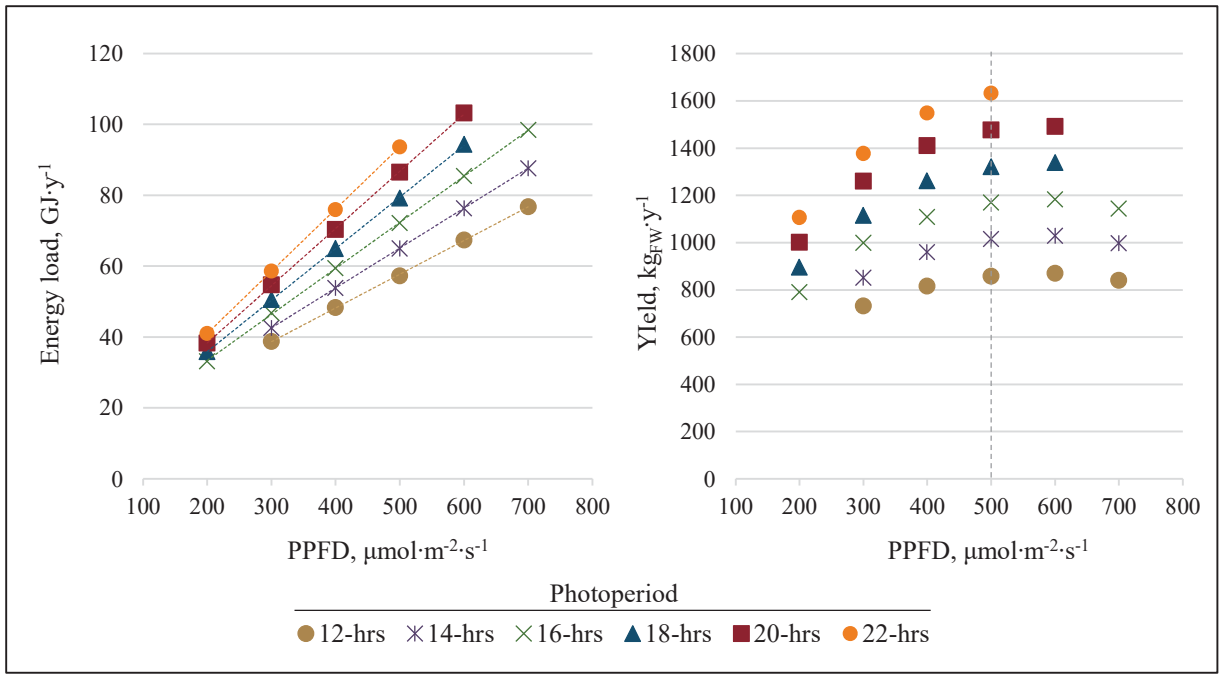

Figure 6.10 Variation in annual energy load and yield with PPFD at an air temperature of 24°C, VPD of 0.54 kPa, and photoperiods of 12 to 22 hours

6.3.4 Yield for different combinations of PPFD/photoperiod for a constant DLI

Additional results are generated at an air temperature of 24C° and VPD of 0.54 kPa to investigate the influence of varying the PPFD while maintaining a constant DLI of 14, 18 and 20 $mol \cdot m^{-2} \cdot d^{-1}$. Table 6.7 tabulates the selected PPFD and their corresponding photoperiods for DLI of 14, 18, 20, 22 and 24 $mol \cdot m^{-2} \cdot d^{-1}$.

Table 6.7 Resulting photoperiod (hours) for PPFD of 200 to 700 µmol·m^{-2}·s^{-1} combined to a DLI of 14, 18, 20, 22 and 24 mol·m^{-2}·day^{-1}

DLI, mol·m^{-2}·d^{-1} / **PPFD, µmol·m^{-2}·s^{-1}**	**14**	**18**	**20**	**22**	**24**
200	19.4	-	-	-	-
300	13.0	16.7	18.5	20.4	-
400	-	12.5	13.9	15.3	16.7
500	-	-	-	12.2	13.3
600	-	-	-	-	-
700	-	-	-	-	-

Figure 6.11 illustrates how energy load and crop yield vary with the PPFD for an air temperature of 24°C, VPD of 0.54 kPa, and DLI of 14, 18, 20, 22 and 24 mol·m^{-2}·d^{-1}. When PPFD is lowered by 100 µmol·m^{-2}·s^{-1} while maintaining a constant DLI, it leads to a modest reduction in energy load of 2 to 7%. Although scenarios with the same DLI have identical lighting loads, reducing the PPFD and extending the photoperiod slightly decrease the cooling, dehumidification and heating loads. Regarding crop yield, extending the photoperiod while maintaining a constant DLI increases crop yield, ranging from 20% to 24%. Lowering the PPFD while extending the photoperiod is particularly interesting as it substantially impacts crop productivity and, to a lesser extent, holds the potential to improve energy load, ultimately improving the specific energy load.

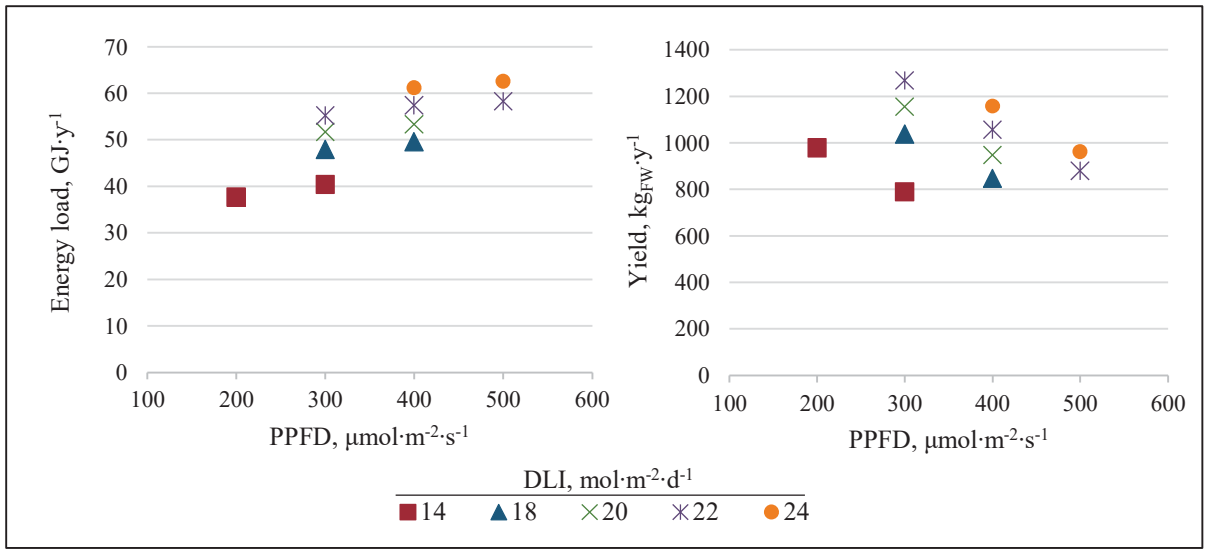

Figure 6.11 Variation in annual energy load and yield with PPFD at an air temperature of 24°C and VPD of 0.54 kPa for DLI of 14, 18, 20, 22 and 24 mol·m^{-2}·d^{-1}

6.4 Discussion

The results obtained, the energy intensity, production intensity, and specific energy load of the scenarios at 24°C and 0.54 kPa, are compared with data reported in the literature, as illustrated in Figure 6.12. The additional data included are from two studies (Blom et al., 2023; Graamans et al., 2018) that have estimated the energy load associated with space energy demands. It is important to specify that for a vertical farm with negligible heat exchanges through the building envelope, the impact of the size of the high-density CEA space has minimal impact under similar growing conditions. As an example, the numerically estimated annual energy load intensities for cooling and dehumidification were within 5% and 1%, respectively, for vertical farms having a footprint of 7.4 m^2 and 50,000 m^2 (Talbot & Monfet, 2024).

The energy intensity and production intensity estimated by Blom et al. (2023) are respectively 22% and 44% lower than the corresponding value for nearly identical growing conditions (24°C / 0.54 kPa / 200µmol·m^{-2}·s^{-1} / 16-hrs). The lower energy intensity from Blom et al. (2023) is primarily attributed to using a higher PPE (3.5 vs 2.6 µmol·J^{-1}) and excluding energy load during the dark period. The results obtained using the proposed modelling approach

estimated the energy load during the dark period to account for approximately 12% of the total energy load for this particular set of conditions. When considering all the modelled scenarios, the energy load during the dark period ranges from 1% to 19% of the total energy load. The lower production intensity is linked to the light productivity Blom et al. (2023) used based on their operational conditions. Blom et al. (2023) stated that higher production intensity could be achieved using light productivity data experimentally obtained by Carotti et al. (2021).

The energy intensity and production intensity estimated by Graamans et al. (2018) are respectively 15% lower and 25% higher than the nearest corresponding value for nearly identical growing conditions (28°C / 0.54 kPa / 500µmol·m^{-2}·s^{-1} / 16-hrs). The difference in energy intensity can be primarily attributed to temperature and VPD setpoints. In their study, floating setpoints allowed the air temperature and relative humidity to reach 30°C and 90% (VPD of 0.42 kPa), reducing the energy load associated with cooling and dehumidification. Additionally, there are other differences in the energy modelling approach, as reported by Talbot and Monfet (2024). The discrepancy in production intensity is attributed to the growth model used by Graamans et al. (2018), which tends to overestimate the growth rate in CEA applications, as demonstrated by Talbot and Monfet (2024).

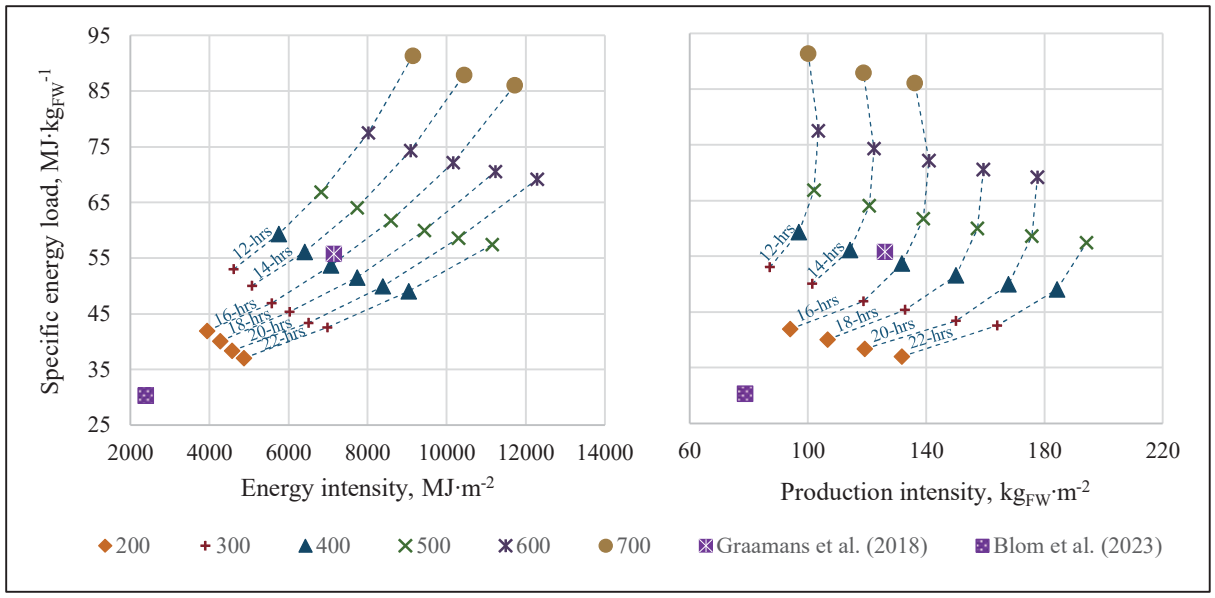

Figure 6.12 Energy intensity, production intensity and specific energy load for the scenarios at 24°C and 0.54 kPa and from other studies

The obtained yield in section 6.3.4 for different combinations of PPFD and photoperiod, while maintaining a constant DLI, aligns with findings reported by Elkins and van Iersel (2020), who observed an increase in shoot dry weight of 18% to 30% for DLI of 16 and 12 mol·m^{-2}·d^{-1}, respectively, when the photoperiod was extended from 10 to 20 hours. Similar results were reported by Kelly et al. (2020) for a DLI of 15.6 mol·m^{-2}·d^{-1}, with dry weight increasing by 23-26%, depending on the cultivar when the PPFD is decreased by 90 µmol·m^{-2}·s^{-1}. Additionally, they observed an increase in fresh weight of 18%-22% but also noted that at a lower DLI of 10.4 mol·m^{-2}·d^{-1}, there was no difference in growth when changing the PPFD. This approach can potentially reduce the energy load while increasing the yield, reduce tip burn incidence and lower the purchase and installation cost of electric lighting with a low PPFD (Kelly et al., 2022). It also reduces the dehumidification load per fresh yield, which is noteworthy given that dehumidification units are typically less efficient than cooling units. Additionally, using electric lighting with a low PPFD decreases power demand, leading to potential cost savings. This is significant because, in many locations, electricity prices are often a combination of energy load and power demand.

6.5 Conclusion

This study assessed the annual energy load, distribution per category and fresh yield for various growing conditions. It provided insight into the influence of the growing conditions on energy load and crop yield using a modelling approach, specifically focusing on energy load associated with space energy demands, excluding HVAC equipment. To improve energy efficiency, lowering the energy requirements through energy efficiency measures becomes as important as improving the energy performance of the HVAC equipment. The analysis presented in this study provides a comprehensive understanding of how growing conditions influence energy load and crop yield. The yield predicted with the model was compared and cross-referenced with existing literature. The key findings of the analysis can be summarised as follows:

- Most energy load can be attributed to lighting, which influences the demand for electricity and cooling. Both account for 50% to 87% of the energy load, with a noticeable increase as the PPFD rises. Consequently, for most scenarios, implementing energy efficiency measures such as improving PPE or implementing pulsing light strategies is crucial.
- Scenarios with a 24°C air temperature resulted in higher energy load compared to scenarios at 20°C and 28°C. However, they also led to a substantial increase in crop yield, resulting in a consistent improvement in specific energy load.
- For most conditions, lowering the VPD setpoint is favourable as it reduces energy load without causing water stress that might hinder growth. Under certain conditions, notably at higher PPFD levels, changing the VPD no longer significantly influences energy load.
- At PPFD levels exceeding 500 $\mu mol \cdot m^{-2} \cdot s^{-1}$, the results showed that growth was limited, while the energy load continued to increase linearly with PPFD.
- When maintaining a constant DLI, lowering the PPFD and extending the photoperiod reduced the energy load and significantly increased yield, resulting in a consistent improvement of the specific energy load. Additionally, this approach offers other advantages, such as lowering the cost of purchasing the lighting system and reducing the power demand of the space.

- Dehumidification is a highly energy-intensive process, but specific changes in the growing conditions consistently reduce its energy load. These include changing the temperature setpoint to 20°C or 28°C, reducing the VPD setpoint and decreasing the PPFD while extending the photoperiod for a constant DLI.

This study provided a better understanding of how growing conditions influence energy load and crop yield. The results of this study or the energy modelling approach could be leveraged for implementing energy efficiency measures. However, it is essential to note that the dynamic crop model is still limited to lettuce cultivation under constant CO_2 concentration and for air temperatures of 20°C, 24°C and 28°C. Future work would expand it to include other crops usually grown indoors, such as leafy greens, microgreens and strawberries.

Acknowledgements

This work was supported by the Fonds de recherche du Québec – Nature et technologies (Quebec, Canada), PhD scholarship for the first co-author, as well as NSERC research grants RGPIN-2020-04576 and ALLRP 561361-21.

Declaration of competing interest

The authors declare that they have no known competing financial interests or personal relationships that could have appeared to influence the work reported in this paper.

Declaration of Generative AI and AI-assisted technologies in the writing process

While preparing this work, the authors used ChatGPT (GPT-3.5) to improve the language and readability of a few sentences (less than 10% of the text). After using this tool/service, the authors reviewed and edited the content as needed and took full responsibility for the publication's content.

CRediT authorship contribution statement

Marie-Hélène Talbot: Conceptualization, Software, Visualization, Methodology, Validation, Formal analysis, Writing - original draft. **Danielle Monfet:** Methodology, Visualization, Writing - review & editing, Supervision, Funding Acquisition.

CHAPTER 7

DISCUSSION

The previous four chapters represent four contributions to the field of research on modelling CEA-HD spaces. These contributions addressed specific research gaps identified in the literature review (CHAPTER 1). This global discussion synthesizes the insights from each article, highlights their main limitations, and offers recommendations regarding modelling approaches for CEA-HD spaces and improvements of the current research project. Furthermore, future works are proposed.

7.1 Assessment of the impact of various factors on energy load

Article #1 (CHAPTER 3) and *Article #2* (CHAPTER 4) were exploratory, aiming to assess the impact of selected phenomena on energy loads and to evaluate whether certain modelling simplifications could be justified. For thermal storage, the primary limitation lies in the lack of validation for the hydroponic system model developed. As future work, this model could be validated experimentally, operating a CEA-HD space without any crops. Preliminary results suggested that under long photoperiods (e.g., 22 hours), heating loads may approach zero due to excess heat accumulated during lighting periods, and this is a key insight for CEA-HD modelling: heating systems might not be necessary.

Conversely, the influence of thermal storage on annual cooling loads was found to be minimal, with a maximum impact of 9% on cooling loads. Therefore, omitting thermal storage modelling in hydroponic systems appears to be a reasonable simplification and was not pursued in subsequent articles. However, for larger-scale CEA-HD spaces, the influence could be either higher or lower, depending on the configuration, and should be reassessed accordingly.

Regarding light interception, the main limitation was the use of Tei et al. (1996) cultivation cover area correlation, which is constrained to a specific crop density. Due to the lack of

flexibility in this method, later studies adopted an alternative approach for estimating light interception. Preliminary results showed that light interception has a significant impact, particularly in reducing cooling loads. As it is relatively simple to implement, it is recommended that this factor be included in CEA-HD models, especially as PPE continues to improve, increasing the importance of this effect. For the variation in LED heat fractions, a key limitation was the empirical growth model used to generate the results, as it employed PPFD values associated with lighting efficiencies (both low and high) outside the model's validated range. Nevertheless, the findings remain valuable: they demonstrated that accurate knowledge of heat fractions becomes increasingly important for cooling and dehumidification loads as the crop canopy expands. Given the substantial variation between lighting technologies, the primary takeaway is the need for better characterization of horticultural LED lamps by manufacturers.

Concerning crop growth, the main limitation was the empirical model used, which was validated under specific conditions and required the fresh weight on the 30th day, an approach that lacks flexibility and limits its usefulness for yield prediction. For modelling both energy consumption and crop yield in operational CEA-HD systems, the use of a more robust crop growth model is recommended. Even in cases of diversified stage growth management methods, a growth model could assist in selecting a more appropriate LAI value, potentially deviating from the commonly assumed fixed LAI value of 2.1.

7.2 Development of a dynamic crop model for CEA-HD spaces

Article #3 (CHAPTER 5) focused on the development of a crop model for yield and energy analysis, integrating a growth model adapted to CEA-HD cultivation. Although the crop growth model was designed to be versatile, accounting for dynamic air moisture properties, heat of vaporization, and adaptable to a range of cultivation parameters such as planting density, photoperiod, transplant and harvest sizes, temperature, PPFD, and humidity, it still presents some limitations.

Although the total energy of incoming light was considered, the photon spectral distribution was not accounted for in the growth model developed. This is a limitation, as spectral distribution can significantly influence plant development, particularly by affecting light interception and biomass accumulation (Abedi et al., 2023). This gap was addressed by Abedi et al. (2023), who modified the Van Henten (1994) growth model to incorporate the effect of photon spectral distribution on lettuce biomass accumulation. Unlike the work presented in *Article #3*, which involved modifying some of the equations of Van Henten (1994) model, Abedi et al. (2023) only adjusted some parameters, i.e., they selected slightly higher values for the boundary layer and stomatal conductance (g_{bnd} and g_{stm}) based on Stanghellini (1987). They then assessed the performance of their model, which closely resembles the Van Henten (1994) model, observing that it consistently overestimated biomass accumulation across 20 experimental datasets with varying spectral distributions. This finding aligns with the results of *Article #3,* for which it was clear that the use of the Van Henten (1994) model led to overestimation of the growth rate in CEA-HD spaces. Abedi et al. (2023) also demonstrated that the margin of error with results from the Van Henten (1994) model varied significantly depending on the spectral treatment. Based on the main assumption that the light use efficiency coefficient (c_ε) is influenced by the spectral composition of the incoming light, Abedi et al. (2023) numerically determined a specific c_ε for each experiment, allowing the accurate prediction of the final lettuce dry weight with the growth model. The c_ε values were derived from experiments where the harvested lettuces weighed less than 3 g_{DW},, which is more than three times smaller than a marketable head size of 250 g_{FW}. Subsequently, Abedi et al. (2023) developed a mathematical model to estimate c_ε. It is worth noting that their work was intended solely for yield prediction, rather than combined energy and yield analysis, which would also require accurate prediction of LAI. Abedi et al. (2023) reported $c_\varepsilon$values ranging from 9 to 14 $\times 10^6$ $g \cdot J^{-1}$, for PPFD levels between 174 and 216 $\mu mol \cdot m^{-2} \cdot s^{-1}$, with one outlier at about 17 $\times 10^6$, as illustrated in Figure 7.1. In comparison, the calibrated c_ε at 200 $\mu mol \cdot m^{-2} \cdot s^{-1}$ in *Article #3* for different air temperatures led to values ranging between 10.5 and 11 $\times 10^6$ $g \cdot J^{-1}$, which fall within the range of Abedi et al. (2023). Notably, both studies began with a default c_ε value of 17 $\times 10^6$, reinforcing confidence in the model developed in *Article #3* (CHAPTER 5).

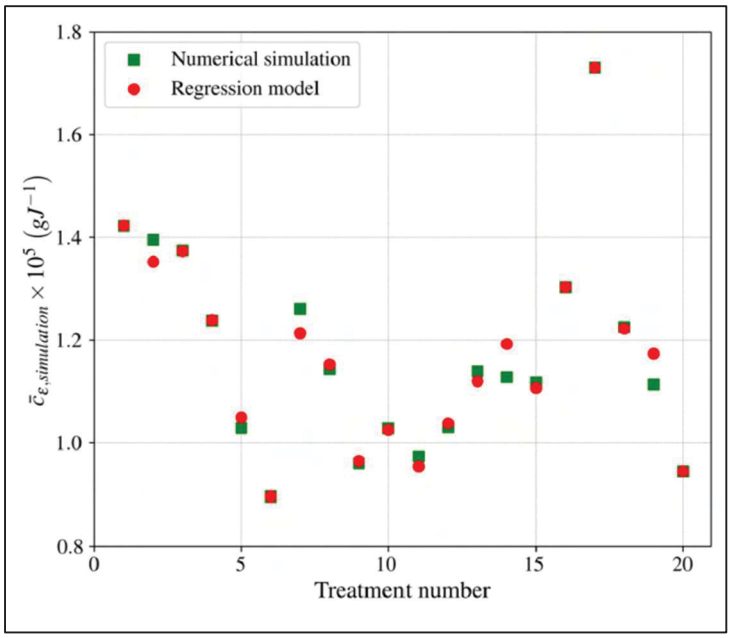

Figure 7.1 Comparison of c_ε from numerical simulation and a regression model

Taken from Abedi et al. (2023, p.13)

Given the demonstrated sensitivity of c_ε to spectral composition, it would be advisable to integrate spectral effects into future versions of the growth model. One possible approach could involve using a correction factor to adjust the c_ε value calibrated in this thesis. This would significantly enhance the model's versatility, especially for applications involving modulating spectral distribution, which is gaining attention.

Another limitation of the model lies in its inability to integrate dynamically modulated lighting intensity, an increasingly important strategy for optimizing CEA-HD spaces. In its current form, the model treats SLA as a fixed parameter dependent on temperature and PPFD, which drives leaf expansion and thus, LAI. However, this approach assumes a static SLA over the cultivation period, whereas leaf expansion could be impacted if there are changes in PPFD and temperature. Sun et al. (2025) incorporated this dynamic behaviour into their lettuce growth model designed for semi-controlled greenhouses. Based on their approach, several modifications could be applied to the model developed in this thesis:

- Convert SLA from a parameter to a variable.

- Recalculate SLA at each timestep as a function of indoor conditions.
- Estimate the rate of change in LAI based on biomass accumulation and the current SLA.
- Treat LAI as a state variable rather than a derived one.

Currently, the model uses SLA values from Carotti et al. (2021) as input parameters. These values represent the slope of the measured leaf area versus measured dry weight at different growth stages and inherently reflect an average SLA across both light-on and light-off periods. As a first step, it would be useful to estimate separate SLA values for the lights-on and lights-off periods, which is relatively straightforward. Additionally, Sun et al. (2025) accounted for the influence of humidity on SLA. Building on this, further investigation is needed to assess whether relatively slight variations in humidity level occurring in CEA-HD space significantly influence SLA dynamics, or if the humidity effect can be considered negligible.

The last limitation regarding the developed growth model concerns the two state variables of the model: structural and non-structural dry weight. The proposed calibration method involved fitting total dry weight, defined as the sum of the two state variables, by adjusting sensitive parameters. However, there is a known relationship between these variables: non-structural dry weight rarely exceeds 25% of total dry weight (Goudriaan et al., 1985). Van Henten and Van Straten (1994) illustrated that this relationship is respected in their model after a particular stage of growth, as shown in Figure 7.2.

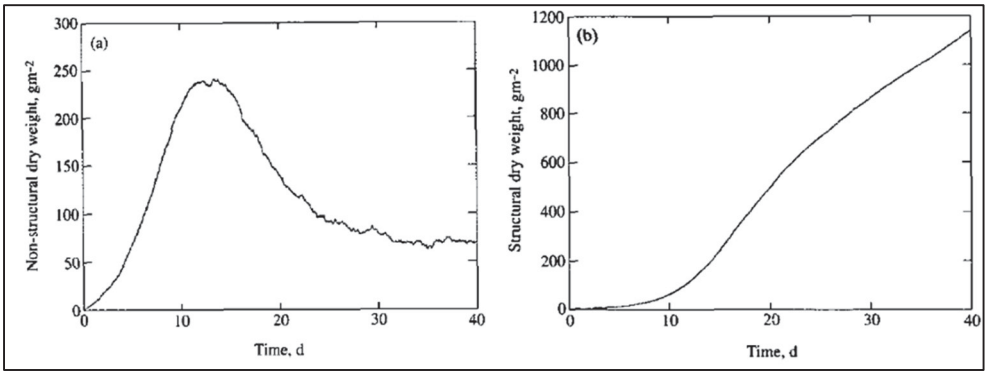

Figure 7.2 Growth trajectories of (a) non-structural dry weight, (b) structural dry weight, as an example of Van Henten (1994) growth model
Taken from Van Henten and Van Straten (1994, p.25)

In contrast, when examining the state variables produced by the calibrated model, the non-structural dry weight frequently exceeds the expected 25% threshold. This kind of inconsistency is not uncommon in grey-box models, where intermediate variables can deviate from expected values. To address this, a revised calibration process should be considered, one that incorporates the relationship between structural and non-structural dry weight as a constraint in the genetic algorithm to ensure biologically plausible results.

Another avenue worth exploring is the modelling approach developed by Sun et al. (2025), who proposed a lettuce growth model for low-tech greenhouse applications, characterized by a wide range of indoor climatic conditions. They observed that the Van Henten (1994) growth model tends to overestimate crop growth in such environments, suggesting that this overestimation is not confined to CEA-HD spaces, as found in *Article #3* (CHAPTER 5). To address this, Sun et al. (2025) proposed a simplified modelling framework wherein total dry weight is equated with structural dry weight. In their model, non-structural carbohydrates serve as a temporary buffer for assimilated carbon, primarily functioning to regulate photosynthesis rather than contributing directly to dry matter accumulation. This approach allows the model to account for carbon balance without inflating biomass accumulation.

Finally, the crop energy balance model was refined by explicitly introducing moist air thermophysical properties through the intrinsic TRNSYS subroutines *MoistAirProperties* and

AirProp. As previously noted, the procedure proposed by Graamans et al. (2017) approximates the leaf vapour pressure term using a first-order linearization obtained at the indoor air temperature, thereby partially decoupling this term from the resolved leaf temperature. In the new model developed in Article #3 (Chapter 5), Type 211, the leaf vapour pressure is evaluated psychometrically directly at the leaf temperature and updated at each iteration. This approach eliminates the linearization and improves the thermodynamic consistency of the model. To further enhance thermodynamic coherence, an additional heat exchange could be introduced in the airnode heat balance: when water vapour leaves the leaf surface at leaf temperature and mixes with the surrounding air, a small sensible heat exchange arises from bringing the newly added vapour to the indoor air temperature. However, sensitivity analyses performed under the four operating conditions used by Graamans et al. (2017) indicate that this sensible contribution represents approximately 0.1–0.2 % of the convective heat exchange between the leaf surface and the indoor air.

7.3 Energy and yield analysis

Article #4 (CHAPTER 6) focused on assessing the impact of a broad range of growing conditions on both energy load and crop yield. Various scenarios were tested by varying temperature, light intensity, and photoperiod. This required the interpolation of several crop model parameters: c_{ε}, $c_{gr,max}$, c_{β}, SLA and $DW_{content}$. As detailed in Appendix A of the article, most of these parameters were interpolated across different PPFD values using second-degree polynomials. However, this interpolation approach could be improved. For instance, in Figure 6.10, yield does not follow the expected saturating exponential function with increasing PPFD. As illustrated in Figure 1.11, yield should exhibit a saturating response, especially within the range of 400 to 750 $\mu mol \cdot m^{-2} \cdot s^{-1}$. Adjusting the fitting function accordingly could enhance model accuracy in that specific range. Another potential improvement involves adjusting SLA values based on photoperiod. As discussed in section 7.2, the SLA values from Carotti et al. (2021) reflect an average for a 16-hour photoperiod. Using SLA values estimated for different photoperiods could lead to more accurate estimates of crop heat exchanges under varying photoperiods.

CONCLUSION

This thesis addressed gaps and inconsistencies in current modelling practices for high-density controlled environment agriculture (CEA-HD) spaces, which are expected in an emerging research field. The work aimed at developing a modelling approach adapted to CEA-HD spaces to support energy and yield analysis across a wide range of growing conditions and crop management strategies. The approach could support the development of optimized solutions that balance energy consumption and crop yield. The objective was divided into specific objectives, leading to the following key outcomes:

(1) Assessment of the impact of different modelling approaches:

The findings highlighted the significant influence of light interception, variability of the light heat fractions, and crop growth on the sensible cooling and latent loads. As a result, these factors should be carefully considered when modelling CEA-HD spaces.

(2) Development of a dynamic crop model:

A crop model incorporating both an energy balance and growth sub-model was developed specifically for lettuce cultivation in CEA-HD spaces. An existing greenhouse lettuce growth model was adjusted, as it initially overestimated growth rates under CEA-HD conditions. The result is a grey-box mechanistic model, integrated into a building performance simulation tool, designed to simulate a wide range of growing conditions and operational scenarios.

(3) Assessment of the impact of different growing conditions on energy and yield:

A case study was conducted by combining different temperatures, vapour pressure deficits, photosynthetic photon flux densities, and photoperiods, resulting in a total of 180 simulation scenarios. The analysis provided a comprehensive understanding of how growing conditions influence energy load and crop yield.

This thesis has led to several contributions to the field, including four peer-reviewed and published papers, as well as three crop models made available to the community on GitHub as TRNSYS components.

RECOMMENDATIONS

Additional features and several improvements could enhance the proposed modelling approach. A promising direction is to increase the model's versatility in handling dynamic lighting strategies, including spectrum and intensity modulation. These capabilities would enable the simulation of innovative growth management methods that are gaining traction in CEA applications. Another avenue for development is to evaluate the model's performance across different lettuce cultivars and other leafy greens. In this research, the selected cultivar was *Othilie*, which is known for its relatively low dry matter content compared to other cultivars. Expanding the model's applicability to a broader range of genotypes would enhance its utility. As outlined in section 7.3, further refinements to the growth model itself could be required. Incorporating a carbohydrate buffer or introducing constraints on the structural and non-structural dry weight state variables may help ensure biologically plausible outputs. However, such refinements may not be necessary for energy and yield analysis alone, in which case the existing grey-box model may remain sufficient.

To further validate the findings of this thesis, particularly the preliminary results on the hydroponic system's thermal behaviour presented in Article #1 (CHAPTER 3), additional experiments could be conducted. Furthermore, to strengthen the model's robustness across a wider range of growing conditions and applications, such experiments could involve collaboration with universities specializing in agronomy. This approach would help ensure that the experiments are designed to meet the specific requirements for validating the model developed for yield and energy modelling. For instance, the model's temperature range could be extended, or CO_2 concentration introduced as an additional variable, since Carotti et al. (2021) did not investigate its impact on crop growth.

In the field of energy modelling, subsequent work should focus on modelling HVAC systems. While this research emphasized energy load estimation, a critical and often overlooked step, energy loads do not directly translate to actual energy consumption. Final energy consumption depends heavily on system design and control strategies. Therefore, modelling HVAC systems is essential to optimize both energy consumption and the yield of CEA-HD spaces.

Finally, adapting the model for greenhouse applications could represent a valuable contribution. Closed greenhouses may serve as an ideal starting point, given their similarity to fully controlled CEA-HD spaces. For semi-closed greenhouses with higher variations in indoor conditions, the lettuce growth model developed by Sun et al. (2025) could be a suitable foundation. However, since that model was designed for yield prediction only, modifications would be required to integrate it into a crop energy balance model. The methodology developed in this thesis could offer useful insights for such adaptations.

ANNEX I

SUPPLEMENTARY TABLES OF CHAPTER 5

Table-A I-1 Equations of the growth model of Van Henten (1994)
Taken and adapted from Van Henten (1994)

Variable	Equation	
Carboxylation conductance, $m \cdot s^{-1}$	$g_{car} = c_{car,1} \cdot {T_a}^2 + c_{car,2} \cdot T_a + c_{car,3}$	(I-1)
Canopy conductance to CO_2, $m \cdot s^{-1}$	$g_{CO_2} = ({g_{bnd}}^{-1} + {g_{stm}}^{-1} + {g_{car}}^{-1})^{-1}$	(I-.2)
Compensation point, $g \cdot m^{-3}$	$\Gamma = c_\Gamma \cdot {c_{Q10,\Gamma}}^{(T_{a,i}-20)/10}$	(I-3)
Light use efficiency, $g \cdot J^{-1}$	$\varepsilon = c_\varepsilon \cdot \frac{CO_2 - \Gamma}{CO_2 + 2\Gamma}$	(I-4)
Response to canopy photosynthesis, $g \cdot m^{-2} \cdot s^{-1}$	$f_{phot,max} = \frac{\varepsilon \cdot PAR \cdot g_{CO_2}(CO_2 - \Gamma)}{\varepsilon \cdot PAR + g_{CO_2}(CO_2 - \Gamma)}$	(I-5)
Leaf area index, $m^2_{leaves} \cdot m^{-2}$	$LAI = c_{lar} \cdot (1 - c_\tau) \cdot X_{sdw}$	(I-6i)
	$LAI = SLA \cdot (1 - c_\tau) \cdot \frac{DW_{leaf}}{DW_{sht}} \cdot (X_{sdw} + X_{nsdw})$	(I-6m)
Gross canopy photosynthesis[1], $g \cdot m^{-2} \cdot s^{-1}$	$f_{phot} = f_{phot,max} \cdot (1 - e^{-k_s \cdot LAI})$	(I-7)
Maintenance respiration rate, $g \cdot m^{-2} \cdot s^{-1}$	$f_{resp} = {c_{Q10.resp}}^{(T_{a,i}-25)/10} \begin{bmatrix} c_{resp,sht} \cdot (1 - c_\tau) \cdot X_{sdw} \\ + c_{resp,rt} \cdot c_\tau \cdot X_{sdw} \end{bmatrix}$	(I-8)
Specific growth rate, s^{-1}	$r_{gr} = c_{gr,max} \cdot \frac{X_{nsdw}}{X_{sdw} + X_{nsdw}} \cdot {c_{Q10.gr}}^{(T_{a,i}-20)/10}$	(I-9)
Grow rate of the structural and non-structural dry weight, $g \cdot m^{-2} \cdot s^{-1}$	$\frac{dX_{sdw}}{dt} = r_{gr} \cdot X_{sdw}$ $\frac{dX_{nsdw}}{dt} = \begin{bmatrix} c_\alpha \cdot f_{phot} - r_{gr} \cdot X_{sdw} \\ -f_{resp} - \frac{1 - c_\beta}{c_\beta} r_{gr} \cdot X_{sdw} \end{bmatrix}$	(I-10)
Structural and non-structural dry weight, $g \cdot m^{-2}$	$X_{sdw}(t) = X_{sdw}(t-1) + dX_{sdw}$ $X_{nsdw}(t) = X_{nsdw}(t-1) + dX_{nsdw}$	(I-11)
Total dry weight, $g \cdot plant^{-1}$	$DW_{tot} = \frac{X_{sdw} + X_{nsdw}}{PCD}$	(I-12)

Table-A I-2 Parameters of the growth model of Van Henten (1994)
Taken and adapted from Van Henten (1994)

Parameter	Description	Initial value	Modified value
$c_{car,1}$, $m \cdot s^{-1} \cdot K^{-2}$ $c_{car,2}$ $m \cdot s^{-1} \cdot K^{-1}$ $c_{car,3}$, $m \cdot s^{-1}$	Carboxylation parameters	$-1.32 \cdot 10^{-5}$ $5.94 \cdot 10^{-4}$ $-2.64 \cdot 10^{-3}$	-
$g_{bnd} = 1/r_a$, $m \cdot s^{-1}$	Boundary layer conductance (Van Henten & Van Straten, 1994)	0.004	0.01 $m \cdot s^{-1}$ (Graamans et al., 2017)
$g_{stm} = 1/r_s$, $m \cdot s^{-1}$	Stomatal conductance (Van Henten & Van Straten, 1994)	0.002	$\frac{200+PPFD}{60 \cdot (1500+PPFD)}$ (Graamans et al., 2017)
c_Γ, $g \cdot m^{-3}$	CO_2 compensation point (it corresponds to 40 ppm)	$7.32 \cdot 10^{-2}$	-
$c_{Q10,\Gamma}$	Q_{10} factor to account the effect of temperature	2	-
c_ε[1], $g \cdot J^{-1}$	Light use efficiency at very high CO_2 concentration	$17 \cdot 10^{-6}$	Refer to Figure 5.8 for calibrated values.
k_s[1]	Extinction coefficient of lettuces	0.9	Refer to Figure 5.8 for calibrated values.
c_{lar}, m^2/g	Structural leaf area ratio	$75 \cdot 10^{-3}$	Using the SLA in Equation (A6.m) to estimate the LAI instead of the c_{lar} in Equation (A6.i)
c_τ	Ratio of the root dry weight to the total dry weight for lettuces grown in soil	0.15	-
$c_{resp,sht}$, s^{-1}	Maintenance respiration coefficient for the shoot at 25°C	$3.47 \cdot 10^{-7}$	-
$c_{resp,rt}$, s^{-1}	Maintenance respiration coefficient for the root at 25°C	$1.16 \cdot 10^{-7}$	-
$c_{gr,max}$[1], s^{-1}	Saturation growth rate at 20°C	$5 \cdot 10^{-6}$	Refer to Figure 5.8 for calibrated values.
$c_{Q10,resp}$	Q_{10} factor for maintenance respiration	2	-
$c_{Q10,gr}$	Q_{10} factor for growth	1.6	-
c_α	Ratio of the CH_2O molar mass to the CO_2 molar mass	0.68	-
c_β[1]	Yield factor indicating the respiratory and synthesis losses of non-structural material due to growth	0.8	Refer to Figure 5.8 for calibrated values.

[1] Most sensitive parameters of the growth model (aside from the initial values of X_{sdw} and X_{sndw}) according to Van Henten and Van Straten (1994).

ANNEX II

SUPPLEMENTARY TABLE OF CHAPTER 6

Table-A II-1 Parameters of the crop model

<table>
<tr><th>Parameter</th><th>Description</th><th>Value</th><th>Interpolation method</th></tr>
<tr><td>r_a, s·m^{-1}</td><td>Aerodynamic resistance</td><td>100 (Graamans et al., 2017)</td><td>N/A</td></tr>
<tr><td>r_s, s·m^{-1}</td><td>Stomatal resistance</td><td>$\frac{60\cdot(1500+PPFD)}{200+PPFD}$ (Graamans et al., 2017)</td><td>N/A</td></tr>
<tr><td>c_ε, g·J^{-1}</td><td>Light use efficiency at a very high CO_2 concentration</td><td>
<table>
<tr><td>$T_{a,i}$, °C</td><td colspan="3">PPFD, µmol·m^{-2}·s^{-1}</td></tr>
<tr><td></td><td>200</td><td>400</td><td>750</td></tr>
<tr><td>20</td><td>10.5324E-6</td><td>10.5901E-6</td><td>7.7421E-6</td></tr>
<tr><td>24</td><td>11.0025E-6</td><td>11.6375E-6</td><td>7.8226E-6</td></tr>
<tr><td>28</td><td>10.7513E-6</td><td>9.5993E-6</td><td>6.9296E-6</td></tr>
</table>
Calibrated values by Talbot and Monfet (Talbot & Monfet, 2024)
</td><td>Second-degree polynomial regression</td></tr>
<tr><td>$k_{s,el}$</td><td>Extinction coefficient of lettuces</td><td>0.66
Calibrated values by Talbot and Monfet (2024)</td><td>N/A</td></tr>
<tr><td>$c_{gr,max}$, s^{-1}</td><td>Saturation growth rate at 20°C</td><td>
<table>
<tr><td>$T_{a,i}$, °C</td><td colspan="3">PPFD, µmol·m^{-2}·s^{-1}</td></tr>
<tr><td></td><td>200</td><td>400</td><td>750</td></tr>
<tr><td>20</td><td>7.576E-7</td><td>10.474E-7</td><td>11.433E-7</td></tr>
<tr><td>24</td><td>6.715E-7</td><td>8.733E-7</td><td>8.988E-7</td></tr>
<tr><td>28</td><td>1.764E-7</td><td>4.679E-7</td><td>5.264E-7</td></tr>
</table>
Calibrated values by Talbot and Monfet (2024)
</td><td>Second-degree polynomial regression</td></tr>
<tr><td>c_β</td><td>Yield factor indicating the respiratory and synthesis losses of non-structural material due to growth</td><td>
<table>
<tr><td>$T_{a,i}$, °C</td><td colspan="3">PPFD, µmol·m^{-2}·s^{-1}</td></tr>
<tr><td></td><td>200</td><td>400</td><td>750</td></tr>
<tr><td>20</td><td>0.401</td><td>0.402</td><td>0.403</td></tr>
<tr><td>24</td><td>0.400</td><td>0.400</td><td>0.402</td></tr>
<tr><td>28</td><td>0.425</td><td>0.404</td><td>0.403</td></tr>
</table>
Calibrated values by Talbot and Monfet (2024)
</td><td>Linear</td></tr>
<tr><td>SLA, cm^2·g$_{DW}^{-1}$</td><td>Specific leaf area</td><td>
<table>
<tr><td>$T_{a,i}$, °C</td><td colspan="3">PPFD, µmol·m^{-2}·s^{-1}</td></tr>
<tr><td></td><td>200</td><td>400</td><td>750</td></tr>
<tr><td>20</td><td>327</td><td>261</td><td>218</td></tr>
<tr><td>24</td><td>452</td><td>365</td><td>272</td></tr>
<tr><td>28</td><td>400</td><td>314</td><td>250</td></tr>
</table>
Extracted from Carotti et al. (2021) experiments
</td><td>Second-degree polynomial regression</td></tr>
<tr><td>$DW_{content}$, %</td><td>Dry weight content at harvest</td><td>
<table>
<tr><td colspan="3">PPFD, µmol·m^{-2}·s^{-1}</td></tr>
<tr><td>200</td><td>400</td><td>750</td></tr>
<tr><td>2.6</td><td>3.8</td><td>4.2</td></tr>
</table>
Extracted from Carotti et al. (2021) experiments
</td><td>Second-degree polynomial regression</td></tr>
</table>

LIST OF REFERENCES

Abedi, M., Tan, X., Stallknecht, E. J., Runkle, E. S., Klausner, J. F., Murillo, M. S., & Bénard, A. (2023). Incorporating the effect of the photon spectrum on biomass accumulation of lettuce using a dynamic growth model [Original Research]. *Frontiers in Plant Science*, *14*. https://doi.org/10.3389/fpls.2023.1106576

Agritecture, & WayBeyond. (2021). *Global CEA Census Report*. https://www.agritecture.com/census

Ahamed, M. S., Sultan, M., Monfet, D., Rahman, M. S., Zhang, Y., Zahid, A., Bilal, M., Ahsan, T. M. A., & Achour, Y. (2023). A critical review on efficient thermal environment controls in indoor vertical farming. *Journal of Cleaner Production*, *425*, 138923. https://doi.org/https://doi.org/10.1016/j.jclepro.2023.138923

Arcasi, A., Mauro, A. W., Napoli, G., Tariello, F., & Vanoli, G. P. (2024). Energy and cost analysis for a crop production in a vertical farm. *Applied Thermal Engineering*, *239*, 122129. https://doi.org/https://doi.org/10.1016/j.applthermaleng.2023.122129

Armanda, D. T., Guinée, J. B., & Tukker, A. (2019). The second green revolution: Innovative urban agriculture's contribution to food security and sustainability – A review. *Global Food Security*, *22*, 13-24. https://doi.org/https://doi.org/10.1016/j.gfs.2019.08.002

ASHRAE. (2013a). *ASHRAE Handbook - Fundamentals : Energy estimating and modeling methods*. American Society of Heating, Refrigerating and Air-Conditioning Engineers, Inc. http://app.knovel.com/hotlink/toc/id:kpASHRAEC1/ashrae-handbook-fundamentals/ashrae-handbook-fundamentals

ASHRAE. (2013b). *ASHRAE Handbook - Fundamentals : Nonresidential cooling and heating load calculations*. American Society of Heating, Refrigerating and Air-Conditioning Engineers, Inc. http://app.knovel.com/hotlink/toc/id:kpASHRAEC1/ashrae-handbook-fundamentals/ashrae-handbook-fundamentals

ASHRAE. (2021). *2021 ASHRAE Handbook - Fundamentals*. American Society of Heating Refrigerating and Air-Conditioning Engineers Inc. (ASHRAE. http://ezaccess.libraries.psu.edu/login?url=https://app.knovel.com/hotlink/toc/id:kpASHRAEZ2/2021-ashrae-handbook?kpromoter=marc

Baba, F. M., Ge, H., Zmeureanu, R., & Wang, L. (2022). Calibration of building model based on indoor temperature for overheating assessment using genetic algorithm: Methodology, evaluation criteria, and case study. *Building and Environment*, *207*, 108518. https://doi.org/https://doi.org/10.1016/j.buildenv.2021.108518

Baglivo, C., Mazzeo, D., Panico, S., Bonuso, S., Matera, N., Congedo, P. M., & Oliveti, G. (2020). Complete greenhouse dynamic simulation tool to assess the crop thermal well-being and energy needs. *Applied Thermal Engineering*, *179*, 115698. https://doi.org/https://doi.org/10.1016/j.applthermaleng.2020.115698

Benis, K., Reinhart, C., & Ferrão, P. (2017a). *Building-Integrated Agriculture (BIA) In Urban Contexts: Testing A Simulation-Based Decision Support Workflow*.

Benis, K., Reinhart, C., & Ferrão, P. (2017b). Development of a simulation-based decision support workflow for the implementation of Building-Integrated Agriculture (BIA) in urban contexts. *Journal of Cleaner Production*, *147*, 589-602. https://doi.org/https://doi.org/10.1016/j.jclepro.2017.01.130

Blom, T., Jenkins, A., Pulselli, R. M., & van den Dobbelsteen, A. A. J. F. (2022). The embodied carbon emissions of lettuce production in vertical farming, greenhouse horticulture, and open-field farming in the Netherlands [Article]. *Journal of Cleaner Production*, *377*, Article 134443. https://doi.org/10.1016/j.jclepro.2022.134443

Blom, T., Jenkins, A., & van den Dobbelsteen, A. (2023). Synergetic integration of vertical farms and buildings: reducing the use of energy, water, and nutrients [Original Research]. *Frontiers in Sustainable Food Systems*, *7*. https://doi.org/10.3389/fsufs.2023.1227672

Both, A.-J. (1995). *Dynamic simulation of supplemental lighting for greenhouse hydroponic lettuce production* [Ph.D., Cornell University]. ProQuest Dissertations & Theses Global. Ann Arbor.

Bu, K., Yu, Z., Lai, D., & Bao, H. (2024). Energy-saving effect assessment of various factors in container plant factories: A data-driven random forest approach. *Cleaner Energy Systems*, *8*, 100122. https://doi.org/https://doi.org/10.1016/j.cles.2024.100122

Carotti, L., Graamans, L., Puksic, F., Butturini, M., Meinen, E., Heuvelink, E., & Stanghellini, C. (2021). Plant Factories Are Heating Up: Hunting for the Best Combination of Light Intensity, Air Temperature and Root-Zone Temperature in Lettuce Production. *Frontiers in Plant Science*, *11*, 592171-592171. https://doi.org/10.3389/fpls.2020.592171

Carotti, L., Pistillo, A., Zauli, I., Pennisi, G., Martin, M., Gianquinto, G., & Orsini, F. (2024). Far-red radiation management for lettuce growth: Physiological and morphological features leading to energy optimization in vertical farming. *Scientia Horticulturae*, *334*, 113264. https://doi.org/https://doi.org/10.1016/j.scienta.2024.113264

Casey, L., Freeman, B., Francis, K., Brychkova, G., McKeown, P., Spillane, C., Bezrukov, A., Zaworotko, M., & Styles, D. (2022). Comparative environmental footprints of lettuce supplied by hydroponic controlled-environment agriculture and field-based supply

chains. *Journal of Cleaner Production*, *369*, 133214. https://doi.org/https://doi.org/10.1016/j.jclepro.2022.133214

Chang, C.-L., Chung, S.-C., Fu, W.-L., & Huang, C.-C. (2021). Artificial intelligence approaches to predict growth, harvest day, and quality of lettuce (Lactuca sativa L.) in a IoT-enabled greenhouse system. *Biosystems Engineering*, *212*, 77-105. https://doi.org/https://doi.org/10.1016/j.biosystemseng.2021.09.015

Coakley, D., Raftery, P., & Keane, M. (2014). A review of methods to match building energy simulation models to measured data. *Renewable and Sustainable Energy Reviews*, *37*, 123-141. https://doi.org/https://doi.org/10.1016/j.rser.2014.05.007

Cohen, A. R., Chen, G., Berger, E. M., Warrier, S., Lan, G., Grubert, E., Dellaert, F., & Chen, Y. (2022). Dynamically Controlled Environment Agriculture: Integrating Machine Learning and Mechanistic and Physiological Models for Sustainable Food Cultivation. *ACS ES&T Engineering*, *2*(1), 3-19. https://doi.org/10.1021/acsestengg.1c00269

Crawley, D. B., Lawrie, L. K., Pedersen, C. O., & Winkelmann, F. C. (2000). Energy plus: energy simulation program. *ASHRAE journal*, *42*(4), 49-56.

Critten, D. (1991). Optimization of CO2 concentration in greenhouses: A modelling analysis for the lettuce crop. *Journal of Agricultural Engineering Research*, *48*, 261-271.

Davis, M. M., & Hirmer, S. (2015). The potential for vertical gardens as evaporative coolers: An adaptation of the 'Penman Monteith Equation'. *Building and Environment*, *92*, 135-141. https://doi.org/https://doi.org/10.1016/j.buildenv.2015.03.033

Decardi-Nelson, B., & You, F. (2024). Artificial intelligence can regulate light and climate systems to reduce energy use in plant factories and support sustainable food production. *Nature Food*, *5*(10), 869-881. https://doi.org/10.1038/s43016-024-01045-3

Dorais, M. (2003). The use of supplemental lighting for vegetable crop production: light intensity, crop response, nutrition, crop management, cultural practices.

Eaton, M., Shelford, T., Cole, M., & Mattson, N. (2023). Modeling resource consumption and carbon emissions associated with lettuce production in plant factories. *Journal of Cleaner Production*, *384*, 135569. https://doi.org/https://doi.org/10.1016/j.jclepro.2022.135569

El Ghoumari, M. Y., Tantau, H. J., & Serrano, J. (2005). Non-linear constrained MPC: Real-time implementation of greenhouse air temperature control. *Computers and Electronics in Agriculture*, *49*(3), 345-356. https://doi.org/https://doi.org/10.1016/j.compag.2005.08.005

Elkins, C., & van Iersel, M. W. (2020). Longer Photoperiods with the Same Daily Light Integral Increase Daily Electron Transport through Photosystem II in Lettuce. *Plants (Basel)*, *9*(9). https://doi.org/10.3390/plants9091172

Engler, N., & Krarti, M. (2021). Review of energy efficiency in controlled environment agriculture. *Renewable and Sustainable Energy Reviews*, *141*, 110786. https://doi.org/https://doi.org/10.1016/j.rser.2021.110786

EPRI. (2018). *Indoor Agriculture : A Utility, Water, Sustainability, Technology and Market Overview*.

Fraile-Robayo, R. D., Álvarez-Herrera, J. G., Reyes M, A. J., Álvarez-Herrera, O. F., & Fraile-Robayo, A. L. (2017). Evaluation of the growth and quality of lettuce (Lactuca sativa L.) in a closed recirculating hydroponic system. *Agronomía Colombiana*, *35*, 216-222. http://www.scielo.org.co/scielo.php?script=sci_arttext&pid=S0120-99652017000200216&nrm=iso

Golzar, F., Heeren, N., Hellweg, S., & Roshandel, R. (2018). A novel integrated framework to evaluate greenhouse energy demand and crop yield production. *Renewable and Sustainable Energy Reviews*, *96*, 487-501. https://doi.org/https://doi.org/10.1016/j.rser.2018.06.046

Goudriaan, J., Van Laar, H., Van Keulen, H., & Louwerse, W. (1985). Photosynthesis, CO2 and plant production. In *Wheat growth and modelling* (pp. 107-122). Springer.

Graamans, L., Baeza, E., van den Dobbelsteen, A., Tsafaras, I., & Stanghellini, C. (2018). Plant factories versus greenhouses: Comparison of resource use efficiency. *Agricultural Systems*, *160*(Supplement C), 31-43. https://doi.org/https://doi.org/10.1016/j.agsy.2017.11.003

Graamans, L., van den Dobbelsteen, A., Meinen, E., & Stanghellini, C. (2017). Plant factories; crop transpiration and energy balance. *Agricultural Systems*, *153*(Supplement C), 138-147. https://doi.org/https://doi.org/10.1016/j.agsy.2017.01.003

Guzmán-Valdivia, C., Talavera-Otero, J., & Désiga-Orenday, O. (2019). Turbulent Kinetic Energy Distribution of Nutrient Solution Flow in NFT Hydroponic Systems Using Computational Fluid Dynamics. *AgriEngineering*, *1*, 283-290. https://doi.org/10.3390/agriengineering1020021

Hang, T., Lu, N., Takagaki, M., & Mao, H. (2019). Leaf area model based on thermal effectiveness and photosynthetically active radiation in lettuce grown in mini-plant factories under different light cycles. *Scientia Horticulturae*, *252*, 113-120. https://doi.org/https://doi.org/10.1016/j.scienta.2019.03.057

Harbick, K., & Albright, L. (2016). Comparison of energy consumption: greenhouses and plant factories. VIII International Symposium on Light in Horticulture 1134,

Holden, N. M., Wolfe, M. L., Ogejo, J. A., & Cummins, E. J. (2021). *Introduction to Biosystems Engineering*.

Horomia, K., & Gordon-Smith, H. (2021). Global CEA Census Report. *Auckland: WayBeyond Ltd and Agritecture LLC*.

Hoyt, T., Arens, E., & Zhang, H. (2015). Extending air temperature setpoints: Simulated energy savings and design considerations for new and retrofit buildings. *Building and Environment*, *88*, 89-96. https://doi.org/https://doi.org/10.1016/j.buildenv.2014.09.010

Hydro-Québec. (2025). *Efficient Solutions for agricultural operations*. https://www.hydroquebec.com/business/energy-savings-business/efficient-solutions-agricultural-operations/innovative-greenhouses.html

Iddio, E., Wang, L., Thomas, Y., McMorrow, G., & Denzer, A. (2020). Energy efficient operation and modeling for greenhouses: A literature review. *Renewable and Sustainable Energy Reviews*, *117*, 109480. https://doi.org/https://doi.org/10.1016/j.rser.2019.109480

Jans-Singh, M., Ward, R., & Choudhary, R. (2021). Co-simulating a greenhouse in a building to quantify co-benefits of different coupled configurations. *Journal of Building Performance Simulation*, *14*(3), 247-276. https://doi.org/10.1080/19401493.2021.1908426

Jin, W., Formiga Lopez, D., Heuvelink, E., & Marcelis, L. F. M. (2023). Light use efficiency of lettuce cultivation in vertical farms compared with greenhouse and field. *Food and Energy Security*, *12*(1), e391. https://doi.org/https://doi.org/10.1002/fes3.391

Jin, W., Ji, Y., Larsen, D. H., Huang, Y., Heuvelink, E., & Marcelis, L. F. M. (2023). Gradually increasing light intensity during the growth period increases dry weight production compared to constant or gradually decreasing light intensity in lettuce. *Scientia Horticulturae*, *311*. https://doi.org/10.1016/j.scienta.2022.111807

Jonlin, D. L., & Lewellen, D. J. (2017). A Low-energy High Managing Energy Use for Commercial Indoor Cannabis Cultivation. *Energy Engineering*, *114*(4), 69-79. https://doi.org/10.1080/01998595.2017.11876936

Jung, D. H., Kim, D., Yoon, H. I., Moon, T. W., Park, K. S., & Son, J. E. (2016). Modeling the canopy photosynthetic rate of romaine lettuce (Lactuca sativa L.) grown in a plant factory at varying CO2 concentrations and growth stages [journal article]. *Horticulture, Environment, and Biotechnology*, *57*(5), 487-492. https://doi.org/10.1007/s13580-016-0103-z

Katsoulas, N., & Stanghellini, C. (2019). *Modelling Crop Transpiration in Greenhouses: Different Models for Different Applications* (Vol. 9). https://doi.org/10.3390/agronomy9070392

Kelly, N., Choe, D., Meng, Q., & Runkle, E. S. (2020). Promotion of lettuce growth under an increasing daily light integral depends on the combination of the photosynthetic photon flux density and photoperiod. *Scientia Horticulturae*, *272*, 109565. https://doi.org/https://doi.org/10.1016/j.scienta.2020.109565

Kelly, N., Meng, Q., & Runkle, E. S. (2022, March). Photoperiod, light intensity and daily light intergral. *Produce grower*, 16-19.

Keyvan, P., & Roshandel, R. (2024). An integrated Energy-Yield-Cost model to evaluate clean energy solutions for vertical farms. *Computers and Electronics in Agriculture*, *219*, 108809. https://doi.org/https://doi.org/10.1016/j.compag.2024.108809

Kim, C., & van Iersel, M. W. (2022). Morphological and Physiological Screening to Predict Lettuce Biomass Production in Controlled Environment Agriculture. *Remote Sensing*, *14*(2), 316. https://www.mdpi.com/2072-4292/14/2/316

Klein, S. A., & al., e. (2017). TRNSYS 18: A Transient System Simulation Program. *Solar Energy Laboratory, University of Wisconsin, Madison, WI, USA*.

Kokogiannakis, G., & Cooper, P. (2015). Evaluating the environmental performance of indoor plants in buildings. 14th International Conference of IBPSA - Building Simulation 2015, BS 2015, Conference Proceedings,

Kozai, T. (2016). Why LED lighting for urban agriculture? In *LED lighting for urban agriculture* (pp. 3-18). Springer.

Kozai, T. (2018). *Smart Plant Factory: The Next Generation Indoor Vertical Farms*. Springer.

Kozai, T. (2019). Towards sustainable plant factories with artificial lighting (PFALs) for achieving SDGs. *International Journal of Agricultural and Biological Engineering*, *12*(5), 28-37.

Kozai, T., Niu, G., & Takagaki, M. (2015). *Plant factory: an indoor vertical farming system for efficient quality food production*. Academic Press.

Kusuma, P., Pattison, P. M., & Bugbee, B. (2020). From physics to fixtures to food: current and potential LED efficacy. *Horticulture Research*, *7*(1), 56. https://doi.org/10.1038/s41438-020-0283-7

Lalonde, T., Talbot, M.-H., & Monfet, D. (2019, 2-4 September 2019). *The Impact Of Plants On HVAC System Performance In Cold Climate: A Parametric Study* Building Simulation 2019, Rome.

Ledesma, G., Nikolic, J., & Pons-Valladares, O. (2022). Co-simulation for thermodynamic coupling of crops in buildings. Case study of free-running schools in Quito, Ecuador. *Building and Environment*, *207*, 108407. https://doi.org/https://doi.org/10.1016/j.buildenv.2021.108407

Léveillé-Guillemette, F. (2019). *Évaluation des impacts énergétiques et environnementaux de différents modes d'agriculture urbaine en environnement contrôlé* École de technologie supérieure.

Li, K., Fang, H., Zou, Z.-r., & Cheng, R.-f. (2021). Optimization of rhizosphere cooling airflow for microclimate regulation and its effects on lettuce growth in plant factory. *Journal of Integrative Agriculture*, *20*(10), 2680-2695. https://doi.org/https://doi.org/10.1016/S2095-3119(20)63382-2

Li, L., Li, X., Chong, C., Wang, C.-H., & Wang, X. (2020). A decision support framework for the design and operation of sustainable urban farming systems. *Journal of Cleaner Production*, *268*, 121928. https://doi.org/https://doi.org/10.1016/j.jclepro.2020.121928

Liebman-Pelaez, M., Kongoletos, J., Norford, L. K., & Reinhart, C. (2021). Validation of a building energy model of a hydroponic container farm and its application in urban design. *Energy and Buildings*, *250*, 111192. https://doi.org/https://doi.org/10.1016/j.enbuild.2021.111192

Liu, R., Zhou, X., Lochhead, S. J., Zhong, Z., Huynh, C. V., & Maxwell, G. M. (2017). Low-energy LED lighting heat gain distribution in buildings, part II: LED luminaire selection and test results. *Science and Technology for the Built Environment*, *23*(4), 688-708. https://doi.org/10.1080/23744731.2016.1250563

Lopez-Cruz, I. L., Ruiz-GarcÃ-a, A., Fitz-RodrÃ-guez, E., Salazar-Moreno, R., & Rojano-Aguilar, A. (2017). A comparison of Bayesian and classical methods for parameter estimation in greenhouse crop models.

McCartney, L., & Lefsrud, M. (2018). Protected Agriculture in Extreme Environments: A Review of Controlled Environment Agriculture in Tropical, Arid, Polar, and Urban Locations. *Applied Engineering in Agriculture 34*(2), 455-473.

Meinen, E., Dueck, T., Kempkes, F., & Stanghellini, C. (2018). Growing fresh food on future space missions: Environmental conditions and crop management. *Scientia Horticulturae*, *235*, 270-278. https://doi.org/https://doi.org/10.1016/j.scienta.2018.03.002

Miserocchi, L., & Franco, A. (2025). Benchmarking energy efficiency in vertical farming: Status and prospects. *Thermal Science and Engineering Progress*, *58*, 103165. https://doi.org/https://doi.org/10.1016/j.tsep.2024.103165

Monteith, J. L. (1965). Evaporation and environment. Symp. Soc. Exp. Biol,

Nadal, A., Llorach-Massana, P., Cuerva, E., López-Capel, E., Montero, J. I., Josa, A., Rieradevall, J., & Royapoor, M. (2017). Building-integrated rooftop greenhouses: An energy and environmental assessment in the mediterranean context. *Applied Energy*, *187*, 338-351. https://doi.org/http://dx.doi.org/10.1016/j.apenergy.2016.11.051

Ohyama, K., Yamaguchi, J., & Enjoji, A. (2018). Evaluating Labor Productivity in a Plant Production System with Sole-source Lighting: A Case Study. *HortTechnology hortte*, *28*(2), 121-128. https://doi.org/10.21273/HORTTECH03886-17

Ohyama, K., Yamaguchi, J., & Enjoji, A. (2020). Resource Utilization Efficiencies in a Closed System with Artificial Lighting during Continuous Lettuce Production. *Agronomy*, *10*(5), 723. https://www.mdpi.com/2073-4395/10/5/723

Okayama, T., Okamura, K., Park, J.-E., Ushada, M., & Murase, H. (2008). A Simulation for Precision Airflow Control using Multi-Fan in a Plant Factory. *Environment Control in Biology*, *46*, 183-194. https://doi.org/10.2525/ecb.46.183

Pearson, S., Wheeler, T. R., Hadley, P., & Wheldon, A. E. (1997). A validated model to predict the effects of environment on the growth of lettuce (Lactuca sativa L.): Implications for climate change. *Journal of Horticultural Science*, *72*, 503-517.

Pennisi, G., Orsini, F., Landolfo, M., Pistillo, A., Crepaldi, A., Nicola, S., Fernández, J., Marcelis, L., & Gianquinto, G. (2020). Optimal photoperiod for indoor cultivation of leafy vegetables and herbs.

Prenger, J. J., Fynn, R. P., & Hansen, R. C. (2002). *A Comparison of Four Evapotranspiration Models in a Greenhouse Environment* (Vol. 45). https://doi.org/10.13031/2013.11429

Puccinelli, M., Malorgio, F., Pintimalli, L., Rosellini, I., & Pezzarossa, B. (2022). Biofortification of Lettuce and Basil Seedlings to Produce Selenium Enriched Leafy Vegetables. *Horticulturae*, *8*(9), 801. https://doi.org/10.3390/horticulturae8090801

Ramirez, A., Rodriguez, F., Berenguel, M., & Heuvelink, E. (2003). Calibration and validation of complex and simplified tomato growth models for control purposes in the southeast of Spain. International Workshop on Models for Plant Growth and Control of Product Quality in Horticultural Production 654,

Sabeh, N. C., Ross, D., Miner, L., & Everett, S. (2022). *Literature Review of Energy and Water Use in Controlled Environment Horticulture and Potential Efficiency Opportunities*.

https://www.etcc-ca.com/reports/literature-review-energy-and-water-use-controlled-environment-horticulture-and-potential

Schymanski, S. J., & Or, D. (2017). Leaf-scale experiments reveal an important omission in the Penman–Monteith equation. *Hydrol. Earth Syst. Sci.*, *21*(2), 685-706. https://doi.org/10.5194/hess-21-685-2017

Seginer, I., Straten, G., & Buwalda, F. (1998). Nitrate concentration in greenhouse lettuce : a modeling study.

Shahbandeh, M. (2023). *Global vertical farming market projection 2022 -2032*. https://www.statista.com/statistics/487666/projection-vertical-farming-market-worldwide/

Shimizu, H., Kushida, M., & Fujinuma, W. (2008). A growth model for leaf lettuce under greenhouse environments. *Environmental Control in Biology*, *46*(4), 211-219.

Silva, L. M., Cruz, L. P., Pacheco, V. S., Machado, E. C., Purquerio, L. F. V., & Ribeiro, R. V. (2022). Energetic efficiency of biomass production is affected by photoperiod in indoor lettuce cultivation. *Theoretical and Experimental Plant Physiology*, *34*(2), 265-276.

Song, R., Liu, D., Pan, Y., Cheng, Y., & Meng, C. (2023). Container farms: Energy modeling considering crop growth and energy-saving potential in different climates. *Journal of Cleaner Production*, 138353. https://doi.org/https://doi.org/10.1016/j.jclepro.2023.138353

Stanghellini, C. (1987). *Transpiration of greenhouse crops. An aid to climate management*.

Stanghellini, C., & Katzin, D. (2023). The dark side of lighting: a critical analysis of vertical farms' environmental impact. https://doi.org/10.31219/osf.io/nsu8h

Sun, W., Coules, A., Zhao, C., & Lu, C. (2025). A lettuce growth model responding to a broad range of greenhouse climates. *Biosystems Engineering*, *250*, 285-305. https://doi.org/https://doi.org/10.1016/j.biosystemseng.2025.01.008

Sweeney, D., Hand, D. W., Slack, G., & Thornley, J. H. M. (1981). Modelling the growth of winter lettuce.

Talbot, M.-H., Lalonde, T., Beaulac, A., Haillot, D., & Monfet, D. (2022, 22-23 June 2022). *Comparing the energy performance of different controlled environment agriculture spaces using TRNSYS* eSim2022, Ottawa.

Talbot, M.-H., & Monfet, D. (2020). Estimating the impact of crops on peak loads of a Building-Integrated Agriculture space. *Science and Technology for the Built Environment*, *26*(10), 1448-1460. https://doi.org/10.1080/23744731.2020.1806594

Talbot, M.-H., & Monfet, D. (2021). Estimated energy demand and sensible heat ratio of a controlled-environment agriculture space for a growth cycle. *ASHRAE Transactions*, *127*(2), 211-219.

Talbot, M.-H., & Monfet, D. (2024). Development of a crop growth model for the energy analysis of controlled agriculture environment spaces. *Biosystems Engineering*, *238*, 38-50. https://doi.org/https://doi.org/10.1016/j.biosystemseng.2023.12.012

Talbot, M.-H., Monfet, D., Lalonde, T., & Haillot, D. (2021). *Impact of Modelling Thermal Phenomena in a High-Density Controlled Environment Agriculture (CEA-HD) Space* Building Simulation 2021, Bruges.

Tei, F., Scaife, A., & Aikman, D. P. (1996). Growth of Lettuce, Onion, and Red Beet. 1. Growth Analysis, Light Interception, and Radiation Use Efficiency. *Annals of Botany*, *78*(5), 633-643. https://doi.org/10.1006/anbo.1996.0171

Van Henten, E. J. (1994). Validation of a dynamic lettuce growth model for greenhouse climate control. *Agricultural Systems*, *45*(1), 55-72. https://doi.org/https://doi.org/10.1016/S0308-521X(94)90280-1

Van Henten, E. J., & Van Straten, G. (1994). Sensitivity Analysis of a Dynamic Growth Model of Lettuce. *Journal of Agricultural Engineering Research*, *59*(1), 19-31. https://doi.org/https://doi.org/10.1006/jaer.1994.1061

Vanthoor, B. H. E., de Visser, P. H. B., Stanghellini, C., & van Henten, E. J. (2011). A methodology for model-based greenhouse design: Part 2, description and validation of a tomato yield model. *Biosystems Engineering*, *110*(4), 378-395. https://doi.org/http://dx.doi.org/10.1016/j.biosystemseng.2011.08.005

Villarreal-Guerrero, F., Kacira, M., Fitz-Rodríguez, E., Kubota, C., Giacomelli, G. A., Linker, R., & Arbel, A. (2012). Comparison of three evapotranspiration models for a greenhouse cooling strategy with natural ventilation and variable high pressure fogging. *Scientia Horticulturae*, *134*, 210-221. https://doi.org/https://doi.org/10.1016/j.scienta.2011.10.016

Waldron, D. (2018). EVOLUTION OF VERTICAL FARMS AND THE DEVELOPMENT OF A SIMULATION METHODOLOGY. *WIT Transactions on Ecology and the Environment*, *217*, 975-986.

Wang, A., Lv, J., Wang, J., & Shi, K. (2022). CO2 enrichment in greenhouse production: Towards a sustainable approach [Review]. *Frontiers in Plant Science*, *Volume 13 - 2022*. https://doi.org/10.3389/fpls.2022.1029901

Ward, R., Choudhary, R., Cundy, C., Johnson, G., & McRobie, A. (2015). Simulation of plants in buildings; incorporating plant-Air interactions in building energy simulation. 14th Conference of International Building Performance Simulation Association, BS 2015, December 7, 2015 - December 9, 2015, Hyderabad, India.

Watson, D. J. (1947). Comparative physiological studies on the growth of field crops: I. Variation in net assimilation rate and leaf area between species and varieties, and within and between years. *Annals of Botany*, *11*(41), 41-76.

Weidner, T., Yang, A., & Hamm, M. W. (2021). Energy optimisation of plant factories and greenhouses for different climatic conditions. *Energy Conversion and Management*, *243*, 114336. https://doi.org/https://doi.org/10.1016/j.enconman.2021.114336

Yeo, U.-H., Lee, S.-Y., Park, S.-J., Kim, J.-G., Choi, Y.-B., Kim, R.-W., Shin, J. H., & Lee, I.-B. (2022). Rooftop Greenhouse: (1) Design and Validation of a BES Model for a Plastic-Covered Greenhouse Considering the Tomato Crop Model and Natural Ventilation Characteristics. *Agriculture*, *12*(7), 903. https://www.mdpi.com/2077-0472/12/7/903

Zhang, K., Burns, I. G., & Turner, M. K. (2008). Derivation of a Dynamic Model of the Kinetics of Nitrogen Uptake Throughout the Growth of Lettuce: Calibration and Validation. *Journal of Plant Nutrition*, *31*(8), 1440-1460. https://doi.org/10.1080/01904160802208345

Zhang, S., & Schulman, B. (2017). A Numerical Model for Simulating the Indoor Climate inside the Growing Chambers of Vertical Farms with Case Studies. *International Journal of Environmental Science and Development*, *8*(10).

Zhang, Y., & Kacira, M. (2020a). Comparison of energy use efficiency of greenhouse and indoor plant factory system. *European Journal of Horticultural Science*, *85*(5), 310-320.

Zhang, Y., & Kacira, M. (2020b). Enhancing resource use efficiency in plant factory.